Bacterial degradation of dissolved organic carbon in the water column

An experimental and modelling approach

The research presented is this thesis was carried out at the Department of Theoretical Biology, Vrije Universiteit Amsterdam, The Netherlands and at the Laboratory of Marine Microbiology, Geochemistry and Ecology, University of Aix-Marseille II, Marseille France.

VRIJE UNIVERSITEIT

Bacterial degradation of dissolved organic carbon in the water column

An experimental and modelling approach

ACADEMISCH PROEFSCHRIFT

ter verkrijging van de graad Doctor aan
de Vrije Universiteit Amsterdam,
op gezag van de rector magnificus
prof.dr. L.M. Bouter,
in het openbaar te verdedigen
ten overstaan van de promotiecommissie
van de faculteit der Aard- en Levenswetenschappen
op woensdag 23 januari 2008 om 13.45 uur
in de aula van de universiteit,
De Boelelaan 1105

door

Marie Eichinger

geboren te Mulhouse, Frankrijk

promotoren:	prof.dr. S.A.L.M. Kooijman
	prof.dr. J.C. Poggiale

Contents

Chapter III: Biodegradation experiments in variable environments: substrate pulses and impact on growth efficiencies 45

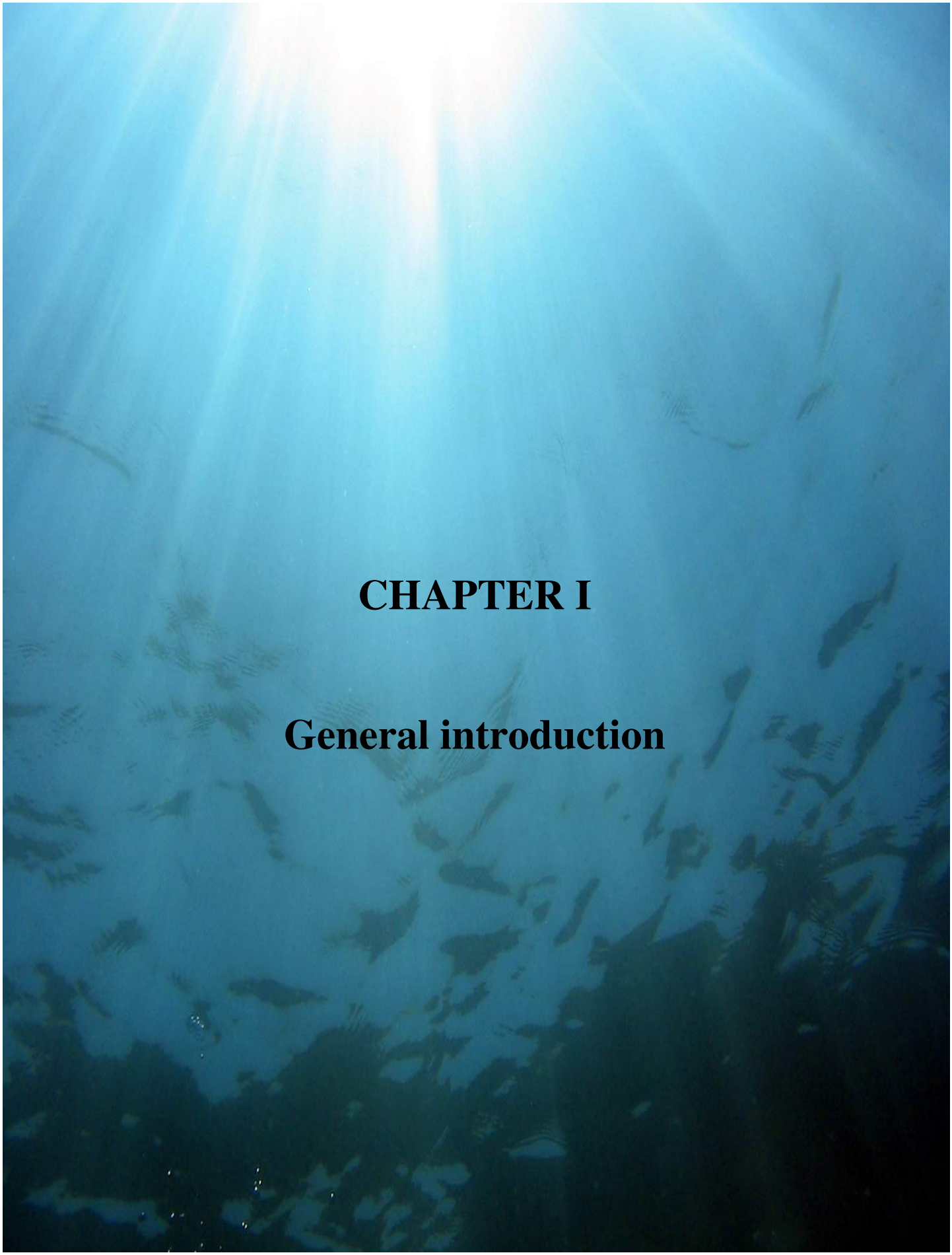

CHAPTER I

General introduction

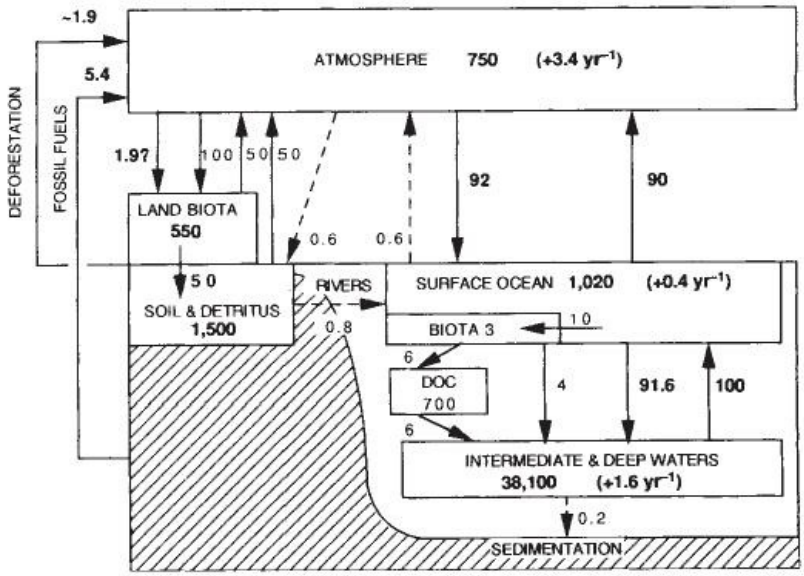

Figure I- 1: Reservoirs (Gt C) and flows (Gt C yr^{-1}) of the global carbon cycle (Siegenthaler & Sarmiento 1993).

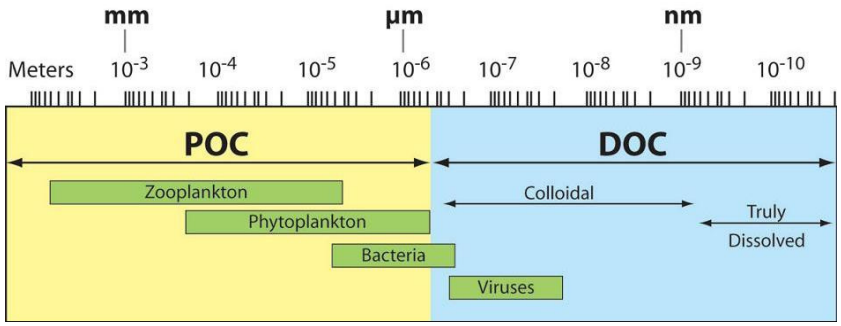

Figure I- 2: Size continuum spectrum of organic carbon, with the distinction between the particulate phase (POC > 0.7 µm) and the dissolved one (DOC < 0.7 µm). Adapted from Verdugo et al. (2004)**.**

I. The carbon cycle and the importance of processes of bacterial degradation of dissolved organic matter in aquatic systems

1. The role of dissolved organic carbon and of bacteria in the global carbon cycle

The global carbon cycle takes place inside and between the 4 spheres at the surface of the planet: lithosphere, hydrosphere, biosphere and atmosphere. The global stocks and flows of each of these reservoirs are given in Figure I-1. The ocean, covering approximatively 70 % of the earth surface, plays an important role in the carbon cycle and the global climate system. Indeed, at the global scale, seawater is an important component of the carbon cycle and constitutes one of the larger carbon reservoirs: the dissolved inorganic carbon amounts to 40 000 Gt C, thus approximatively 6 times the amount of atmospheric carbon dioxide (CO_2).

Carbon is fractionated into 2 categories: inorganic carbon (IC) and organic carbon (OC). IC is associated to compounds which are or were not living and which do not contain any C-C or C-H link, as for example the carbon from CO_2 or those from carbonate calcium $CaCO_3$. OC is produced by living organisms and is chemically linked to other carbon atoms or to elements as hydrogen (H), nitrogen (N) or phosphor (P). OC is subdivided into 2 classes: dissolved organic carbon (DOC) and particulate organic carbon (POC). Separation between both stocks is based on their size: all compounds that pass a filter with a given retention size (generally 0.7 µm) are considered as dissolved, the rest as particulate (Figure I-2). However, some living organisms, thus particulate, such as bacteria, are in the boundary of this separation and may partially be considered as DOC.

From a biological point of view, the carbon cycle typically starts from the conversion of CO_2 and other inorganic nutrients to OC and O_2 by photosynthesis (Figure I-3). In pelagic environments, photosynthesis is realised by phytoplankton, marine plants and algae but also by other autotrophic organisms such as cyanobacteria. This first step requires light and constitutes the primary production. OC produced by primary production can be consumed by higher trophic levels such as zooplanktonic organisms and fishes. DOC and POC are produced all along this trophic chain. DOC includes excretion of small molecules and POC includes fecal pellets. POC can be transformed into DOC according to several processes such as dissolution and enzymatic processes. DOC is used by heterotrophic bacteria

which remineralise organic matter, producing CO_2 and inorganic nutrients. These remineralised compounds can be reused for photosynthesis purposes if required conditions are met, and thus heterotrophic bacteria maintain the carbon cycle.

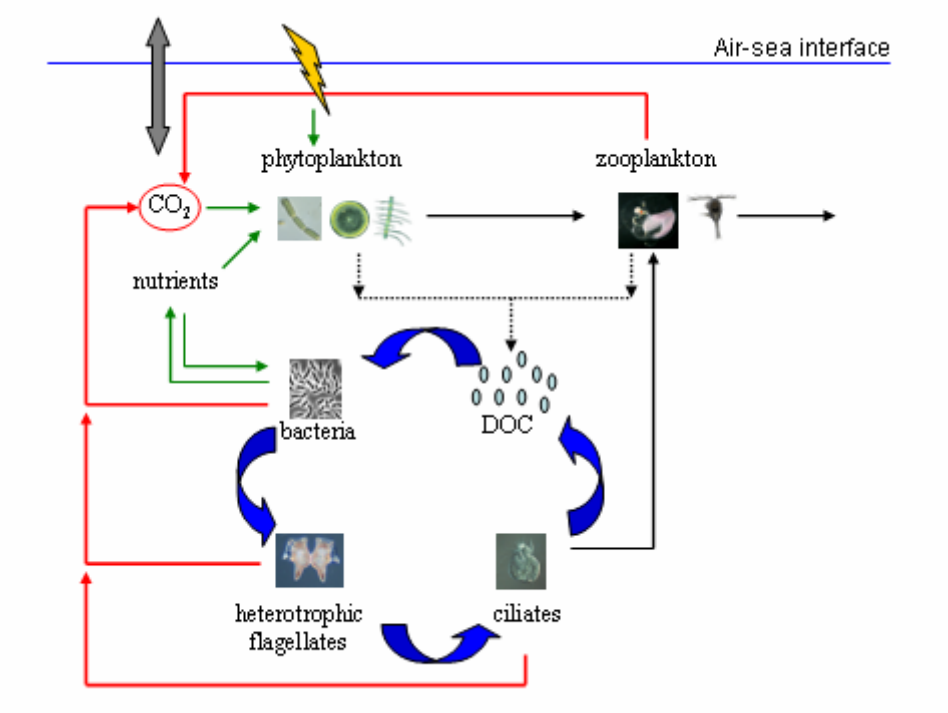

Figure I- 3: schematic and simplified representation of the aquatic carbon cycle. Green arrows represent photosynthetic requirements and constitute the start of the cycle. The full black arrows represent the traditional food chain (the last arrow coming from zooplankton being directed to the higher trophic levels), and the dashed black arrows the DOC production along this trophic chain. The full blue arrows represent the microbial loop, the start point being DOC, and all red arrows represent CO_2 production at each trophic level. Bacteria contribute not only to matter remineralisation by CO_2 production but also to nutrient regeneration required for photosynthesis. Finally, CO_2 is permanently exchanged between the ocean and the atmosphere by gas transfer (full grey arrow).

It is widely recognised that heterotrophic bacteria play a predominantly role in the carbon cycle. Indeed, they represent the most important living biomass in aquatic ecosystems. They also constitute the major DOC consumers (Pomeroy 1974), this latter being the second most important stock of bioreactive carbon in ocean (680 – 700 Pg C) (Williams & Druffel 1987, Hansell & Carlson 1998) after the very large stock of dissolved IC (38 000 Pg C) (Hansell 2002). DOC dynamic is thus important for understanding global carbon cycle and changes of atmospheric CO_2, the most critical greenhouse gas on our planet (Siegenthaler & Sarmiento 1993). DOC, after being consumed by heterotrophic bacteria, is either incorporated in the food chain or respired as CO_2. Bacteria represent thus either a sink or a source of carbon. DOC may also be photooxidised and remineralised in the surface layer (Tedetti 2007 et al. and references therein) or exported into the deep ocean by winter convection of the surface water masses (Copinmontegut & Avril 1993).

2. The dissolved organic carbon

i. Composition

DOC has a very heterogeneous nature and has thus been classified into different categories, which differ according to the studies. Some authors classify DOC pools between material that disappears rapidly to that which accumulates (Anderson & Williams 1999, Christian & Anderson 2002). Three distinct pools have been determined according to their reactivity towards heterotrophic bacteria: labile DOC (L-DOC) that is consumed in hours to days, semi-labile DOC (SL-DOC) that has a turnover time of weeks to years and refractory DOC (R-DOC) that has a turnover rate of millennia (Williams & Druffel 1987, Bauer et al. 1992, Druffel et al. 1992, Carlson & Ducklow 1995, Hansell et al. 1995, Carlson & Ducklow 1996, Carlson 2002). L-DOC represents DOC fraction which may be directly utilised by bacteria whereas SL-DOC needs bacterial enzymatic activity to be transformed in L-DOC and being consumed. R-DOC can be transformed into L-DOC only after photooxydation. When working on natural seawater samples, the separation of R-DOC from L-DOC and SL-DOC stocks may be performed by subtracting the values of DOC in deep waters (> 1000 m) to that of total DOC in surface waters, assuming an uniform distribution of R-DOC thorough the water column (Carlson & Ducklow 1995) (Figure I- 4). However, the separation of L-DOC from SL-DOC is more difficult as only a very small fraction of DOC can be chemically identified. Biological assays of bacterial degradation must be realised to fractionate these stocks (Wheeler et al. 1996, Hansell & Peltzer 1998, Wiebinga & de Baar 1998, Dafner et al. 2001, Sohrin & Sempéré 2005).

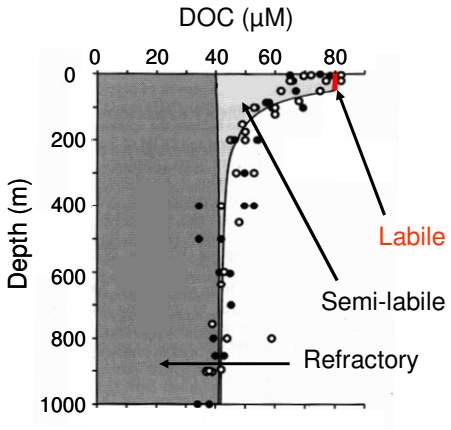

Figure I- 4: The distribution of DOC in the water column (Anderson & Williams 1999). L-DOC is only present in small concentrations in the surface layer.

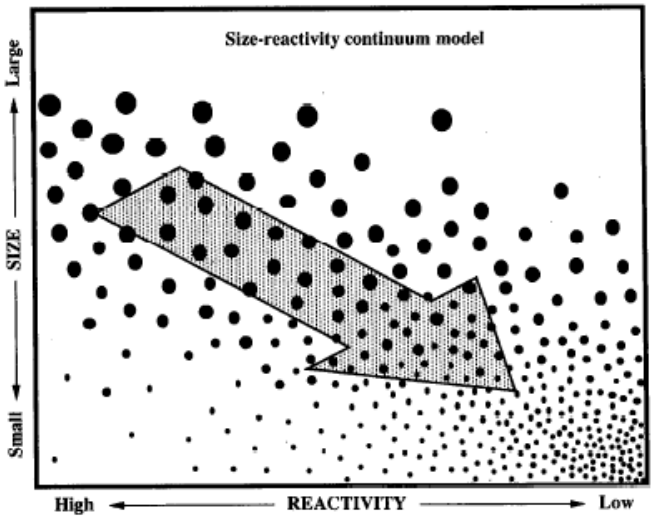

Figure I- 5: schematic diagram of the size continuum model of the reactivity for organic matter (OM) decomposition in aquatic environment. Dot size is representative of OM size and arrows indicate the reactivity direction, from very reactive HMW compounds to LMW compounds more recalcitrant to degradation (Amon & Benner 1996).

DOC may also be fractionated with respect to their molecular weight (Amon & Benner 1996). Low molecular weight (LMW) compounds, with a size less than 1 kDa, can be distinguished from DOC compounds with a high molecular weight (HMW), with a size between 1 kDa and 30 kDa, and from DOC with a very high molecular weight (VHMW) with a size greater than 30 kDa. However, the relationship between this latter classification and the previous one based on lability is not very clear. Most studies assimilate LMW compounds to labile material, and inversely HMW compounds to more refractory material (Saunders 1976). In contrast, some studies demonstrate that HMW compounds are more reactive (Amon & Benner 1996) and a new size continuum model has been created, where the bioreactivity of DOC decreases with decreasing size (Figure I- 5). Authors supposed that freshly produced organic matter (OM) is HMW and that during decomposition OM continuously becomes less bioreactive and smaller in physical size, giving rise to LMW molecules with a low reactivity (Amon & Benner 1996).

DOC may also be classified with respect to its chemical nature (carbohydrate, lipid, nucleic acid), but currently only approximatively 30 % of the bulk DOC pool have been chemically characterised. In order to try to understand which compounds are preferentially utilised by bacteria, and thus to determinate the labile nature of these compounds, numerous authors have used biodegradation experiments with seawater samples by adding model compounds. Inorganic nutrients are also often added in these cultures. The observation that added inorganic nutrients do not stimulate bacterial production or DOC utilisation indicates that growth is limited by the OC availability (Carlson & Ducklow 1996, Carlson et al. 2002). Other experiments showed that compounds such as glucose, dissolved free amino acids (DFAA) and natural plankton extracts stimulate bacterial production as well as OM utilisation with turnover rates of some days (Cherrier et al. 1996). These compounds may thus be classified as L-DOC. Carlson (2002) states that the most biologically reactive organic compounds in seawater include dissolved free compounds such as neutral monosaccharides (MCHO) and DFAA. Another experiments, where OM addition consists of plankton extracts, showed that only 28 % of this extract have been chemically characterised and consists of DFAA, dissolved combined amino acids (DCAA) and MCHO (Cherrier & Bauer 2004). In addition, only 31 % of this added DOC were used by bacteria during short biodegradation experiments, and may thus be classified in L-DOC, but only 75 % of the utilised compounds have been chemically characterised (Cherrier & Bauer 2004). This study proves thus the complexity of associating chemical compounds with a labile nature of OC.

ii. Production

Numerous mechanisms of DOC production have been highlighted. The main source of DOC production seems to come from release by phytoplankton (Nagata 2000). However, other processes are involved in DOC production, as egestion, excretion and "sloppy feeding" by grazers, and cell lysis induced by viruses (Nagata 2000, Carlson 2002). The quantitative role of DOC release by phytoplankton is assessed by the percent extracellular release (PER). This latter have been extensively studied and present a high variability depending on whether it was estimated from phytoplanktonic cultures or from natural seawater. PER fluctuates between 2 and 10 % in cultures (Nagata 2000) and between 0 and 80 % in the field for a variety of coastal and oceanic systems (Carlson 2002). Grazers also participate substantially to DOC production. Indeed, the magnitude of potential DOC release by protozoa, that feed on small phytoplankton and bacteria, is equivalent to or even exceeds that of phytoplankton (Nagata 2000). In addition, zooplankton, i.e. grazers that feed on large phytoplankton, could release DOC by four main processes: excretory release, egestion, sloppy feeding (breakage of large prey during handling and feeding) and release from fecal pellets (Carlson 2002). Production rates are highly variable according to the considered process (Nagata 2000). Viral lysis plays also an important role among these DOC production processes. Finally, even bacteria may participate to DOC production. Indeed, structural components of bacterial cells including membranes and peptidoglycan can be introduced to seawater as DOC during bacterial death due to protozoan grazing and viral infection (Nagata & Kirchman 1999).

However, we don't get any information about DOC lability else than via the process by which it is produced. The labile character of a compound is very difficult to estimate. Indeed, if DOC consumption is studied in cultures including one DOC producer and bacteria, these flows being direct, we cannot measure the fraction of DOC that is really assimilated by bacteria. On the other hand, studying only DOC production does not allow estimating its potential utilisation by bacteria.

iii. Spatial and temporal variability of DOC

From a general point of view, DOC concentration is higher in the surface layer than in deep waters. In deep waters, DOC concentration is considered constant around 34 µM C but may vary slightly due to marine currents. For example, 29 % decrease in DOC concentration has been observed between north of the North Atlantic and north of the North Pacific (Hansell & Carlson

1998). Surface concentrations are more variable, due to more pronounced spatial and temporal influences. The DOC mean surface concentration may be estimated to 90 µM C (Hansell 2002). Its spatial variation may be affected by physical phenomenona such as (1) upwelling which will reduce the DOC concentration, (2) terrigenous inputs such as the highly concentrated DOC inputs by riverines. In this latter case, the DOC concentration may exceed 200 µM C. The temporal DOC variation is principally due to seasonal phytoplankton blooms. However, the magnitude of this variability differs with the region. So, strong increases in DOC concentration are characteristic of high latitude systems which receive high fresh nutrients inputs during winter periods. For example, the DOC concentration in surface waters increases from 42 µM C in winter to 65-70 µM C in summer in the Ross Sea (Carlson et al. 1998). In oligotrophic zones, with medium latitudes, oceans do not exhibit the same seasonality (Hansell 2002). The changes in DOC concentration is on average only about 3-6 µM C, that is small amplitudes compared to the high latitude systems (Hansell 2002). This phenomenon is due to mixing between surface and deep waters, with a small DOC concentration, when primary production is high. Consequently, when stratification becomes established with the heating of the top layer, the phytoplanktonic bloom will cease and the DOC concentration increases again to normal levels. Oceanic systems at low latitude do not undergo winter refreshment of the surface layer and thus seasonality in DOC concentration (Hansell 2002). It is therefore important to be aware that spatial and temporal variabilities are tightly coupled, implying that impacts from spatial or temporal variability are difficult to discriminate.

3. DOC utilisation by pelagic heterotrophic bacteria

Heterotrophic bacteria are considered as major consumers and remineralisers of dissolved organic matter (DOM) in the ocean (Pomeroy 1974). They also represent a very dynamic compartment in the interaction between geosphere, hydrosphere and biosphere and as such has the potential to influence the global carbon cycle and climate change (Farrington 1992). The interactions between DOM and bacteria play a central role in the aquatic carbon cycle; thus, the factors regulating DOM production and consumption profoundly influence carbon fluxes (Amon & Benner 1996). Moreover, since Azam et al. (1983) have highlighted the ecological role of bacteria in the water column, numerous studies have tried to understand how bacteria utilised and transformed DOM.

The bacterial growth efficiency (BGE) is a factor allowing the determination of the DOM utilised by bacteria for their growth, the remaining being remineralised. Indeed, at low BGE, more DOM will be remineralised, keeping the nutrient cycling within the microbial cycle; at high BGE the OM is transferred from the dissolved phase to the particulate phase and with increased probability into the larger trophic size fractions (del Giorgio & Cole 1998, del Giorgio & Duarte 2002, Cajal-Medrano & Maske 2005). BGE allows thus estimating bacterial impact in marine ecosystems as carbon source or sink. Numerous environmental factors may affect BGE (del Giorgio & Cole 1998): DOC quality in term of molecular weight (Amon & Benner 1996), chemical nature of DOC (Carlson & Ducklow 1996, Cherrier et al. 1996, Cherrier & Bauer 2004), substrate C:N ratio (Goldman et al. 1987), distance of the study site from the shore (del Giorgio & Cole 1998, La Ferla et al. 2005), season (Reinthaler & Herndl 2005, Eichinger et al. 2006), temperature (Rivkin & Legendre 2001) and depth (Eichinger et al. 2006). However, BGE comparison between studies is made difficult due to the diversity of methods used and the utilisation of conversion factor.

BGE is estimated from experimental data generally obtained from batch cultures. BGE is calculated from bacterial production (BP), bacterial respiration (BR) and/or bacterial carbon demand (BCD) according to the following formula BGE=BP/BCD where BCD=BP+BR (Carlson & Ducklow 1996, del Giorgio & Cole 1998, Rivkin & Legendre 2001, Sempéré et al. 2003, Cherrier & Bauer 2004). BP may be estimated from tritiated leucine or thymidine incorporation, but its estimation requires the utilisation of conversion factors which are not necessarily constant. BR is estimated from a linear regression on the increasing CO_2 concentration in incubations that last few days, or more generally from a linear regression on the decreasing O_2 concentration. However, the conversion from O_2 consumption to CO_2 production which corresponds to BR requires the utilisation of an assumed respiratory quotient (RQ). This latter is considered constant and is often approximated to 1 for sake of simplicity or to 0.8 as a mean of literature values (Sempéré et al. 2003). BCD is calculated either as the sum of BP and BR or as the decrease of DOC in cultures. However, BGE values resulting from the estimation of BCD as BP+BR or as the rate of decrease of DOC concentration may be different (Cherrier et al. 1996). Consequently, the sole utilisation of a conversion factor biases BGE estimation.

II. Modelling organic matter and bacterial dynamics

This section focuses on the different models which have been used to describe bacterial growth utilising DOC as nutritive resource. Since Azam et al. (1983) allocated the term microbial loop for the set of interacting processes responsible for the recycling of dead OM into particulate biomass, there was an increasing number of studies trying to estimate the carbon flow through microbial loop. Heterotrophic bacteria represent the major organisms that consumed and remineralised DOM (Pomeroy 1974) and are the central component of the microbial food web (Legendre & Rassoulzadegan 1995). Consequently, an understanding of the relevant aspects of bacterial physiology is a prerequisite for any detailed understanding of how heterotrophic bacteria interact with DOC and organisms at other trophic levels in the microbial loop (Martinussen & Thingstad 1987). Many experimental studies were conducted and models proposed to explore the bacterial link-sink problem (Touratier et al. 1999). Mathematical models provide tools which allow investigation of complex dynamics such as microbial food webs. However, the design of a particular model may vary greatly and depends on the particular purpose of the modelling exercise, as modelling of an ecosystem as a whole and modelling of the physiology of the individual physiology are carried out with different objectives and often using different approaches (Davidson 1996). We have thus decided to describe the various models in relation to their complexity at the level of bacterial physiology, and not in relation to the complexity of the global model, that is to say if the considered study presents a simple bacterial growth model or an ecosystem model dealing with numerous parameters and state variables. The bacterial growth formulation may however be the same depending on whether the model is a growth model or a trophic chain model. Models describing carbon utilisation by bacteria were developed by various authors and the system complexity varies (Cajal-Medrano & Maske 1999) from simple models with 2 state variables (Monod 1942) to very complex bioenergetic models with many state variables (Vallino et al. 1996).

1. Utilisation of models with Michaelis-Menten kinetics

The Monod (Monod 1942) model uses Michaelis-Menten (Michaelis & Menten 1913) kinetics and is certainly the most extensively used formulation for describing bacterial growth with DOC as nutritive resource. This model assumes that substrate (X) is directly and instantaneously assimilated by bacteria (B) with a constant growth efficiency (BGE). The substrate

utilisation is described by a Michaelis-Menten formulation with a maximum specific assimilation rate (V_{max}) and a half-saturation constant (K):

$$\frac{dX}{dt} = -V_{max}\frac{X}{K+X}B$$
$$\frac{dB}{dt} = BGE\,V_{max}\frac{X}{K+X}B$$

This model assumes that a proportion BGE of the assimilated substrate is utilised for growth, and that the complementary proportion (1-BGE) is thus used for respiration. At the bacterial level, this model has been used to describe *in situ* data on growth and L-DOC utilisation (Eichinger et al. 2006), as well as in a chemostat-type theoretical study dealing with 2 potentially limiting substrates (C and N) (Thingstad & Pengerud 1985). The Monod model has been more extensively used in studies at a wider scale, i.e. studies describing the microbial loop or global models aiming to represent elemental cycles in marine systems. Among these studies, microbial loop models including heterotrophic bacteria have been realised, the aim being generally to investigate the carbon flow through microbial loop and the interactions between bacteria and other organisms constituting the microbial loop. However, most of these works investigated models at their steady-state and compare model outputs with stock data (Taylor & Joint 1990, Blackburn et al. 1996, Anderson & Ducklow 2001) or considered the model only on a theoretical point of view without comparison with data (Thingstad & Pengerud 1985). In addition, parameter values of the four last cited models came from literature or were assumed. This latter fact, in addition to the absence of model validation with dynamical data, complicates the evaluation of the pertinence of these models in the context of this thesis. Moreover, substrate quality was taken into account but the various studies did this in different ways: quality may be converted to a lability, which is expressed as a fraction of the DOC production by the considered source (phytoplankton exudation, bacterial lysis, grazing) (Taylor & Joint 1990, Anderson & Ducklow 2001) or taken to be a function of elemental C:N ratios (Thingstad & Pengerud 1985, Blackburn et al. 1996).

Finally, many studies, focusing mainly on cycling of elements in marine systems, have used this formulation to describe DOC utilisation by bacteria (Davidson 1996, Christian & Anderson 2002). Some studies specifically investigated oceanic DOC cycling and have used a Monod-type formulation (Connolly & Coffin 1995, Anderson & Williams 1998, 1999), a simplified Monod-type formulation (Bendtsen et al. 2002), or a slightly more complicated Monod-type formulation by adding for example a temperature-

dependant relationship (Bissett et al. 1999) or by taking into account a carbon absorption threshold (Tian et al. 2000). All these models, except the last one, considered several DOC labilities. However, even if the global dynamics of these models match DOC distribution in marine systems well, the validity of these models is limited due to (1) the parameter values that were assumed or taken from literature and (2) the comparison of model outputs with data comprising either only few variables of the model or few data points. Other ecosystem models utilised also Monod-type formulations for the DOC utilisation by bacteria, but without specific attention for the carbon cycle (Billen & Becquevort 1991, Vallino 2000, Spitz et al. 2001, Lancelot et al. 2002, Raick et al. 2005).

2. Utilisation of models with reserve

The ability of carbon storage by heterotrophic bacteria has been demonstrated for carbon limited systems (Baxter & Sieburth 1984) as well as for systems not limited by carbon availability (Kooijman 2000). Production and accumulation of carbon products, such as polymeric carbohydrates, has been shown to be a survival mechanism to dispose of the excess MCHO taken up (Baxter & Sieburth 1984). This storage capacity provides an explanation of the continued cell growth after depletion of the substrate (Martinussen & Thingstad 1987). This experimental result has thus to be taken into account in models simulating bacterial growth and utilisation of carbon substrate. To take this storage material into consideration, growth models often used the Droop (Droop 1968) model or an adaptation of this latter. This model has been originally constructed to describe nutrient-limited growth of a monospecific phytoplankton strains. Since then, it has been extensively used and extended to study heterotrophic bacteria. Some studies have used an adapted form of this model to describe carbon utilisation and bacterial growth in chemostat-type theoretical situations (Thingstad & Pengerud 1985, Thingstad 1987) or in comparison with batch or chemostat data (Martinussen & Thingstad 1987). In these studies, this model has been used to describe limitation by nitrogen (N), phosphor (P) or carbon (C). This allows flexibility in biomass composition in term of C, N and P, whereas Monod model assumes constant composition. In this kind of model, growth depends on a surplus pool of nutrients inside the cell, named cell quota, and not on the outside concentration of limiting nutrient directly as in Monod model. The growth rate is controlled only by the cell quota (C, N or P) which is closest to its minimum value. In the works cited previously, model formulation for the substrate utilisation and growth of bacterial biomass has evolved in the course of years and has been adapted to match experimental results. The model considered different formulations for the growth in term of biomass

(C, N or P) and the growth in term of cell number which only depends of one of the three elements.

Contrary to the Monod model, quota models have been rarely used in microbial loop or ecosystem models. Some microbial loop models have used cell quota (Baretta-Bekker et al. 1998) to describe element fluxes and to allow bacteria using inorganic nutrients, a capability not utilised in their previous model; Baretta-Bekker *et al.* (1994) allowed only OC utilisation. A complex biogeochemical model, following from the ERSEM model of Baretta-Bekker *et al.* (1998), used also the notion of cell quota. This was to decouple OC assimilation from nitrogenous and phosphorous nutrient utilisation rather than to create material storage in the cell. Contrary to the studies of Thingstad *et al.* cited previously where each quota comprises only 1 element (C, N or P) and where growth depends on the ratio between the minimum quota and the current quota value, cell quota correspond here to C:N and C:P ratios and permit to determine the limiting element.

Dynamic energy budget (DEB) theory (Kooijman 2000) considers storage of nutrients as well as energy substrates. This theory provides laws for energy and substrate absorption and their utilisation by organisms. One organism is quantified by at least 2 state variables: reserve and structure (see chapter IV). Reserve is thus considered as a state variable as well and the number of reserves might equal that of nutrients. This theory has been extensively applied to the growth of heterotrophic bacteria (Kooijman et al. 1991, Hanegraaf & Muller 2001, Brandt et al. 2003, Brandt et al. 2004) and to the growth of bacteria implied in prey-predator interactions and in small trophic chains (Kooi & Kooijman 1994, Kooijman et al. 1999, Hanegraaf & Kooi 2002). In all of these studies models have been compared to data and match very well. However, DEB theory has currently not been used for describing microbial loop or complex ecosystems, certainly because resulting models are complex and the calibration of their numerous parameters and state variables is complicated.

3. Maintenance implementation

Some of the models cited previously used also the notion of maintenance to translate the fact that organisms provide energy not only for biosynthetic processes producing growth but also for physiological activity that does not produce new biomass but maintain cell integrity (Cajal-Medrano & Maske 2005). This energy is utilised for the turnover of cell constituents, ionic equilibrium and repair processes (Cajal-Medrano & Maske 1999). This maintenance activity is decoupled from growth and is necessary for cell

survival even if concentration of bioavailable substrate is not sufficient to ensure growth. First authors having pointing out maintenance requirements were Herbert (1958), Marr et al. (1963) and Pirt (1965). This maintenance activity is often represented in models by respiration, accounting for a term of basal respiration and one of activity linked to the growth. Cajal-Medrano and Maske (1999, 2005) have used a model which links the respiration rate, taking into account both terms, and the growth rate together. These studies aimed to interpret published data concerning BGE values obtained with natural bacterial population from temperate, pelagic systems. However, these studies did not compare the model with dynamical data of DOC and bacteria. Other studies, based on bacterial growth, have taken the maintenance process into account in models. Some of these models assessed the influence of substrate quality, in terms of C:N ratio, on growth, respiration and excretion, but they described growth according to Michaelis-Menten kinetics (Touratier et al. 1999). Other studies have also incorporated maintenance as respiration; contrary to most studies, this latter is realised from carbon cell quota and not directly from assimilated substrate (Martinussen & Thingstad 1987, Thingstad 1987). This model has been calibrated and compared to steady-state and transient data, coming from batch and chemostat experiments, and showed a good match.

Some microbial loop models also take maintenance into account by fractioning respiration into a part dedicated to growth and the other one linked to maintenance (Baretta-Bekker et al. 1994, Blackburn et al. 1996, Baretta-Bekker et al. 1998). The presence of maintenance in bacteria is rare in ecosystem models. Connolly and Coffin (1995) took basal respiration into account, but not that linked to growth. In most other models, growth is realised with a constant fraction BGE, thus considering or assuming that respiration is the part of the assimilated carbon not utilised for growth, which means that respiration is only linked to growth by a fraction (1-BGE) (Anderson & Williams 1998, 1999, Bissett et al. 1999, Tian et al. 2000, Vallino 2000, Spitz et al. 2001, Pahlow & Vézina 2003, Raick et al. 2005).

DEB theory is based on 3 main processes: assimilation, maintenance and growth (Kooijman 2000). Consequently, all models constructed from this theory account for cell maintenance. Maintenance costs are also paid from reserve. Contrary to all models cited previously that include maintenance, DEB theory, being based on energy, does not identify maintenance to respiration and maintenance costs can be paid in different ways. Consequently, maintenance may result in biomass loss and/or in product formation that are not necessary CO_2 (see chapter IV).

III. Objectives and thesis outline

This thesis aims to investigate growth of pelagic heterotrophic bacteria that utilise DOC as nutritive resource by using both experimental and modelling approaches. Two main axes merge from this work: (1) the study of growth models, constructed from experimental results, with a view to implement them in ecosystem models, and (2) the investigation of the environmental factors influencing the BGE with these models. The main objective consists of the study of bacterial growth in different environmental contexts and to deduce a suitable mathematical formulation for describing the interaction between growth and DOC to include this in a biogeochemical model later on. To do that, a strong coupling between experimentation and modelling was required. The various growth models described previously, with different levels of complexity, have been studied and have been confronted to data, these latter coming either from natural seawater or from experiments in artificial conditions.

This thesis is divided into 4 parts.

The first chapter concerns the utilisation of the Monod model for describing bacterial growth and DOC assimilation in *in situ* conditions. 36 biodegradation experiments have been performed during the POMME program in Atlantic Ocean, corresponding to several water depths and seasons. The various measurements realised during the experiments allowed the determination of bacterial biomass and DOC concentration dynamics for each experiment. However, the small number of measurements did not allow the use of a mechanistic model. We have thus decided to utilise the Monod model as it takes only 2 state variables and 3 parameters into account. Moreover, this model is the most used to describe the utilisation of carbon substrate by heterotrophic bacteria in biogeochemical models, and we were thus able to test its pertinence towards *in situ* data. This model has been calibrated for each experiment and we were thus able to estimate BGE and the assimilation rate for each of them. The model parameters, including BGE, varied according to depth and season and demonstrated that the Monod model is not sufficient for describing the DOC utilisation by bacteria in biogeochemical models.

The second chapter concerns the investigation of biodegradation in a perturbed system, carried out with an artificial medium and a monospecific bacterial strain using a single carbon substrate. Previous experiments required a lot of assumptions to apply a model, which complicates further analysis and

interpretation of results. In addition, the experimental setup did not allow the application of a complex model. Utilisation of artificial culture medium permitted the control of experimental conditions and thus allowed not only numerous measurements and application of less restrictive models, but also applying experimental perturbations in order to be close to natural conditions from a qualitative point of view. This chapter focuses especially on the comparison of 2 experiments carried out under the same experimental conditions, the difference being the input regime of the carbon substrate in the batch cultures. In the first experiment, whole substrate was loaded as soon as the experiment began, as for the experiments realised during the POMME program. In the second experiment, substrate was periodically pulsed, the total substrate amount being the same as the first experiment. BGE have been estimated for both experiments. Its estimation was realised not only directly from experimental data, as is done by most authors, but also from 3 models, each of them comprising a different complexity level. This study demonstrated that the Monod model is unable to fit bacterial dynamics under starvation. Starvation occurs regularly in oceanic ecosystem since the DOC distribution is spatially and temporally variable. We have also highlighted that BGE values were always larger in the pulse experiment, whatever the estimation method we used. This result is profoundly important in the current marine microbiological context as numerous authors work on the influence of environmental factors on the BGE dynamics. Even the isolation of bacteria from their environment, which is a prerequisite to study carbon flow through bacteria, affects the obtained BGE values.

The third chapter presents a model, formulated from DEB theory, which has specifically been constructed for the pulse experiment cited previously. This model has been calibrated on experimental data and matched the data very well. However, this model was too complex to be introduced in biogeochemical models. We thus have simplified it and showed that it may reduce to a logistic equation, with a variable carrying capacity. We reduced the original set of 4 differential equations to a system of 2 differential equations. Moreover, this simplified model did not reduce model performance when compared to data as it exhibits exactly the same dynamics. This result is very important in the current context of the development of biogeochemical models, as more and more processes are taken into account to be close to reality, but simplification of these formulations is required to accurately calibrate, simulate and understand model results.

The last chapter concludes on all results, on the BGE estimation and dynamics as well as on the simplification of bacterial growth model to implement them into global models. This chapter presents also some perspectives for further research.

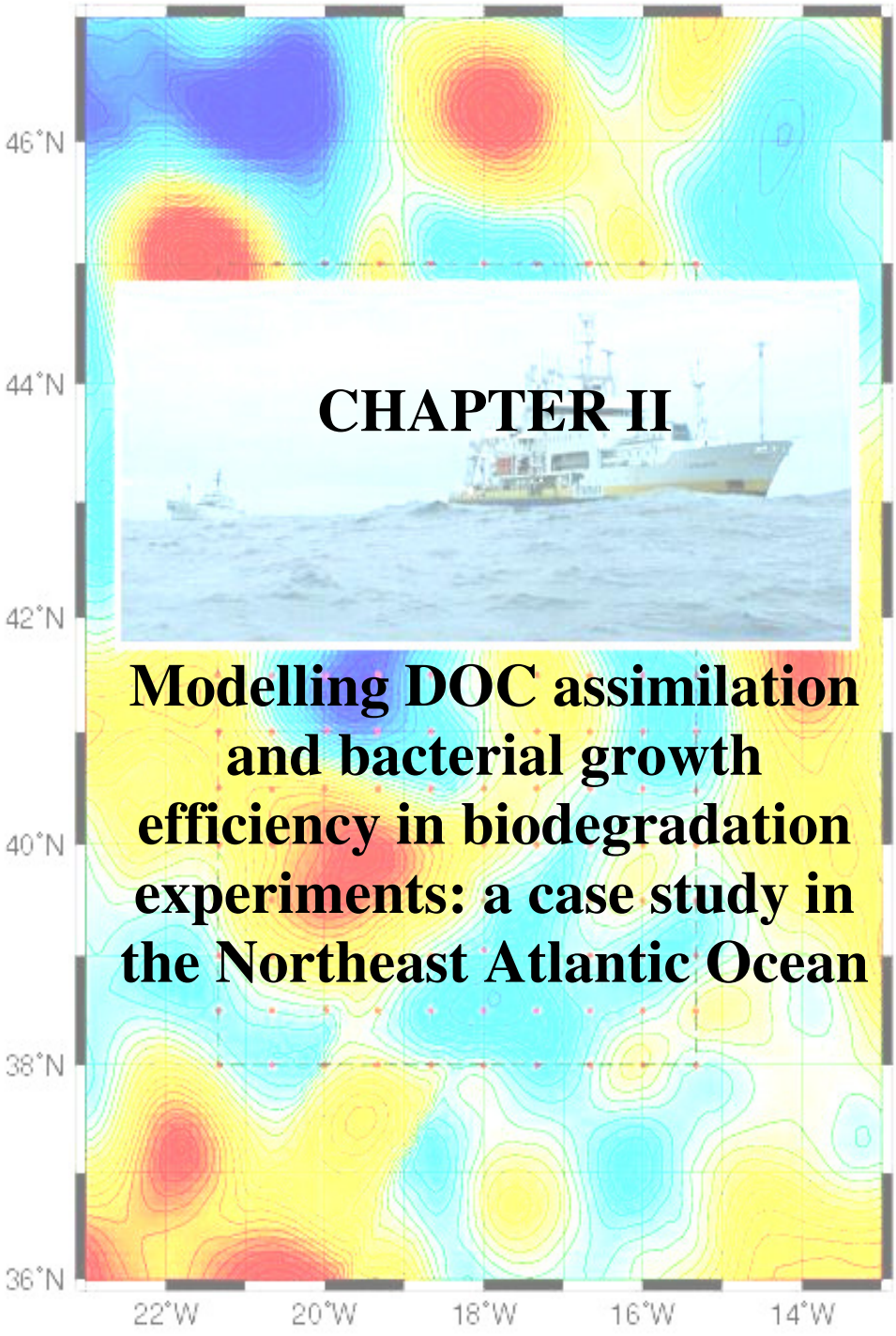

CHAPTER II

Modelling DOC assimilation and bacterial growth efficiency in biodegradation experiments: a case study in the Northeast Atlantic Ocean

Eichinger M, Poggiale JC, Van Wambeke F, Lefèvre D, Sempéré R

(2006) Aquatic Microbial Ecology 43:139-151

Abstract

A Monod (1942) model was used to describe the interaction and dynamics between marine bacteria and labile-dissolved organic carbon (L-DOC) using data obtained from 36 biodegradation experiments. This model is governed by 2 state variables, DOC and bacterial biomass (BB) and 3 parameters, specific maximum assimilation rate (V_{max}), half-saturation constant (k) and bacterial growth efficiency (BGE). The calibrations were obtained from biodegradation experiments carried out in the Northeast Atlantic Ocean over different seasons and at different depths. We also conducted a sensitivity analysis to determine (1) which parameter had the greatest influence on the model, and (2) whether the model was robust with regard to experimental errors. Our results indicate that BGE is greater in surface layer than in deeper waters, with minimum values being observed during winter. In contrast, the V_{max}/k ratio is inversely dependent on depth and does not show any seasonal trend. This reflects an increase in bacterial affinity for substrate with increasing depth (decrease of k) and/or better specific maximum assimilation rates (increase of V_{max}). The sensitivity and robustness analyses demonstrate that the model is more sensitive to the V_{max}/k ratio than to BGE, and that the parameters estimated are reliable. However, although the BGE values are close to those estimated experimentally, the use of a constant V_{max}/k and BGE in a 1-dimensional model is not appropriate as these parameters should be described as variables that take depth and season into account.

I. Introduction

The global oceanic dissolved organic carbon (DOC) reservoir is about 685 x 10^{15} gC (Hansell & Carlson 1998a), is recognised as one of the largest pools of reduced carbon on the planet (Carlson & Ducklow 1995) and is directly related to atmospheric CO_2 (Siegenthaler & Sarmiento 1993). Dissolved organic compounds are almost exclusively consumed by bacteria and are either incorporated into the microbial food web and/or respired as CO_2, in proportions that are difficult to determine. Depending on the bacterial reactivity, DOC can be fractionated into several components. These include refractory material with turnover times of millennia, semi-labile material with turnover times of months to years and labile material with turnover times of hours to days (Williams & Druffel 1987, Bauer et al. 1992, Druffel et al. 1992, Carlson & Ducklow 1995, Hansell et al. 1995, Carlson 2002). The labile component of DOC (L-DOC) can be studied by measuring bacterial DOC consumption in biodegradation experiments (Amon & Benner 1996, Carlson & Ducklow 1996, Sempéré et al. 1998). Semi-labile and refractory-DOC are usually determined by examining DOC profiles throughout the water column (Wheeler et al. 1996, Hansell & Peltzer 1998, Wiebinga & de Baar 1998, Dafner et al. 2001, Sohrin & Sempéré 2005).

Bacterial respiration (BR) represents ~ 50 to 90 % of the total community respiration (Sherr & Sherr 1996, del Giorgio & Duarte 2002). Understanding heterotrophic bacterial metabolism (production of biomass plus respiration) is therefore paramount in determining the role of the biological pump in the carbon cycle. More recently, an effort has been made to provide a more accurate description of the relationship between DOC assimilation and bacterial production (BP) (Anderson & Williams 1999, Lancelot et al. 2002, Vichi et al. 2003). The bacterial carbon demand (BCD) can be calculated from BP by the use of the bacterial growth efficiency (BGE = BP/BCD and BCD = BP + BR) (del Giorgio & Cole 1998, Rivkin & Legendre 2001). BGE ranges from < 5 to 60 %, median value being 24 % (Jahnke & Craven 1995, del Giorgio & Cole 1998), and is usually determined by DOC biodegradation experiments or locally computed from *in situ* size-fractionated community respiration measurements and BP data (del Giorgio & Cole 1998).

Some biogeochemical models describe the interaction between DOC and bacteria but include other processes such as DOC production, the transfer of matter to higher trophic levels and different DOC pools (Baretta-Bekker et al. 1995, Blackburn et al. 1996, Anderson & Williams 1998, 1999, Anderson & Ducklow 2001, Spitz et al. 2001, Lancelot et al. 2002, Dearman et al. 2003).

In these models, DOC uptake by bacteria is generally computed from Monod kinetics, which suggests a constant BGE (Taylor & Joint 1990, Baretta-Bekker et al. 1995, Blackburn et al. 1996, Anderson & Williams 1998, 1999, Lancelot et al. 2002). Biodegradation experiments produce a simple ecosystem (no autotrophs, no source of DOC, and no grazers) which provide a reasonable data set that is easier to use for modelling bacterial utilisation of DOC. First order kinetic models are often used in describing DOC and particulate organic carbon (POC) degradation (Harvey et al. 1995, Sempéré et al. 2000, Fujii et al. 2002, Panagiotopoulos et al. 2002), but these models only take into account the concentration of organic matter (OM) at any given time. Recent studies have indicated that a better understanding of the dynamics of OM in models requires an appropriate knowledge of the dynamics of the bacterial community (Talin et al. 2003 and references therein). Only a few aquatic biogeochemical studies describe model performance for bacteria, which is a poorly modelled state variable (Arhonditsis & Brett 2004). Some models have been developed to describe the interaction between bacteria and OM, but these include a mathematical formula for more than 1 potentially limiting factor, several bacterial communities and/or the respiration process (Thingstad & Pengerud 1985, Martinussen & Thingstad 1987, Thingstad 1987, Cajal-Medrano & Maske 1999, Touratier et al. 1999, Miki & Yamamura 2005).

Here, we report on the determination of BGE, estimated using 2 different methods: (1) experimental, by calculations obtained from BP and BR measured using biodegradation experiments, and (2) numerical, by estimating the parameter values by finding the minimum distance between the experimental kinetics and the numerical simulations using the Monod (1942) model. The data used to determine both BGE come from the same experiments. However, in these experiments only BP, bacterial abundance and oxygen consumption were measured. Thus, numerous hypotheses have to be made in order to estimate the necessary DOC data set and then estimate the parameters numerically. We are aware that these assumptions increase the errors in data, and thus in parameter estimations, but the current state of microbial knowledge and techniques precludes the achievement of better estimations with these data sets. Consequently, our approach is qualitative by suggesting a new method of BGE estimation and a new way of improving biogeochemical models. We show that BGE values obtained using both approaches are within the same range, varying with depth and season. We also demonstrate how robust the model is with regard to sensitivity to BGE and to parameter estimations using perturbed experimental data. Finally, we discuss the use of this model for describing bacterial and DOC dynamics in biodegradation experiments and thus in biogeochemical models.

II. Materials and methods

1. Experimental design

i. Study area

As part of the "Programme Océan Multidisciplinaire Méso Echelle" (POMME), seawater samples were collected in the Northeast Atlantic Ocean (Figure II-1) over three seasons; winter (POMME 1; P1), spring (POMME 2; P2) and summer (POMME 3; P3) 2001 (for further details on POMME and on sampling techniques, see Mémery et al. 2005). It is beyond the scope of this study to present a detailed protocol and mesoscale variability aspects, and such data are available elsewhere (F. Van Wambeke et al. unpubl. data).

ii. General design

Seawater was collected from 3 depths (5, 200 and 400 m) using Niskin bottles, then transferred immediately into large polycarbonate bottles without tubing. The protocol for seawater collection and for minimising organic carbon contamination is described in Sempéré et al. (2003). Following collection, seawater was filtered, using a low vacuum (<50 mm Hg) through pre-combusted (450°C, 6 hours) GF/F glass fibre filters in order to obtain bacterial seawater cultures. This experimental design removes all DOC sources and all predators, except for some viruses. A mean of 46 % of the *in situ* bacterial cells was passed through the filters (F. Van Wambeke et al. unpubl. data). DOC was not measured. However, we could not exclude the possibility that the filtration process might induce some increase in DOC concentration and slightly modify the bacterial activity, particularly in the deep samples, as in some cases specific activity of bacteria after filtration increased compared to that *in situ* (F. Van Wambeke et al. unpubl. data). The bulk incubation culture was then sub-sampled by dispension into duplicate pre-combusted borosilicate bottles to determine BP and bacterial abundance, and also into quadruplicate 125 ml Winkler bottles for dissolved oxygen determination. The latter samples were fixed with Winkler reagents, and measurements were made using an automated Winkler titration system based on that described by Williams & Jenkinson (1982). Experimental bottles were incubated in the dark in a temperature controlled room (± 1°C) over the course of the experiments. Samples were sacrificed and analysed for BP and dissolved oxygen using a time series of 0, 0.5, 1, 2, 5, 10 d. Consequently, we must hypothesise that dynamics are identical in all bottles.

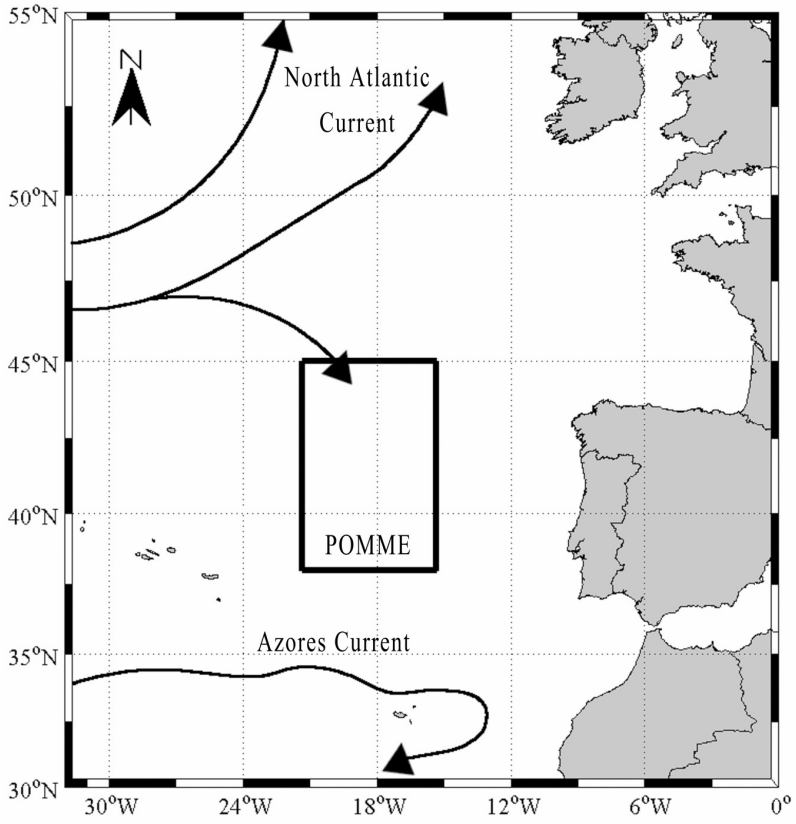

Figure II-1. POMME zone in the Northeast Atlantic Ocean studied during Leg 2 of POMME 1 (P1: 1-15 March 2001), POMME 2 (P2: 18 April – 2 May 2001) and POMME 3 (P3: 19 September – 3 October 2001) for BGE determination. Arrows represent principal currents: North Atlantic Current and Azores Current. See Mémery et al. (2005), Maixandeau et al. (2005) and Karayanni et al. (2005) for details on hydrological situations occurring at each site. Adapted from Guidi et al. (2007).

BP was calculated using the tritiated leucine method (Kirchman 1993). The experimental estimation for BGE (BGE_E) was calculated by integrating data from time zero (t_0) to the BP peak, which refers to the maximum BP value in the time series, as follows:

$$BGE_E = \frac{IBP}{IBP + \frac{\Delta O_2}{\Delta t}\, t\, RQ} \qquad \text{(II.1)}$$

where IBP (µM C) was time-integrated BP from t_0 to the BP peak with trapezoidal integration of discrete data. The conversion factor of leucine-carbon was 1.5 kg C mol^{-1} of leucine incorporated assuming an isotopic dilution of 1. The oxygen consumption rate $\Delta O_2/\Delta t$ (µM d^{-1}) was calculated assuming a linear regression model for the decrease in dissolved oxygen concentration with time (t). The respiratory quotient (RQ) was 0.8 (F. Van Wambeke et al. unpubl. data).

iii. DOC and bacterial biomass estimations

Initial bacterial biomass (BB) was determined by epifluorescence microscopy after DAPI staining, assuming a carbon conversion factor (CCF) of 20 fg C $bacterium^{-1}$ (Lee & Fuhrman 1987). In order to estimate BB increase, the IBP (derived from the leucine method, see equation II.1) was added to this initial value of BB for computing the BB for all other time points. Numerous hypotheses were made to assess DOC dynamics. Total organic carbon (TOC) was measured using high temperature catalytic oxidation (Sohrin & Sempéré 2005) on the *in situ* vertical profiles, but not for the biodegradation experiments. Initial values of DOC were thus estimated as the difference between *in situ* TOC and POC, which was deduced from total particulate carbon (TPC) measurements obtained using an optical particle counter (HIAC) (Merien 2003). As the proportion of DOC to TOC fraction increases globally from 83 % at 5 m to 92 % at 200 m, we estimated that at 400 m DOC is close to TOC. We then assumed that initial DOC concentration in the batches was close to *in situ* DOC concentration. Finally, we estimated DOC concentrations over the course of the experiments on the assumption that the quantity of DOC consumed over a short period, which we assumed to be only L-DOC according to duration of experiments, is equal to the sum of BB increase and CO_2 produced over the same period, estimated as:

$$\Delta CO_2 / \Delta t = - RQ \times \Delta O_2 / \Delta t \qquad \text{(II.2)}$$

2. Monod (1942) model

The biodegradation model was set up on the basis of the following assumptions. (1) There is no source of DOC in the cultures. (2) Bacteria are the only organisms present (no flagellates and no virus) (these first 2 assumptions are likely to be valid, since only the growth phase, and thus a short period of time, is considered). (3) L-DOC was the limiting factor on bacterial growth, which is a reasonable assumption since nutrient concentrations measured in water column profiles during the cruises were sufficient to sustain bacterial growth in the experiments considered (NO_3 concentrations ranged from 1.9 to 13.1 µM, except one value of 0.39 µM in spring, and PO_4 concentrations from 0.1 to 1.04 µM), except perhaps in surface water in late summer where values were lower (from undetectable to 0.04 µM for NO_3 and from 0.01 to 0.02 µM for PO_4) (F. Van Wambeke et al. unpubl. data). (4) We assumed that only the L-DOC fraction is consumed by bacteria during the 10 d biodegradation experiments as well as in the model.

The Monod (1942) formula, which uses Michaelis-Menten kinetics, is one of the simplest and most widely used models for describing the interactions between 2 state variables, in this case bacterial C-biomass and DOC. Note that in this model the disappearing DOC is instantaneously taken up by bacteria and converted into C-biomass with a constant efficiency (numerical bacterial growth efficiency, BGE_N). Consequently, BGE_N is estimated using the model calibration and depends on the external limiting food concentration.

$$\frac{dDOC}{dt} = -\frac{V_{\max}\, DOC \text{ x } BB}{k+DOC} \qquad \text{(II.3)}$$

$$\frac{dBB}{dt} = BGE_N \frac{V_{\max}\, DOC \text{ x } BB}{k+DOC} \qquad \text{(II.4)}$$

where BB is in µM C; DOC is concentration in µM C, with the assumption that L-DOC is the limiting food resource and the only fraction of DOC consumed; V_{max} is the specific maximum assimilation rate in d^{-1}; and k is the half-saturation constant for DOC in µM C.

The parameters (BGE_N, V_{max} and k) were estimated, for each experiment, from all available DOC derived values and BB data. The parameter values were thus estimated using a non-linear regression that uses the least-squares

method. The calibration is performed for each experiment in order to compare the parameters obtained from the model for different depths and seasons. Nevertheless, it should be pointed out that DOC estimations are representative of the total pool of DOC (L-DOC, semi-labile-DOC plus refractory-DOC), whereas the model only simulates the decrease of L-DOC, which constitutes the first and only fraction of DOC used by bacteria during the 10 d biodegradation experiments. This does not affect the parameter estimations, as semi-labile-DOC and refractory-DOC are supposed to be constant and unaffected during these biodegradation experiments. Thus, model parameters are representative of bacterial growth in batch cultures.

A sensitivity analysis was carried out to determine (1) which parameter has the most influence on the dynamics, and (2) the validity of parameter estimations according to experimental errors. First, the derivatives of the model were calculated with respect to the parameters, the highest derivative being the most influential parameter. This enables a quantitative comparison of parameter sensitivity. We then analysed the robustness of the parameter estimations with respect to the data. The measurement errors, the variability of environmental forcing parameters on the measurements and the assumptions made to assess DOC data may indeed indicate some variabilities in the observations used to calibrate the model. We have estimated that the sum of these variabilities was ≤ 30 %. For 1 experiment, 500 extra sets of data were obtained by replacing each original data point in the course of the experiments by its value multiplied by $1 \pm p$, where $p \leq 0.3$ and is a random proportion that is uniformly distributed. Thus, 'perturbed' data represent the value that a data point could have if we consider the accuracy of the original data to be within the range of 70 to 100 %. We then estimated parameters of the model for these 500 data sets using the same method as those for data sets without perturbation. This procedure provides information on the parameter distribution and on the robustness of the BGE_N estimations.

3. Comparison of methods for BGE estimation

The present study calculated BGE in 2 ways: as BGE_E and BGE_N. Both estimations implied assumptions about RQ and leucine-carbon conversion factors, which are supposed to be constant and equal in the 2 BGE estimations. The values of the BGE_E may change with respect to BGE_N according to the method used to calculate the O_2 utilisation rate, the assumptions made to assess DOC data (as the CCF) and the integration time considered. BGE_E values are estimated using integrated data from t_0 to the BP peak and assuming a linear regression model for the decrease in dissolved oxygen concentration, whereas values for BGE_N are estimated using the

least-squares method between the outputs of the 2 state variables of the model and the whole data set for each experiment. In order to compare the 2 methods, we calculated the relative quadratic distance (*d*) between BGE_E and BGE_N for each biodegradation experiment by taking BGE_E as reference:

$$d = \frac{|BGE_E - BGE_N|}{BGE_E} \qquad \text{(II.5)}$$

If *d* is low ($d \ll 1$), the 2 methods of BGE estimation are thus considered to be equivalent.

III. Results

1. Model calibration and simulation

We performed a calibration of the model with the data for each experiment. The minimum distance between the model outputs and experimental data are obtained from high values of V_{max} and k in all experiments. Consequently, DOC can be neglected in comparison to k, that is $k + DOC \approx k$. Then, equations (II.3) and (II.4) can be approximated by the following system (equations II.6 and II.7):

$$\frac{dDOC}{dt} = -\alpha\, DOC \text{ x } BB \qquad \text{(II.6)}$$

$$\frac{dBB}{dt} = BGE_N\, \alpha\, DOC \text{ x } BB \qquad \text{(II.7)}$$

where $\alpha = V_{max}/k$ in $\mu M\ C^{-1}\ d^{-1}$ (II.8)

This simplified model can be solved analytically. Equations A.II.3 and A.II.4 in Appendix II-A allow the removal of the integration step for the calibration and simulation. The use of these equations enables analysis to be performed faster and provides a more precise calibration.

For most of the experiments (26 out of 36) the model (equations II.6 and II.7) produces an accurate fit both qualitatively and quantitatively with parameters α and BGE_N (see Figure II-2). However, there is no agreement between the model outputs and data in the case of the other 10 experiments (see Figure II-3). Thus, these results have not been taken into account in the

analysis of the parameter variation according to depth and season. These inaccuracies are related to (1) missing BP or O_2 data due to problems with analysis precision (BP was at the detection limit, or quadruplicate Winkler bottles were highly variable), which made correct estimation of BB or DOC concentration difficult in Expts L, Q, O and FF ('nd' in Table II-1); (2) the shape of the model, which is poorly suited to the shape of data in Expts C, J, II and U (e.g. in Expts C, BB data exhibit an exponential shape whereas the DOC data are linear); and (3) a stationary phase in bacterial data that was observed in Expts T and KK, whereas large amounts of DOC were still available (Figure II-3).

2. Sensitivity and robustness analyses

The derivatives of equations (II.6) and (II.7) with respect to parameters were used in order to study the sensitivity of the model (Figure II-4, Appendix II-B). Equations (A.II.5) to (A.II.8) represent the sensitivity of equations (II.6) and (II.7) with respect to parameters α and BGE_N. In all cases, the sensitivity is equal to the product of $a \times DOC \times BB$, where a = BGE_N, 1, α and 0 respectively, for equations (A.II.5) to (A.II.8). However, in all experiments we observed that $0 < \alpha < BGE_n < 1$ (see Appendix II-B for more details). There is indeed a great difference in the order of magnitude of sensitivity to α as a function of DOC concentration and BB (Figure II-4 b), which is between 20 and 100 times greater than the sensitivity to BGE_N (Figure II-4 a). If we only consider the sensitivity to α, as 1 > BGE_N, for the given values of DOC and BB, then equation (II.6) is more sensitive to a variation of α than equation (II.7) (Figure II-4 b). Only equation (II.7) is sensitive to a variation in BGE_N (Figure II-4 a).

We also analysed the robustness of the estimated parameters α and BGE_N with respect to the estimated data set. For each experimental data set, we simulated 500 extra sets of data with randomly perturbed data up to 30 %, and we estimated model parameters for each of the extra sets. We termed the BGE_N and α estimated with the perturbed data 'BGE_p' and α_p, respectively. Then, for each experiment, we analysed the distribution of the 500 BGE_p estimated with their corresponding extra sets of data, with respect to the BGE_N estimated for the corresponding experiment without perturbation. The same analysis was performed for the parameter α. These simulations, which were performed for all experiments, provide a basis for studying how robust the model is according to the distribution of the parameters (see Figure II-5).

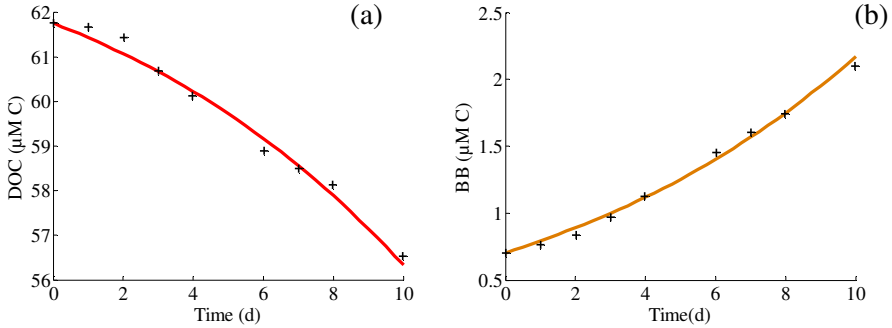

Figure II-2. Dynamics of (a) DOC and (b) BB for the biodegradation experiment carried out during spring at 5 m (Expt M, Table II-1). **+**: data for BB and DOC recalculated from O_2 and BP data during the biodegradation experiment. Lines: results of simulations of the Monod (1942) model with parameters estimated by non-linear regression, where α = 0.007 μMC^{-1} d^{-1} and BGE_N = 0.27.

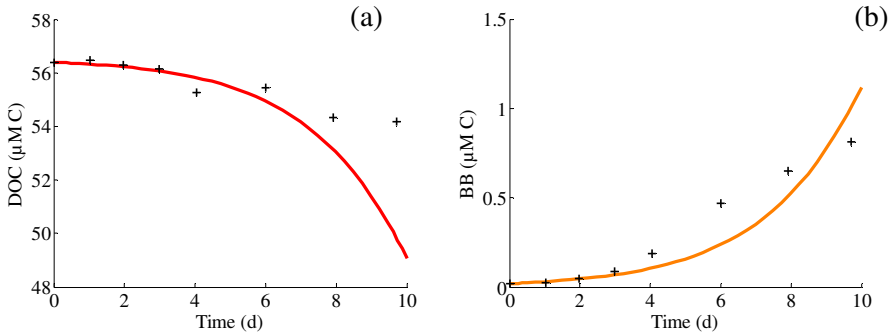

Figure II-3. Dynamics of (a) DOC and (b) BB for the biodegradation experiment carried out during spring at 200m (Expt T, Table II-1). **+**: data for BB and DOC recalculated from O_2 and BP data during biodegradation experiment. Lines: results of simulations of the Monod (1942) model with parameters estimated by non-linear regression, where α = 0.049 μMC^{-1} d^{-1} and BGE_N = 0.15.

In all experiments, the distribution of parameters following perturbation follows a unimodal low, and parameters estimated without perturbation are within or close to the modal class. In each experiment, 90 to 100 % of the 500 perturbation simulations give rise to a $BGE_p < 0.4$, indicating a weak distribution of BGE_p. Moreover, > 50 % of the perturbation experiments give rise to: $BGE_N - 0.1 < BGE_p < BGE_N + 0.1$. A small percentage of the results gives a BGE_p close to 1 (not shown). This result could be related to the scattering of DOC data caused by the perturbation; indeed, this scattering does not give a satisfactory model fit and the calibration method produces a curve with a very small α_p. This indicates that the BB data, where the level of scattering is lower and thus well fitted, needs to be fitted using a very high value of BGE_p in order to balance the weak α_p. The values of α without perturbation are in the middle of the distribution and the highest α_p is double that of α without perturbation.

3. Parameters

For each experiment, values of α and BGE_N obtained by the parameterisation of the model are presented in relation to the BGE_E calculated experimentally from O_2 and BP data (Tables II 1-2). For some experiments, there were no results because of experimental problems (nd in Table II-1). BGE_E ranged from 0.01 to 0.48, whereas α and BGE_N ranged from 0.006 to 0.097 $\mu M\ C^{-1}\ d^{-1}$ and from 0.04 to 0.41, respectively. BGE values were also averaged at each depth for a given season, at each season for a given depth and at each depth for the whole year (Table II-2). By calculating these means, the results where simulations were not possible or seemed inaccurate were excluded (see 'Results; Model calibration and simulation'). As the number of results for a given depth and season were small (n = 4 in general) and some were not taken into account in means, the standard deviations increase rapidly when we remove 1 or 2 results (n = 3 and 2, respectively, Table II-2).

The relative quadratic distances d between BGE_E and BGE_N range from 0.07 to 12.00 (Figure II-6). All distances, except 6 out of 26, have $d < 0.5$ and all except 3 have $d < 1$, which suggests that the 2 methods of BGE estimation are quantitatively equivalent.

The results indicate that mean BGE_N decreases from the surface (5 m) to deeper waters (200 and 400 m) in spring and summer, whereas there is no significant relationship with depth in winter (Table II-2). If we consider the annual means, we observe a decrease in BGE_N with depth. However, the mean BGE_N varies according to season in the surface layer with a minimum

mean in winter (P1). There were no significant differences in seasonal averages in spring and summer, owing to great variability within sites. In contrast, averaged α increased from the surface to deeper water whatever the season; however, there was no significant difference between 200 and 400 m as a results of high standard deviations of data among the stations studied. In contrast to the BGE_N, α did not show any seasonal trend. Although BGE_E values are more abundant, the trends are the same as for BGE_N, i.e. minimum values observed in winter and at greater depths (Table II-2). Finally, we have demonstrated that both BGE_E and BGE_N (experimental and numerical) presented the same variations according to depth, that they were minimum in winter and equivalent from a quantitative point of view.

Table II-1. Comparison of experimental bacterial growth efficiency (BGE_E) and model parameters including numerical BGE (BGE_N) and α, estimated numerically with a non-linear regression, for the 3 depths and 3 seasons studied in Northeast Atlantic Ocean during POMME (P1-3) cruises. Period of sampling for BGE determination: P1: 1-15 March 2001; P2: 18 April-2 May 2001; P3: 19 September-3 October 2001. Values in bold correspond to results that were not taken into account in further analyses because simulations did not match data (see 'Results: Model calibration and simulation'). nd: not determined

Expt	Winter (P1)			Expt	Spring (P2)			Expt	Summer (P3)		
	BGE_E	BGE_N	α		BGE_E	BGE_N	α		BGE_E	BGE_N	α
5 m											
A	0.04	0.07	0.013	M	0.21	0.27	0.007	AA	0.28	0.24	0.011
F	0.13	0.14	0.014	P	0.30	0.41	0.006	DD	0.30	0.28	0.013
I	0.18	0.17	0.016	S	0.36	0.40	0.006	GG	0.48	0.35	0.012
L	nd	nd	nd	V	0.26	0.19	0.011	JJ	0.35	0.29	0.016
200 m											
B	0.04	0.13	0.011	N	0.15	0.27	0.016	BB	0.09	0.11	0.043
D	0.15	0.25	0.007	T	0.16	**0.15**	**0.049**	EE	0.15	0.19	0.016
G	0.05	0.07	0.052	Q	0.20	nd	nd	HH	0.12	0.14	0.024
J	0.05	**0.10**	**0.016**	W	0.07	0.04	0.078	KK	0.18	**0.13**	**0.038**
400 m											
C	0.01	**0.05**	**0.024**	O	0.04	nd	nd	CC	0.08	0.09	0.045
E	0.06	0.09	0.040	R	0.02	0.26	0.017	FF	0.24	nd	nd
H	0.05	0.06	0.049	U	0.03	**0.10**	**0.119**	II	0.33	**0.21**	**0.027**
K	0.05	0.11	0.026	X	0.07	0.06	0.097	LL	0.13	0.14	0.035

Table II-2. Model mean parameters α and BGE_N, and mean BGE_E estimated for different depths at different seasons and for the whole 2001 year (mean ± SD). See Table II-1 for POMME (P1-3) cruise dates. n_N = number of values used to calculate means for numerical parameters α and BGE_N. n_E = number of values used to calculate mean BGE_E. For each individual cruise n_E = 4, except for the mean calculated for P1 at 5 m n_E =3.

Depth (m)	Winter (P1)				Spring (P2)				Summer (P3)				Annual mean				
	α	BGE_N	n_N	BGE_E	α	BGE_N	n_N	BGE_E	α	BGE_N	n_N	BGE_E	α	BGE_N	n_N	BGE_E	n_E
5	0.014 ± 0.002	0.12 ± 0.05	3	0.12 ± 0.07	0.007 ± 0.002	0.32 ± 0.10	4	0.28 ± 0.06	0.013 ± 0.002	0.29 ± 0.05	4	0.35 ± 0.09	0.011 ± 0.004	0.25 ± 0.11	11	0.25 ± 0.12	11
200	0.024 ± 0.025	0.15 ± 0.09	3	0.07 ± 0.05	0.047 ± 0.044	0.15 ± 0.16	2	0.13 ± 0.04	0.028 ± 0.014	0.15 ± 0.04	3	0.13 ± 0.04	0.031 ± 0.025	0.15 ± 0.08	8	0.11 ± 0.05	12
400	0.038 ± 0.012	0.09 ± 0.03	3	0.04 ± 0.02	0.057 ± 0.056	0.16 ± 0.14	2	0.04 ± 0.02	0.040 ± 0.070	0.11 ± 0.04	2	0.18 ± 0.13	0.044 ± 0.026	0.11 ± 0.07	7	0.09 ± 0.10	12

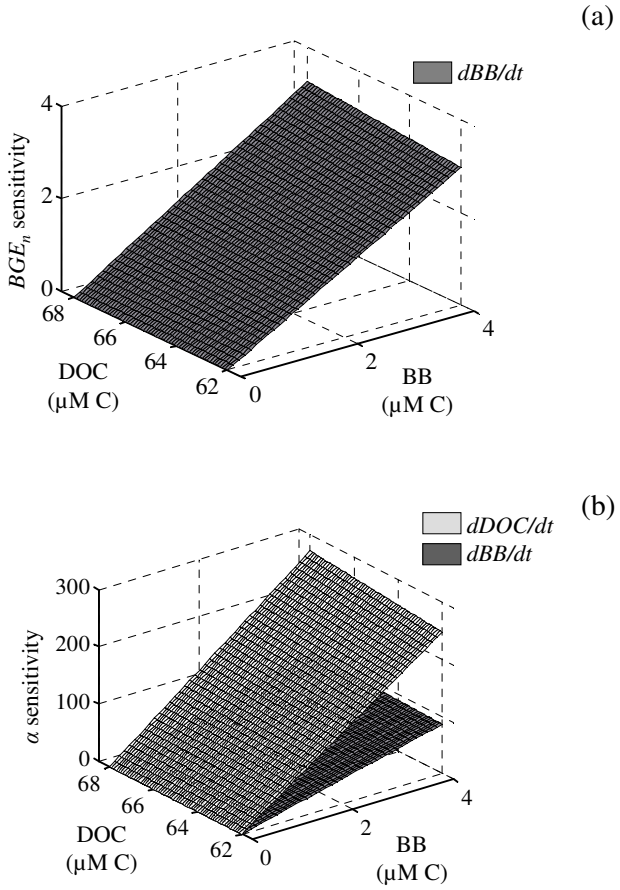

Figure II-4. Representation of the sensitivity of parameters BGE_N and α as a function of variables BB and DOC in biodegradation experiment carried out during summer at 5 m (Expt GG, Table II-1). Sensitivity represented by a surface that corresponds to all possible combinations of the product $a \times DOC \times B$, where a = BGE_N, 1, α or 0, according to the corresponding sensitivity (equations A.II.5 to A.II.8, respectively) (Appendix II-B). DOC and BB can take all possible values in their own range of variation during the experiment (α = 0.012 µM C^{-1} d^{-1} for equation A.II.7 and BGE_N = 0.35 for equation A.II.5) (a): sensitivity of $dBB \times dt^{-1}$ according to BGE_N, which corresponds to equation (A.II.7) (sensitivity of $dDOC \times dt^{-1} = 0$). (b): sensitivity of both parts of model in relation to α (µM C^{-1} d^{-1}), which correspond to equation (A.II.5) and (A.II.6).

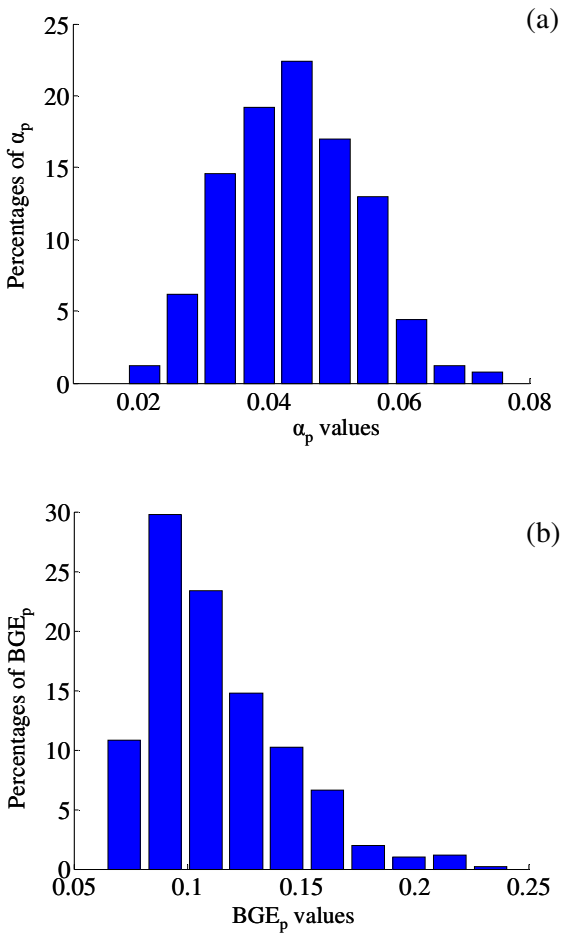

Figure II-5. Distribution of the parameters (a) α_p (µM C^{-1} d^{-1}) and (b) BGE_p after 500 perturbations. Extra sets of data were obtained by replacing each initial data point by its value multiplied by $1 \pm p$, where $p \leq 0.3$ and is a random proportion uniformly distributed, for a biodegradation experiment carried out at 200 m during summer (Expt BB, Table II-1). Results are presented as the percentage of each value of (a) α_p and (b) BGE_p compared to all values obtained after perturbation. The value of α and BGE_N for the data without perturbations are 0.043 µM C^{-1} d^{-1} and 0.11, respectively.

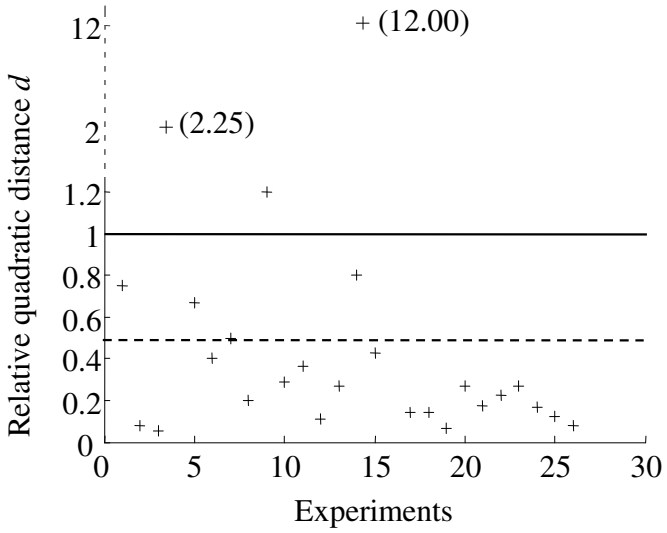

Figure II-6. Distribution of the relative quadratic distance (d) (equation II.5) between BGE_N and BGE_E. If $d > 1$ (dark solid line), the 2 methods of estimation give results that are distant; if $d < 0.5$ (grey dashed line), the 2 methods are considered equivalent; 2 distances are out of the scale and values are indicated in brackets (2.25 and 12.00).

IV. Discussion

1. Analysis of model results

The model fits the data in almost all simulations. However, in some cases, we observed that the model did not match the experimental data. For example, the experimental dynamics of BB seemed to reach a stationary phase even though there was still a significant concentration of DOC (remaining 47 and 54 µM C for Expts KK and T, respectively) (Table II-1, Figure II-3). The stationary phases observed in these experiments are likely to be due to a complete exhaustion of L-DOC, because the remaining DOC in the batch is close to that found in deep waters (40 – 50 µM C) (Sohrin & Sempéré 2005) and *in situ* nutrient concentrations were sufficient to avoid limitation (see 'Materials and Methods; Monod (1942) model'). This remaining DOC is represented by semi-labile and refractory-DOC poorly assimilated by bacteria and not represented in the model, and thus the bacterial stationary phase cannot be simulated.

Except for these biodegradation experiments, the sensitivity analysis has demonstrated that the Monod (1942) model is more sensitive to a variation of $V_{\max}/k$ ratio than to BGE_N, indicating that the best estimations of both parameters require high precision in α values. Our results also demonstrate that a perturbation comprised up to 30 % of total variation in data affects the parameter estimations within a reasonable range: parameters estimated without perturbation are always within or close to the modal class; the distributions of parameters with perturbed experimental data are not very large around the parameters estimated without perturbation; and >50 % of the perturbation simulations give rise to: $BGE_N - 0.1 < BGE_p < BGE_N + 0.1$. As such perturbations only influence the estimation of both parameters to a low order of magnitude, we can be sure that the parameters estimated without perturbation are reliable. However, for some of these perturbations we obtained BGE_p values close to 1. For these perturbations, the model does not match in the case of very small L-DOC variations (e.g. owing to a low signal-to-noise ratio of variations of O_2 data). As the relative quadratic distances *d* for most experiments are ≤ 0.5, our estimations of BGE_N are close to the classical estimations of equation (II.1) (BGE_E). Moreover, we have demonstrated that the tendencies are the same when considering the 2 BGE (BGE_E and BGE_N). Consequently, the overall analysis of the model (qualitative and quantitative comparisons with experimental parameters, sensitivity and robustness analyses) shows that our numerical method of BGE estimation is well suited.

2. Biological analysis

The parameter values, revealed by the calibration of the model, have shown a range of BGE_N values below 0.5 (0.04 to 0.41, Table II-1) which is commonly observed in diverse aquatic habitats (del Giorgio & Cole 1998). The annual mean and standard deviations of BGE_N at 5 m (0.25 ± 0.11) are consistent with published data for the Gulf of Mexico (Pomeroy et al. 1995, Jorgensen et al. 1999), Sargasso Sea (Carlson & Ducklow 1996) and the Atlantic Jet in the Mediterranean Sea (Sempéré et al. 2003). BGE_N at 5 m was greater than at 200 and 400 m, and minimum values were observed in the winter as was also the case in the surface layer of the North Sea (Reinthaler & Herndl 2005). In contrast, minimum values of α were reached at 5 m and no trend emerged with season. The fraction of refractory-DOC increases with depth (Carlson 2002). Bacteria probably consume, in addition to L-DOC, some semi-labile and refractory organic compounds. Therefore, the fraction of assimilated L-DOC probably decreases with depth, and it is conceivable that BGE decreases with depth. As α is the ratio between V_{max} and k, the increase in α reflects an increase in bacterial affinity for substrate with increasing depth (decrease of k) and/or better specific maximum assimilation rates (increase of V_{max}). These results suggest that the more refractory bulk DOC (representative of those observed below the productive layer, i.e. 200 m) (Sohrin & Sempéré 2005), as well as probable patchy distribution of L-DOC in deep waters, would explain lower BGE, higher affinity to the substrate and/or higher specific maximum assimilation rates.

3. Experimental problems

The data needed for the calibration were not directly measured. Patterns of change over time of DOC estimations are based on BP and BR, which were themselves estimated from indirect measurements (leucine incorporation and O_2 variations). Hence, conversion factors (leucine to carbon, RQ) must be applied. The latter is not constant as bacteria can change their RQ (Kooijman 2000) according to changes in the quality and quantity of the substrate over the course of the experiments. However, the changes over time of these conversion factors has no influence on the comparison of BGE, as the same values were used in both cases (BGE_E and BGE_N) and the influence of these factors is discussed elsewhere (F. Van Wambeke et al. unpubl. data). Moreover, these changes of conversion factors over time have to be proven experimentally in order to be taken into account. It further results that the estimations of DOC concentrations may not be accurate and

representative of the real variation in DOC in the experiments. Direct measurements of DOC would be more appropriate, but there is, for instance, no protocol which is sufficiently sensitive for oligotrophic waters. Nevertheless, even if data vary by up to 30 % of the values without perturbation, the method of parameterisation is well suited. Consequently, estimated parameters are reliable. We have also assumed that the DOC concentration at a given time equals the initial DOC, minus the sum of CO_2 respired and BB produced. However, this hypothesis would be accurate only if the system behaves as a Monod (1942) model, i.e. if growth and respiration depend directly on the external concentration of the substrate. The presence of an internal carbon reservoir in bacteria (Ducklow & Carlson 1992, Cherrier et al. 1996) may indeed induce a time lag between assimilation and growth and/or respiration, which has not been taken into account in estimations of the data sets needed for the calibration of the model.

Another bias is the difficulty in placing these results within a natural context. For example, the presence of viruses, which may induce a decrease in BGE and an increase in the growth rate of uninfected cells, cannot be ruled out (Middelboe et al. 1996). These are not represented in the model whereas they may in fact reduce bacterial abundance. Although great care was taken during filtration (Yoro et al. 1999), this process is likely to induce an increase in DOC due to particle breakdown (Carlson et al. 1999, Ducklow et al. 1999). However, increases in specific leucine incorporation rates at t_0 from biodegradation experiments compared to their respective values *in situ* values occurred in less than half of the experiments (F. Van Wambeke et al. unpubl. data). The 10 d incubation experiments could also enable bacteria to use more refractory organic matter, thus lowering natural BGE (del Giorgio & Cole 1998, Carlson et al. 1999). Although these analytical biases are difficult to quantify, they should be kept in mind for comparisons and further interpretation.

4. Improvement of biogeochemical models

We have demonstrated using the Monod (1942) model that (1) parameters BGE_N and α are dependent on depth, and (2) BGE_N varies according to season, especially in the surface layer, in the Northeast Atlantic Ocean. Consequently, the use of a constant BGE_N and α in 1-dimensional biogeochemical models (Anderson & Williams 1999, Lancelot et al. 2002) may not be appropriate. It is necessary to find a better method to simulate the uptake of organic matter by bacteria, for example by expressing BGE_N and α as a function of depth, since the availability of L-DOC varies with depth. The seasonal changes in BGE_N should also be described, for example with

temperature. Other environmental factors such as the composition in organic nutrients, phages and physiological conditions may affect the BGE (Cajal-Medrano & Maske 2005). Moreover, BGE values could influence the existence and competition of bacterial communities living on distinct substrates (Miki & Yamamura 2005).

The time lag between assimilation of the substrate, respiration and growth may require mathematical descriptions for each of these kinetics. Some models that use variable BGE_N, such as the Droop (1968) model, take into account internal variable carbon storage (Grover 1991). In the case of DOC uptake by bacteria, this model allows bacteria to absorb the substrate in part of the cell, referred to here as the quota. Then, carbon stored in the quota will be allocated for different bacterial processes including maintenance and growth. In contrast to the Monod (1942) model, the Droop (1968) model also allows bacteria to survive during a starvation period, and requires differentiation of assimilation and growth processes. These assumptions give a better understanding of the interaction between DOC and bacteria in biogeochemical models (Vichi et al. 2003) and allow a variable BGE to be considered as $BGE = dBB/dDOC$.

Previous studies indicate that bacteria supplied with phosphorus are able to store organic carbon, without dividing, thereby maintaining a higher BGE (Zweifel et al. 1993). The assumption of carbon storage has also been proposed with observation of a non-coupling between (1) the use of DOC and (2) BP and BR (Ducklow & Carlson 1992, Cherrier et al. 1996). It is also important to take into consideration the metabolic energy used for maintenance processes, i.e. processes that do not produce new biomass but maintain cell integrity, in bacterial modelling (Cajal-Medrano & Maske 1999, 2005). Some authors indicate that the addition of reserves and the maintenance in a Monod (1942) model is necessary in order to obtain the bacterial dynamics in chemostats (Kooi & Kooijman 1994, Kooijman 2000). We have to test such models using data from biodegradation experiments and study the effects on biogeochemical models. In the first case, the substrate is constant in the cultures but there are changes in the populations, which proliferate or dominate in cultures; in contrast, in the second case, there are changes in the availability of the substrate over the course of the experiment. Consequently, the description of the interactions between bacteria and DOC in biogeochemical models should be reviewed in order to include some fundamental mechanisms such as the use of reserves and the maintenance processes.

V. Conclusion

We have shown that Monod-type modelling constitutes a fast and cheap method to estimate BGE from bacterial biodegradation experiments (DOC and BB data). This model is not very sensitive to variation in parameters and is robust with regard to experimental errors. However, in order to obtain BGE estimations close to the natural BGE, accurate measured experimental data are required. Moreover, more experiments are needed to observe the decrease in BGE and increase in α with depth with the dynamics of both state variables recorded over different seasons: rigid sampling with regard to depth and time with replicates is essential. An experimental process using the most precise measurements available is crucial for the calibration and validation of any model. Moreover, DOC data is necessary to validate our approach and thus our results. The introduction of BGE as a function of depth and temperature in the model of Anderson & Williams (1999) could prove to be the way forward. Nevertheless, the Monod (1942) model was designed for a system in steady-state in the natural environment; however, there are always perturbations and the steady-state condition is rare. Consequently, models using time variable assimilation rate and BGE such as Droop (1968) and Dynamic Energy Budget models (Kooijman 2000) should be investigated more thoroughly in order to reproduce the observations more accurately.

APPENDIX II-A

Search for the analytical solutions of the model

The mass conservation law of the model (equations II.6 and II.7) gives the following equation:

$$BGE_N \frac{dDOC}{dt} + \frac{dBB}{dt} = 0 \qquad \text{(A.II.1)}$$

Consequently, $\left(BGE_N \text{ x } DOC + BB\right)$ is a constant. If K1 is this constant, then $DOC = \left(K1 - BB\right)/BGE_N$. The model and the conservation law produce the following equation for BB:

$$\frac{dBB}{dt} = \alpha\left(K1 - BB\right)BB = \alpha\, K1\, BB\left(1 - \frac{BB}{K1}\right) \qquad \text{(A.II.2)}$$

Equation (A.II.2) is a logistic equation with an analytic solution as follows:

$$BB(t) = \frac{BB_0\ K1}{BB_0 + \left(K1 - BB_0\right)e^{-\alpha\, K1\, t}} \qquad \text{(A.II.3)}$$

where BB_0 is initial bacterial biomass (µM C), t is time (d), α K1 is intrinsic growth rate (d^{-1}) and K1 is carrying capacity (µM C)
The same reasoning can be applied to the second variable of the model:

$$DOC(t) = \frac{DOC_0\ K2}{DOC_0 + \left(K2 - DOC_0\right)e^{\alpha\, K1\, t}} \qquad \text{(A.II.4)}$$

where DOC_0 is initial DOC concentration (µM C), and $K2 = K1/BGE_N$ (µM C).

APPENDIX II-B

Equations governing the sensitivity analysis

$$\left|\frac{\partial\left(\frac{dBB}{dt}\right)}{\partial\alpha}\right| = BGE_N \times DOC \times BB \quad \text{(A.II.5)} \qquad \left|\frac{\partial\left(\frac{dDOC}{dt}\right)}{\partial\alpha}\right| = DOC \times BB \quad \text{(A.II.6)}$$

$$\left|\frac{\partial\left(\frac{dBB}{dt}\right)}{\partial BGE_N}\right| = \alpha \times DOC \times BB \quad \text{(A.II.7)} \qquad \left|\frac{\partial\left(\frac{dDOC}{dt}\right)}{\partial BGE_N}\right| = 0 \quad \text{(A.II.8)}$$

In all experiments, $0 < \alpha < BGE_N < 1$ (Tables II-1 and II-2). It follows that the values of equations (A.II5) and (A.II.6) are larger than those of equations (A.II.7) and (A.II.8). We thus conclude that the model is more sensitive to $\alpha = V_{max}/k$ than to BGE_N.

CHAPTER III

Biodegradation experiments in variable environments: substrate pulses and impact on growth efficiencies


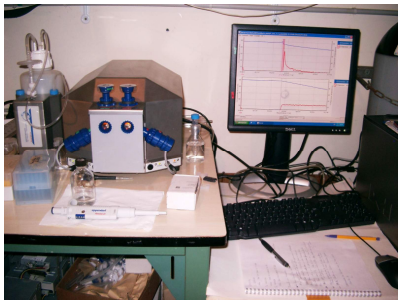


Eichinger M, Sempéré R, Poggiale JC, Grégori G, Charrière B and Lefèvre D (In prep)

Abstract

Biodegradation experiments are often carried out in batch cultures to determine bacterial properties such as the bacterial growth efficiency (BGE). We conducted biodegradation experiments with a unique bacterial strain and a unique carbon limiting substrate in order to study bacterial activities in two kinds of experimental environments. The only difference between these two experiments was the substrate regime. In the first experiment, the substrate was periodically pulsed in the culture. The same concentration was added at each pulse. In the second experiment all the substrate was added in the beginning of the experiment, the total amount of substrate introduced being the same in both experiments. These experiments first allowed pointing out key processes of bacterial growth and degradation activities. We demonstrated that the various bacterial measurements co-vary in both experiments. However, the specific carbon content varied during the experiments. We also observed a production of refractory material during the time course of the experiments. The respiration measurement allowed identifying maintenance process as well as the instantaneous response to the pulse addition. Then, three models were calibrated on the data sets. Two models, the Monod and the Marr-Pirt models, are empiric. The third model originated from the Dynamic Energy Budget (DEB) theory and was especially constructed for the pulse experiment due to the presence of starvation periods. Each of these models allowed the estimation of the BGE. The BGE was also calculated experimentally directly from the data sets. It results that the BGE, what else the method used, was always higher for the pulse than for the batch experiment. It seems that bacteria adapt their metabolism to respond to environmental perturbations, for example by adapting their assimilation or growth efficiencies.

I. Introduction

Dissolved organic carbon (DOC) represents one of the largest active organic carbon reservoirs in the biosphere (Hedges 1992, Amon & Benner 1996). It is widely accepted that DOC represents a dynamic component in the interaction between geosphere, hydrosphere and biosphere and as such has the potential to influence the global carbon cycle and climate change (Farrington 1992). Numerous processes are responsible of DOC production such as release by phytoplankton, egestion, excretion and sloppy feeding from grazers and cellular lysis generated by viruses (Nagata 2000). On the other hand, heterotrophic bacteria are considered as the major consumers and remineralisers of DOC in the ocean (Pomeroy 1974, Williams 2000). According to bacterial reactivity, DOC is usually fractionated into three pools: the refractory DOC (R-DOC) which turns over on the time scale of millennia and that accumulates in ocean, semi-labile DOC (SL-DOC) which turns over on the scale of months to years and labile DOC (L-DOC) which turns over on the scale of hours to days (Williams & Druffel 1987, Carlson & Ducklow 1995, Hansell et al. 1995, Carlson & Ducklow 1996, Nagata 2000, Carlson 2002). The SL-DOC and R-DOC concentrations are usually determined by examining DOC profiles throughout the water column, assuming that in deep-water (> 1000 m) only R-DOC occurs and that the water column has the same R-DOC concentration (Carlson & Ducklow 1995, Wheeler et al. 1996, Wiebinga & de Baar 1998, Sohrin & Sempéré 2005). The L-DOC component can be studied by measuring the bacterial DOC consumption in biological assays (Carlson & Ducklow 1996, Cherrier et al. 1996, Sempéré et al. 1998, Carlson et al. 1999). The fraction of DOC that is transferred to higher trophic levels by bacteria is estimated by the assessment of the L-DOC utilisation in biodegradation experiments. These experiments must be carried out by forcing an uncoupling both of DOC production from consumption, and of bacterial production from bacterivory (Carlson & Ducklow 1996). Consequently, experiments are generally performed either by isolating bacteria from primary producers and grazers by filtering seawater if experiments result from *in situ* sampling, or by working on mono-species strains of bacteria in pure cultures.

Due to physical, chemical and biological processes (Carlson & Ducklow 1995, Carlson et al. 2004, La Ferla et al. 2005) and to the decoupling between the production and consumption terms (Hansell et al. 1995, Carlson et al. 2002), the DOC concentration fluctuates spatially and temporally in oceanic ecosystems. Relatively weak temporal variations in the dynamics of the water column may have a great impact on the functioning of the pelagic system

(González et al. 2002). Thus, it is crucial to study the responses of microbial communities to intermittent or transient forms of reactive DOC (Cherrier & Bauer 2004). The fluctuation of DOC availability varies spatially, from the presence of microzones containing elevated substrate concentration (Williams 2000) to the large scale as the nearshore zone influenced by upwelling events (Mcmanus & Peterson 1988). Temporal fluctuations range from the daily cycle due to highest phytoplankton production during daylight (Coffin et al. 1993) to the seasonal time scale for example due to the release of DOC during a phytoplankton bloom (Miki & Yamamura 2005a, Grossart & Simon 2007). However, experimental studies are generally carried out with natural seawater by adding for example a fresh plankton-derived DOC pulse in the start of the experiment (Cherrier & Bauer 2004). Even if this experimental setup allows alleviating problems due to DOC production and bacterial grazing, it still presents problems due to DOC measurement accuracy, and especially the problem of the assessment of DOC lability. Another difficulty in the interpretation of the results comes from bacterial activity: is the bacterial count or biomass increase related to the DOC utilisation? The final conclusions from results of this experimental design are based on lots of assumptions.

The bacterial growth efficiency (BGE) is a widely used factor that enables the estimation of the carbon flows through the bacterioplankton. BGE indicates the proportion of the dissolved organic matter (DOM) that is made available by the bacteria as particulate organic matter (POM) and that may be consumed by the higher trophic levels (Cajal-Medrano & Maske 2005). It thus has a profound effect on the marine organic carbon cycle (del Giorgio & Cole 1998, del Giorgio & Duarte 2002). BGE is generally experimentally determined from bacterial production (BP) and bacterial respiration (BR) measurements, or from BP and bacterial carbon demand (BCD) according to the following formula: BGE = BP/BCD where BCD = BP+BR (del Giorgio & Cole 1998, Sempéré et al. 1998, Rivkin & Legendre 2001, Reinthaler & Herndl 2005). BGE may also be estimated from mathematical models as it often consists of a model parameter (Eichinger et al. 2006) or is a function of the specific growth rate (Cajal-Medrano & Maske 1999, 2005). However, BGE estimations from different studies are hard to compare with each other due to the widely different methods used to calculate it and the utilisation of conversion factors which also exhibit large variations (Cherrier et al. 1996, del Giorgio & Cole 1998). Nevertheless, a pattern in BGE values appears, with decreasing BGE from coastal to open ocean systems, but with great variability (del Giorgio & Cole 1998). However, physical, chemical and biological processes, acting at several time and space scales as stated previously, affect DOC dynamics and thus

bacterial metabolism. As DOC utilisation by heterotrophic bacteria is separated from the production process in biodegradation experiments, the impact of DOC fluctuation on BGE is never taken into account in these biological assays. Consequently, the influence of the DOC variation on BGE must be investigated, specifically as BGE is often used as a constant parameter in biogeochemical models (Baretta-Bekker et al. 1995, Blackburn et al. 1996, Anderson & Williams 1998, 1999, Lancelot et al. 2002). These models are subsequently used to investigate the carbon cycle (Anderson & Williams 1998, 1999).

In this study we focus on the influence of DOC load in bacterial cultures. Two kinds of experiments were performed: one under the classical conditions of biodegradation experiments, i.e. without any modification of the experimental design during the whole time course of the experiment and one by adding periodically and by pulses the same substrate amount in the culture. The only difference between both experiments is the input regime of the substrate in the batch cultures since the total amount of substrate is the same. To avoid any problems due to the sensibility of DOC measurements, the lability of DOC and the bacterial activity, we decided to carry out biodegradation experiments with a monospecific bacterial strain and a unique, highly labile, carbon substrate source. Thus, we easily might assume that the decreasing DOC concentration is related to the bacterial growth. This assumption was necessary since these data sets were also used to construct and calibrate a mechanistic model (Eichinger et al. submitted) and to estimate BGE (see below). For the same reasons, we applied intensive sampling and used DOC concentrations far from oceanic conditions where DOC concentration range generally from 34 µM C of R-DOC in deep-waters to more than 200 µM C in surface waters, with a high fraction of L-DOC, in ocean margins influenced by riverine inputs (Hansell 2002). In our experiments the total L-DOC concentration added in the cultures was 8 mM C, thus at least 20 times more than ambient L-DOC concentration. In this study, we defined L-DOC as the substrate and thus the DOC that is consumed during the time course of the experiment (with a turnover time of a few hours, approximately) whereas R-DOC was considered as the remaining DOC at the end of the experiments. No reference to SL-DOC was made.

In the first section we present a detailed description of the experiments carried out to assess the influence of DOC load on the BGE, the sampling design as well as the measurements made, and the various methods used to estimate the BGE including experimental calculation and estimation from models. The different processes included in each model as well as their mathematical descriptions are given. The second part focuses on preliminary

experiments realised to determine the initial conditions for the pulse experiment, and to test the reproducibility of our experimental results. This latter step is a requirement allowing the utilisation of deterministic modelling method to describe DOC and bacterial dynamics, and thus to estimate BGE as model parameter. The third section points out the key processes highlighted by both experiments. The fourth part deals with the different methods investigated to estimate the BGE and compares BGE for both experiments, as obtained with each method. Finally, the last section presents the conclusions and discusses their implication for the BGE in aquatic ecosystems.

II. Material and methods

1. General setup

i. Precautions

Biodegradation experiments have been carried out to determinate bacterial and DOC dynamics in several experimental conditions. By dealing with bacteria and carbon, we had to be very careful with contaminations. To prevent bacterial contamination, all culture medium and material used directly to sample the culture batches were sterilised by autoclaving 20 minutes at 110°C, and all samples were handled under a laminary flow air bench. Contamination tests realised at the end of each experiment attested that our experimental setup ensured the sterility of the cultures. To prevent carbon contamination, all glass/borosilicate materials used for the culture or to sample were pre-comusted 6 hours at 450°C. The final volume of the batch cultures was always greater than 50 % of the initial culture volume, to ensure the significance of the results.

ii. Experimental conditions

To ensure reproducibility, all experiments were realised in the same environmental conditions: all experiments were carried out in a temperate room at 25 ± 1°C, all bottles were gently swirled and incubated in the dark. As these data are also used in a modelling framework, the dynamics must be measurable with robust measurements. For this reason we used substrate concentrations well above the ambient ones.

Three experiments were realised including two batch and one pulse experiments. The batch experiment B1 aimed to determine initial conditions as well as the pulse period (see III-1). The batch experiment B2 had exactly the same conditions, except that the initial substrate concentration was 5 times higher. This substrate concentration corresponds to the total amount of substrate added in the pulse experiment, called experiment P. All the other conditions were exactly the same in this latter experiment, compared to the other ones. All experiments were made in 5 litres pre-combusted borosilicate bottles filled up with 4 (experiments B1 and P) or 3 (experiment B2) litres of culture medium. The main aim of this experimental setup is to study the influence of OM loading on bacterial activity, i.e. pulse loading versus one load.

2. Medium constitution, bacterial strain and preculture conditions

The medium culture was composed of artificial seawater (Lyman J. & Fleming R. 1940) containing all salts and ammonium needed to ensure bacterial growth (Appendix III-A). In this seawater, potassium phosphate, iron chloride, NaCl, pyruvate (carbon source) and vitamins were added (Appendix III-A). The pH was adjusted to 7.5. Each medium was autoclaved 20 minutes at 110°C before its utilisation.

The selected bacterial strain was *Alteromonas infernus*. This species originates from a hydrothermal station and can produce exopolysaccharides (EPS) during the stationary phase (Raguénès et al. 1997). This bacterial strain is motile, strictly aerobic, non-fermentative, non-luminescent, non-pigmented, encapsulated. It is a Gram negative rod, with a size about 0.6-0.8 by 1.4-2 µm with a single polar flagellum (Raguénès et al. 1997).

The preculture conditions before the bacterial inoculation in the cultures were always the same and the preculture medium was identical to that of experiments B1 and P, but not identical to the medium of experiment B2 as the initial DOC concentration was five times higher. As the preculture medium and the incubation time before inoculation were the same for all experiments, we can assume that the initial physiological state of bacteria was the same for all experiments. As the preculture was incubated three days before inoculation, and as all the apparent substrate was consumed whereas bacteria were in stationary phase during this lag time (Figure III-4), we can assume that bacteria were starved before being introduced in the batches.

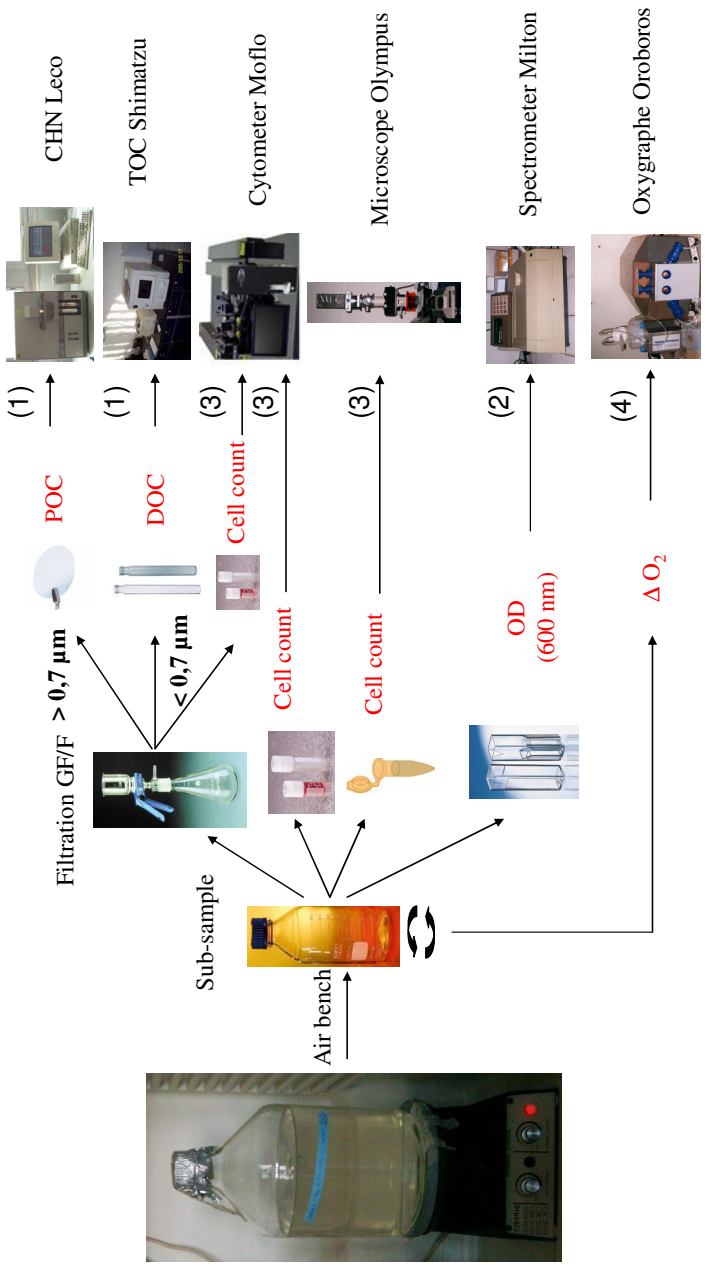

Figure III- 1: resume scheme representing the different steps of the sampling for each measurement. Each number corresponds to the sampling order (see II-3-i)

3. Sampling method and variable measurements

i. Sampling

To prevent any bacterial and carbon contamination, we did not insert any material in the culture bottles and handling of samples was done under laminar flow air bench. Sampling was realised at each point in time by pouring a certain volume of culture in another pre-combusted borosilicate bottle that was used for all sub-samples. This sampling technique allows keeping the culture in the temperate room most of the time. The measurements were always realised in the same order to avoid any bias due to the temporal lag between the different measurements. First sub-sampling was always for carbon measurements (DOC/POC) to prevent any carbon contamination by the other measurement methods. The sampling order was: (1) POC/DOC, (2) optical density (OD), (3) cell count by microscopy and cytometry analyses, and (4) oxygen consumption (Figure III-1). The cultures were always homogenised before sampling.

ii. DOC

Only DOC concentration in the culture was measured by using the total carbon analyses that did not give any information about the pyruvate concentration evolution. At the beginning of the experiment, the other identified carbon source, except pyruvate, was vitamin-DOC that we have estimated to comprise only 3 % of DOC when the initial carbon concentration from pyruvate was 1.6 mM C. When the initial substrate concentration was 8 mM C, this percentage was thus negligible (0.6 %). The medium also comprised more than 1 mM C of $NaHCO_3$ that is inorganic and eliminated by acidification and bubbling before the DOC measurement.

For DOC analyses, a variable amount (10 to 100 cm^3) of the sub-sample was collected in a graduated pre-combusted borosilicate tube and filtered through a pre-combusted GF/F glass fibre filter (0,7 µm nominal retention size). DOC was measured by high temperature catalytic oxidation (HTCO) (Sempéré et al. 2003, Sohrin & Sempéré 2005) using a Shimadzu TOC 5000 Analyzer. Samples were acidified to pH ≈ 1 with 85 % phosphoric acid and bubbled for 10 minutes with CO_2-free air to purge inorganic carbon. Three or four 100 mm^3 replicates of each sample were injected into the column heated at 680 °C. The effluent passed through a drying unit (magnesium perchlorate cartridge), a scrubber to eliminate halogen gas and sulfates, a dust-eliminating membrane filter to remove sea salt and phosphoric acid aerosols, and finally in non-dispersive infrared (NDIR) cell in which CO_2 was detected. The coefficient of variation of DOC replicates was always smaller

than 2 %. Quantification was performed by a four point-calibration curve with standards (from 0 to 2 mM C for the B1 and P experiments and from 0 to 8.5 mM C for the experiment B2) prepared by diluting potassium hydrogen phthalate in Milli-Q water.

iii. POC

In this study, POC refers to the bacterial biomass in carbon and was sampled at the same time as DOC on the filtration column. Indeed, POC is the part of the sub-sample retained on the GF/F filters. A variable but sufficient amount of culture volume was filtered in order to have a reliable POC signal. After the filtration step, each filter was dried in a drying oven, carefully stored in the dark and then analysed with a carbon analyser (Leco SC-144). Filters were introduced in a ceramic carrier and the combustion was carried out at 1350°C in an oxygen flux. The organic carbon is thus transformed in CO_2 and detected by a NDIR cell. Calibration was performed with reference compound in the same order of magnitude than sample. The measurement uncertainty was between 3 and 8 % for these carbon concentrations.

iv. Optical density (OD)

Optical Density (OD) served essentially to check the bacterial growth during the manipulation. We collected 4 cm^3 of the sub-sample to measure the OD with a spectrometer (Milton for experiments B1 and P and Jenway 6310 for experiment B2). OD was measured at 600 nm, wavelength linked to particles density. The OD medium value was subtracted to each OD value.

v. O_2 consumption

O_2 consumption was estimated by measuring the O_2 concentration with the Oroboros-2k oxygraph (OROBOROS, Austria) (Appendix III-B-1). This oxygraph provides the instrumental basis for temporal high-resolution respirometry due to a small lag time between two measurements (2 s). As recommended by the manufacturer the volume of the chambers was set at 2 cm^3, and the stirrer speed at 750 rounds per minute.

Each day, a control sample was made with a sterile medium sample to determine the consumption of the polarographic oxygen sensor (POS). This value was then subtracted from each O_2 consumption value measured the same day. The POS were calibrated with 0 and 100 % oxygen saturation. The calibration with 0 % oxygen saturation was done before the start of each new

experiment. It was calibrated by adding in the chambers anhydre sodium hydrosulfite (Na_2SO_3) in excess in order to complex all the oxygen. The 100 % oxygen saturation was calibrated prior to each measurement, by introducing 2 cm^3 of sterile culture medium in each chamber and by keeping the stopper open to equilibrate the gas with the atmosphere. When the equilibrium was reached (about 10 minutes), the 100 % oxygen saturation was recorded. Then, this medium was replaced by 2 cm^3 of the sub-sample. The stoppers were then closed to prevent oxygen diffusion inside or outside the chambers and the recording of O_2 concentration started at this very time point. After each measurement, both chambers were emptied and stoppers and chambers were cleaned with alcohol then rinsed with sterile medium. The decreasing O_2 concentration allowed estimating the continuous O_2 consumption at each time point. O_2 consumption was calculated by linear regression of the O_2 concentration, where the slope corresponds to the consumption (Appendix III-B-2). In order to get rid of the thermodynamic effects induced by the movement of the stopper when opening and closing the chambers, the O_2 consumption estimation started 10 minutes after the closing of the stopper. The consumption was estimated from 200 seconds measurements.

vi. Bacterial abundance

Total bacterial counts were estimated by two independent ways: microscopy and flow cytometry.

Microscopy counts. Bacteria fixation was performed in an eppendorf by adding 100 mm^3 of a 20 % tetraborated formol solution to 900 mm^3 of the sub-sample. The fixation step took 15 minutes. Then, a few mm^3 were taken out from this formol-mixture and added to a few cm^3 of filtered MilliQ water in a Falcon sterile tube. The volume of the formol-mixture was adjusted according to an estimated bacterial density, so that there were at least 30 bacteria per field under the microscope. We added 5-6 drops of Diamidino-4',6-phénylindol-2 Dichlorhydrate (DAPI) (2.5 µg cm^{-3} final concentration) to stain bacteria and to count these latter by epifluorescent microscopy (Figure III-2). The 10 minutes incubation with DAPI was carried out in the dark and at constant temperature. The final mixture was filtered on a 0.2 µm porosity dark polycarbonate membrane, and this membrane was assembled on a slide with a cover-slip for the final microscopy counting. The counts (in cell cm^{-3}) (Appendix III-C-1) were realised with an epifluorescent microscope (Olympus BH2 or BX61, Olympus, USA) by analysing 30 fields per sample.

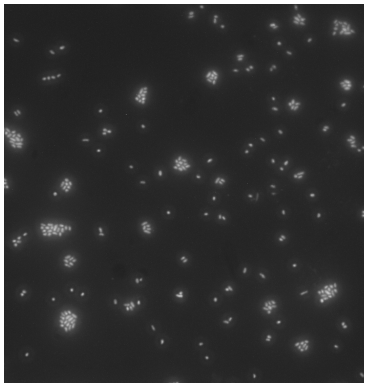

Figure III-2: White and black picture (x 1000) of *Alteromonas infernus* stained with DAPI observed under an epifluorescent microscope.

Flow cytometry counts. Flow cytometry samples were realised by fixing 1.8 cm^3 sample with 0.2 cm^3 of a 20 % para-formaldehyde (PFA) solution in 2 cm^3 cryotubes (Nalgene, USA). These samples were then stored in liquid nitrogen (-180°C) until analysis. Before analysis the samples were gently thawed in a bain-marie at room temperature, then stained with a DAPI solution (2.5 µg cm^{-3} final concentration) and then analysed by flow cytometry. Flow cytometry analyses were carried out on a MoFlo cell sorter (Dako, Dk) (Appendix III-C-2).

Flow cytometry counts were also realised on DOC samples. Indeed, according to their size, bacteria are able to pass through the GF/F filters during the filtration. After we have taken out the DOC sample from the filtration column, we have also collected 1.8 cm^3 of the culture for cytometry counts analysis. We so checked the transfer of bacteria through the GF/F filters and made appropriate POC and DOC corrections.

4. DOC and POC data corrections

Total bacterial density was estimated by flow cytometry and by microscopy for the experiments B2 and P. For both experiments cytometric counts were also realised from the DOC samples in order to estimate the percentage of bacteria passing through the filter for each data point, and to correct DOC and POC values according to this percentage. For the experiment B1 this correction was not possible as only the microscopic total counts were realised.

i. Experiment B2

We noticed that bacterial dynamics are qualitatively identical for both techniques of bacterial density estimation, although the cytometry leads to an overestimation of the total bacterial counts (Figure III-3). This phenomenon has already been mentioned in the literature (Monfort & Baleux 1992). Assuming the flow cytometry as the reference technique, this difference is highly variable during the time course of the experiment, ranging from - 5 to 54 %. This difference is higher during the exponential growth phase (34 to 54 % of difference) than during other growth phases (- 5 to 30 %).

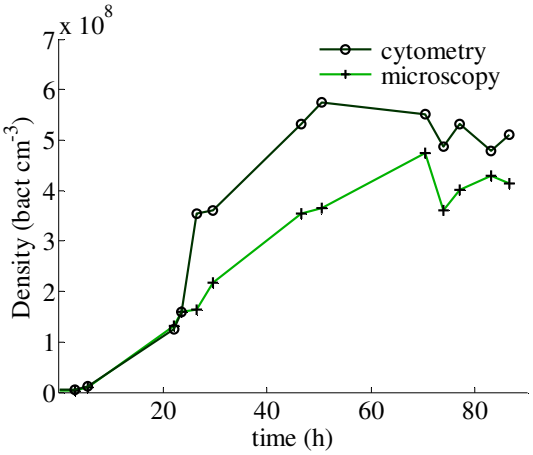

Figure III- 3: Comparison of bacterial density estimated with the MoFlo cytometer (o) and the epifluorescent microscope (+) after DAPI staining for the B2 experiment.

Density of bacteria passing through the filter during DOC/POC separation was estimated by MoFlo flow cytometer. For the B2 experiment, percentage of bacteria in the DOC samples was estimated to range from 0 to 14 %. Higher values were obtained during the exponential growth phase, whereas this percentage was near 0 % during the lag and the stationary phases. This suggests that bacteria are larger during non dividing period, and that the cell division leads to shrinking of bacteria, which subsequently reached the limit size of the filter retention size. We have then multiplied this percentage by the POC value at each point in time to estimate the bacterial biomass that has been considered as DOC instead of POC. This biomass was thus subtracted from the DOC values and added to the POC values for each sampling point.

ii. Experiment P

Unfortunately, unfiltered samples and some filtered samples for the pulse experiment were not measured for bacterial density with cytometry due to technical problems. Thus, the percentage of bacteria passing through the filters was estimated by comparing the bacterial density analysed by epifluorescent microscopy in the full sample to the bacterial density analysed by cytometry after the filtration. In the B2 experiment the density values were always higher (except for one data point) when they were analysed by cytometry. As this phenomenon was already mentioned for other studies (Monfort & Baleux 1992), we can assume that the same result occurs for the P experiment. Thus, by calculating the percentage of bacteria going through the filters with a reference to the microscopic total counts instead of to the cytometric total counts, we introduce a bias, overestimating this percentage. Moreover, except two values of 10.8 and 12.8 %, the percentage of bacteria in the DOC samples was always inferior to 4.5 %. Due to this low percentage, to its overestimation and to the lack of some data, we have decided to not correct the DOC and POC data for the pulse experiment.

5. BGE estimation

For BGE estimation, we focused on the batch experiment B2 and the pulse experiment P. The only difference between both experiments is the way of supplying substrate to the batch cultures. Indeed, all the substrate was available at the beginning of the batch experiment, therefore the culture was not exposed to any perturbation during the time course of the experiment. By contrast, in the pulse experiment, substrate was periodically added in the batch culture. Note that the total substrate quantity added was the same in both experiments. We are specifically interested in the bacterial efficiency to assimilate the C-substrate and in their growth pattern. Here, BGE was calculated by using experimental data points and modelling methods.

i. Experimental BGE estimation

The experimental BGE estimation has been widely used in microbiological studies, especially using *in situ* samples, to compare the ability of bacteria to use DOC for their growth (del Giorgio & Cole 1998). BGE can be experimentally calculated with the following formula: BGE = BP/BCD and BCD = BP + BR (Carlson & Ducklow 1996, del Giorgio & Cole 1998, Rivkin & Legendre 2001, Sempéré et al. 2003, Cherrier & Bauer 2004) where BCD is the bacterial carbon demand, BP the bacterial production and BR the bacterial respiration. In this study, BP was not

measured but it was estimated by the difference between the maximum and initial POC values. BCD was estimated as the difference between the initial (experiment B2) or the total substrate quantity put in the culture (experiment P) and the remaining DOC at the end of the experiment.

ii. BGE estimation from models

BGE has also been estimated by using three models with different levels of detail. The first model originates from the dynamic energy budget (DEB) theory (Kooijman 2000) and has been especially constructed for the pulse experiment due to the presence of the starvation periods. This model comprises a reserve compartment as well as two maintenance processes: maintenance is paid from mobilized reserve if the flux is large enough, but otherwise structure is used to pay the remaining part of the maintenance costs, which causes shrinking of the cell (Tolla et al. 2007, Eichinger et al. submitted – chapter IV) (equations III-3). Consequently, growth is not realised directly from assimilation but is buffered by the reserve compartment. When maintenance is realised from the structural biomass, bacteria release maintenance products in the culture, which correspond to R-DOC. The BGE of this latter model corresponds to the parameter Y, ratio of the two primary parameters y_{EL} and y_{EV} (Table III-1).

The second model is the Marr-Pirt model (Marr et al. 1963, Pirt 1965), which assumes a direct transfer from assimilation to growth, but which also includes a maintenance term. However, maintenance is only realised from the structural biomass as this model does not comprise any reserve compartment (equations III-2). As in the DEB model, R-DOC is produced from the maintenance of the biomass. BGE corresponds to the parameter Y_{VL} of this model (Table III-1).

The third model is the Monod model (Monod 1942), which includes neither reserve nor maintenance. It only assumes that the substrate is directly and instantaneously transformed in biomass with a constant efficiency, the BGE (Table III-1 and equations III-1). Note that here we also report that bacteria were able to produce refractory materials in our systems. However, this model does not allow any product formation. Consequently, in order to compare parameters governing assimilation and growth on L-DOC between the three models, DOC data were modified to deal only with the labile fraction of DOC. DOC values were set to zero during stationary phase. The way to modify data to focus on L-DOC was different for each experiment. For the B2 experiment, R-DOC concentration seems constant. L-DOC values

were thus estimated by offsetting with the R-DOC values to the total DOC values at the end of the experiment. In the P experiment, R-DOC concentration increased after each pulse and a linear regression to R-DOC values for all the experiment was applied and the equation governing this increase was estimated. A value from each DOC concentration was subtracted according to the formula: $DOC^* = DOC - (0.0038\,t + 0.1067)$ where DOC^* represents the corrected data, DOC the original data and t the time. In this way, data were transformed to deal only with the apparent L-DOC fraction, and thus to apply the Monod model on these modified data.

A detailed description of the DEB and Monod models are given in Eichinger et al. (submitted - chapter IV) and Eichinger et al. (2006 - chapter II), respectively. The BGE estimated with the different methods have been compared to each other for each experiment, but also BGE have been compared between the batch and the pulse experiment.

Monod model: (III-1)

$$\frac{dL}{dt} = -\alpha\, L\, M_V$$
$$\frac{dM_V}{dt} = \mathrm{BGE}\,\alpha\, L\, M_V$$

Marr-Pirt model: (III-2)

$$\frac{dL}{dt} = -\alpha\, L\, M_V$$
$$\frac{dM_V}{dt} = \mathrm{Y_{VL}}\,\alpha\, L\, M_V - j_{VM}\, M_V$$
$$\frac{dR}{dt} = y_{RV}\; j_{VM}\, M_V$$

DEB model: (III-3)

$$\frac{dL}{dt} = -\alpha\, L\, M_V$$

if $k_E\, M_E > j_{EM}\, M_V$

$$\frac{dM_E}{dt} = \alpha\, y_{EL}\, L\, M_V - j_{EM}\, M_V - y_{EV}\,\frac{k_E\, M_E - j_{EM}\, M_V}{M_E + y_{EV}\, M_V}\, M_V$$

$$\frac{dM_V}{dt} = \frac{k_E\, M_E - j_{EM}\, M_V}{M_E + y_{EV}\, M_V}\, M_V$$

$$\frac{dR}{dt} = 0$$

if $k_E\, M_E < j_{EM}\, M_V$

$$\frac{dM_E}{dt} = \alpha\, y_{EL}\, L\, M_V - k_E\, M_E - \frac{j_{EM}\, M_V - k_E\, M_E}{M_E + \frac{j_{EM}}{j_{VM}}\, M_V}\, M_E$$

$$\frac{dM_V}{dt} = -\frac{j_{EM}\, M_V - k_E\, M_E}{M_E + \frac{j_{EM}}{j_{VM}}\, M_V}\, M_V$$

$$\frac{dR}{dt} = y_{RV}\,\frac{j_{EM}\, M_V - k_E\, M_E}{M_E + \frac{j_{EM}}{j_{VM}}\, M_V}\, M_V$$

Table III-1: Description and units of model parameters used in this study.

Symbol	Equival.	Unit	Description
Parameters in the DEB model			
j_{LAm}		h^{-1}	Maximum specific absorption rate
K		mM C	Half-saturation constant
α	$\frac{j_{LAm}}{K}$	mM C^{-1} h^{-1}	Ratio between the maximum specific absorption rate and the half saturation constant
y_{EL}		-	Yield coefficient from L-DOC to reserve mass
y_{EV}		-	Yield coefficient from structural to reserve masses
k_E		h^{-1}	Reserve turnover rate
j_{EM}		h^{-1}	Maintenance flux from reserve mass
j_{VM}		h^{-1}	Maintenance flux from structural mass
y_{RV}		-	Yield coefficient from structure to R-DOC
Parameters in the Marr-Pirt model			
α	$\frac{j_{LAm}}{K}$	mM C^{-1} h^{-1}	Ratio between the maximum specific absorption rate and the half saturation constant
Y_{VL}	$\frac{y_{EL}}{y_{EV}}$	-	Growth efficiency
j_{VM}		h^{-1}	Maintenance flux from structural mass
y_{RV}		-	Yield coefficient from structure to R-DOC
Parameters in the Monod model			
α	$\frac{j_{LAm}}{K}$	mM C^{-1} h^{-1}	Ratio between the maximum specific absorption rate and the half saturation constant
BGE	$\frac{y_{EL}}{y_{EV}}$	-	Growth efficiency

III. Description of the experiments: initial conditions and reproducibility tests

1. Determination of initial conditions and the pulse period

The first step consisted in determining the initial conditions so that (1) DOC decrease and bacterial growth were substantial, (2) the pulse period was long enough to allow sample collection between subsequent pulses, and (3) DOC was apparently exhausted and bacteria were in stationary phase at the end of the pulse period. This latter condition allowed us studying bacteria in several states during the same experiment. We have determined the initial conditions as: initial DOC concentration: 1.6 mM C, and initial bacterial concentration: 5.10^6 cells cm^{-3}. A pulse period of 48 h was applied for the initial conditions indicated above (Figure III-4).

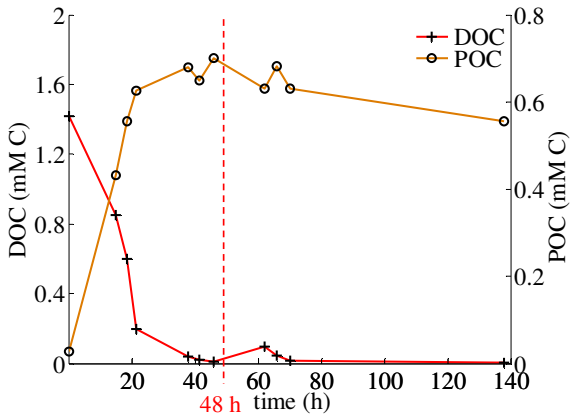

Figure III- 4: DOC and POC (C-bacterial biomass) dynamics for the batch experiment B1 where the initial conditions are: [DOC] = 1.6 mM C and [bact.] = 5.10^6 bact cm^{-3}. This experiment allowed determining the initial conditions for the pulse experiment as well as the pulse period. 48 hours after the start of the experiment, DOC was totally consumed and bacteria were in stationary phase.

2. Reproducibility

i. Batch experiments

Two kinds of batch experiments were carried out, the only difference being the initial DOC concentration. The B1 experiment was realised with an initial DOC concentration of 1.6 mM C in order to determine the pulse concentration and the pulse period (Figure III-4 and section III-1) and also assess the reproducibility of the experimental setup (Figure III-5). The B2 experiment had an initial DOC concentration of 8 mM C, which corresponds to the total DOC concentration added in the longest pulsed experiment (see the following section). In both cases, the initial bacterial concentration was approximately 5.10^6 cells cm^{-3} ($4.6 .10^6$ and 4.1 cells cm^{-3} for the B1 and B2 experiments, respectively).

Several B1 experiments were realised independently with the same initial and external conditions. Dynamics of the data were plotted on the same graph (Figure III-5) in order to test the reproducibility of this experiment. No statistical analysis was applied on these data sets, but we were interested in the qualitative substrate and bacterial dynamics. In the stationary phase, there are some small discrepancies between the experiments (Figure III-5). However, these quantitative differences may be explained by small variations of the initial conditions. As an example, the bacterial density inoculated may vary slightly. Nevertheless, lag, growth and stationary phases occur at the same time for each experiment. We can thus admit that this experimental setup is reproducible.

ii. Pulse experiments

Two pulse experiments were realised independently, the only difference being the total duration, the P experiment considered in this study being the longest of both experiments. The pulse period was based on the previous batch experiment dynamics. We demonstrated reproducibility of results, which is crucial for model applications. As we aimed to carry out a long pulse experiment, a large culture volume was required. This was possible only (1) if we changed the experimental design by using a larger bottle and a different sampling system or (2) if we carried out the experiment in several bottles of 5 litres (like we used in the batch experiment), and assumed almost perfect reproducibility. In this way we don't need to change the experimental protocol. As for the batch experiments, the P experiment was reproducible in a qualitative point of view (Figure III-6). We have thus chosen for the second strategy and used several bottles to realise the experiment.

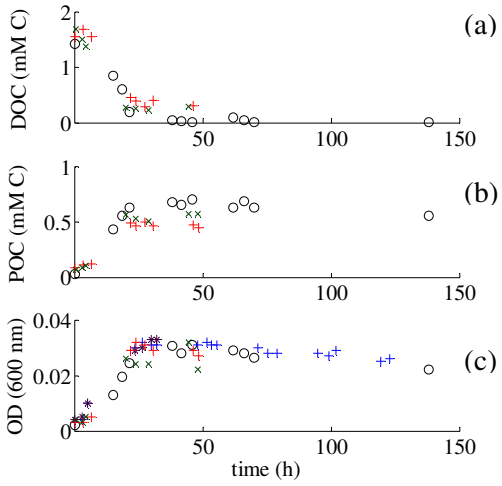

Figure III- 5: Dynamics of DOC (mM C) (a), POC (mM C) (b) and OD (600 nm) (c) of several batch experiments B1 realised with the same conditions. Each symbol corresponds to a different experiment. These graphs have allowed noticing the reproducibility of the experiment B1.

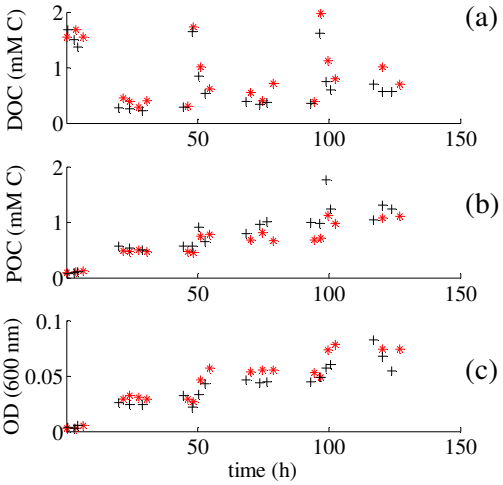

Figure III- 6: Dynamics of DOC (mM C) (a), POC (mM C) (b) and OD (600 nm) (c) of two pulse experiments realised with the same conditions. Each symbol corresponds to a different experiment. These graphs have allowed noticing the reproducibility of the pulse experiment P.

IV. Identification of key processes

1. Autocorrelation of bacterial measurements

For each experiment, we noticed that the dynamics of bacterial variables, i.e. POC, OD and the abundance, were very close, especially for the batch experiments (Figures III-7 and 8 a-b). To test the correlation between these measurements, we applied linear regressions on OD and abundance data against POC data (Figures III-7 to III-9 c-d). The correlation coefficients were always higher than 0.8, except one value (0.38) for the P experiment (Figure III-9-c) and always better for the batch than for the pulse experiments. Bacterial density showed high variations for this experiment. The correlation coefficient for OD against POC is always larger than 0.9, except for the experiment P as we had some technical problems with the spectrometer. We missed some data points due to this problem and needed to change the light source, which may explain some variations in the data set. Correlation coefficients estimated from abundance data are always inferior, which may be explained by the fact that the correlation seems less accurate during the stationary phase (Figures III-7 to III-9 a). However, as critical value $p < 0.005$ for all tests, these results exhibit a significant autocorrelation between the several variables used to measure bacterial growth in this study.

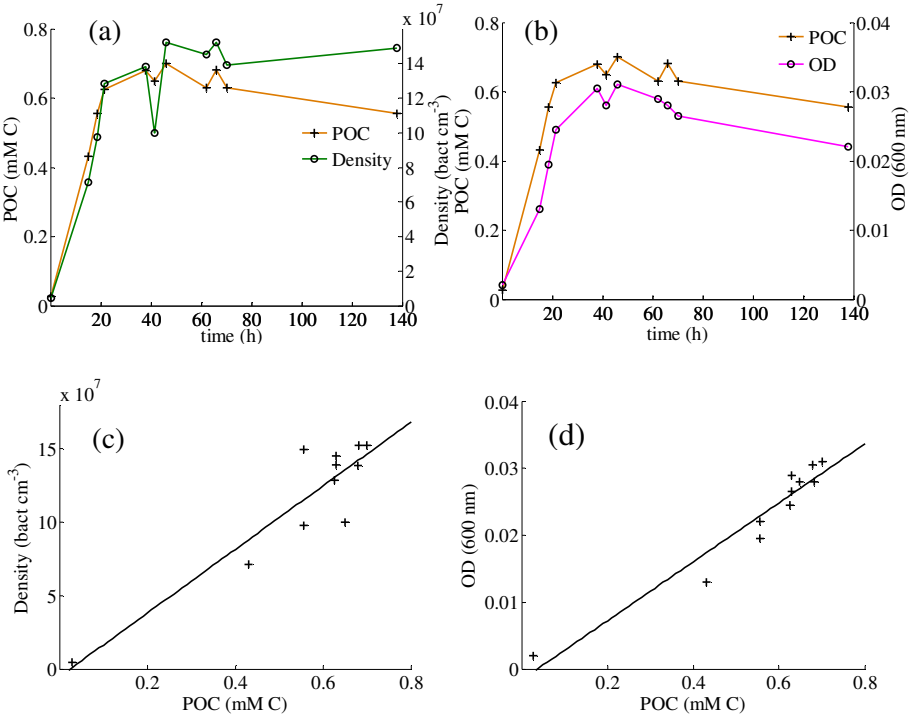

Figure III- 7: POC and bacterial density dynamics (a), and POC and OD dynamics (b) during the time course of the B1 experiment. As dynamics of these state variables are very close, linear regressions on bacterial density data vs POC data (c) and on OD data vs POC data (d) for the experiment B1 were applied. The correlation coefficients are R^2=0.83 (n=11, p=9.10^{-5}) and R^2=0.93 (n = 11, p = 2.10^{-6}), respectively.

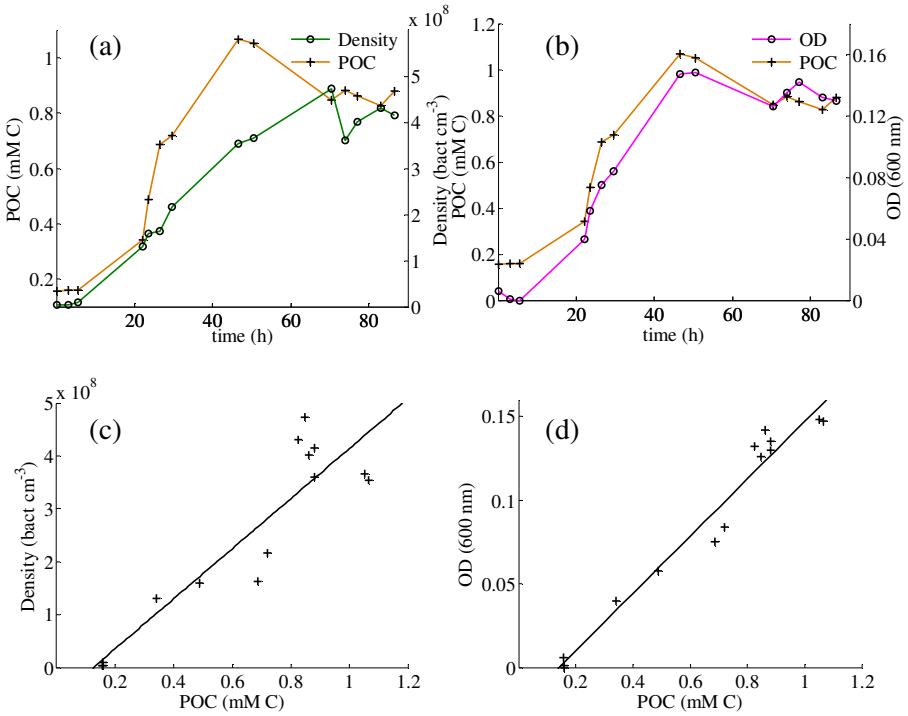

Figure III- 8: POC and bacterial density dynamics (a), and POC and OD dynamics (b) during the time course of the B2 experiment. As the dynamics of these state variables are very close, linear regressions on bacterial density data vs POC data (c) and on OD data vs POC data (d) for the B2 experiment were applied. The correlation coefficients are R^2=0.85 (n=15, p=1.10^{-6}) and R^2=0.96 (n=15, p=9.10^{-11}), respectively.

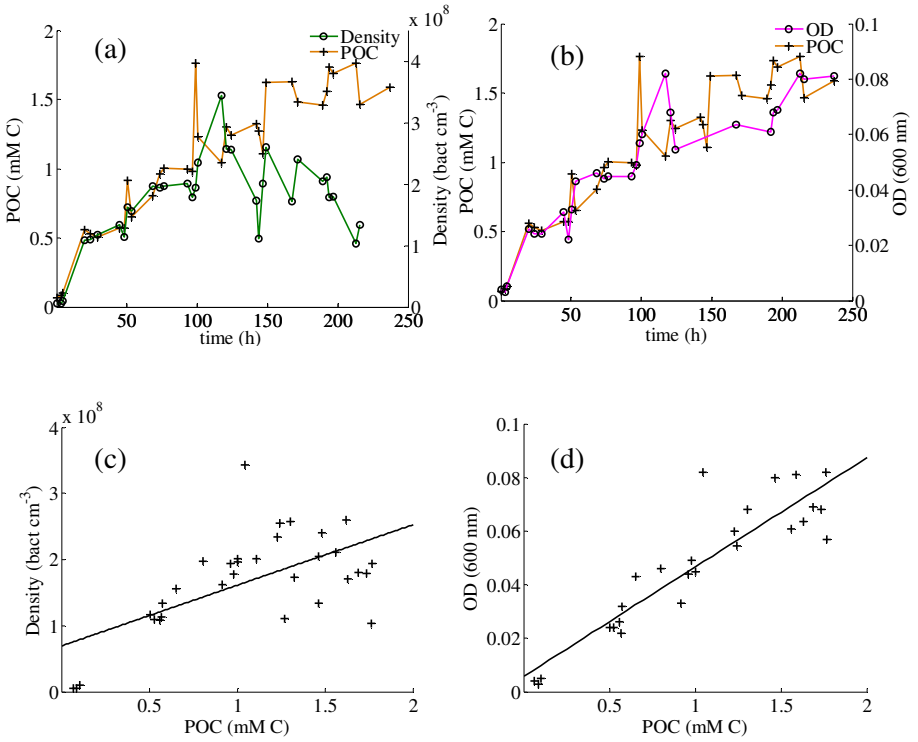

Figure III-9: POC and bacterial density dynamics (a), and POC and OD dynamics (b) during the time course of the P experiment. As dynamics of these state variables are very close, linear regressions on bacterial density data vs POC data (c) and on OD data vs POC data (d) for the pulse experiment were applied. The correlation coefficients are R^2=0.38 (n=32, p=0.0002) and R^2=0.81 (n=26, p=3.10^{-10}), respectively.

2. Production of refractory material

Our results showed DOC remaining in the cultures at the end of the B2 and P experiments (Figure III-10-a). In the P experiment such remaining DOC may consist of refractory material instead of unconsumed L-DOC due to nutrient limitation. Indeed, as bacteria grew after each carbon-pulse (Figure III-10-b), we may assume that bacteria are carbon and not nutrient limited. Moreover, the analysis of the molar ratios may give information about the limiting factor. The molar C:N ratios in the medium were calculated for both experiments and equal to 0.60 and 0.11 for the B2 and P experiments, respectively. The molar C:P ratios were 50 and 10 for B2 and P

experiments, respectively. It has been reported that the molar C:N and C:P ratios in the bacteria in natural environments averaged to 5 and 50, respectively (Fagerbakke et al. 1996, Heldal et al. 1996). From culture experiments, bacterial C:N may vary from 2.3 to 44, with a mean value of 6.1, and C:P from 14 to 358, with a mean value of 45 (Vrede et al. 2002). In this study, BCD was estimated as the difference between the total substrate amount loaded in the system and the smallest DOC value. Here, the bacterial nitrogen demand (BND) and the bacterial phosphorus demand (BPD) were estimated by multiplying the BCD by the inverse of bacterial C:N and C:P ratios, respectively. By considering the wide range of C:N and C:P ratios reported previously, BND and BPD for experiment B2 may vary from 1.40 to 0.14 mM N and from 0.51 to 0.02 mM P, respectively, with a mean value of 1.16 mM N and 0.16 mM P, respectively. For experiment P, BND and BPD may vary from 1.2 to 0.12 mM N and from 0.44 to 0.02 mM P respectively, with mean values of 1 mM N and 0.14 mM P respectively. However, culture media had 14 mM N and 0.17 mM P. Given the wide range of values of the C:P ratios and the elevated concentrations of N and P in the culture media which were always higher than the bacterial demand, we may assume that the cultures were not limited by N and P, but rather by the OC source. This strongly suggests the refractory character of the remaining DOC.

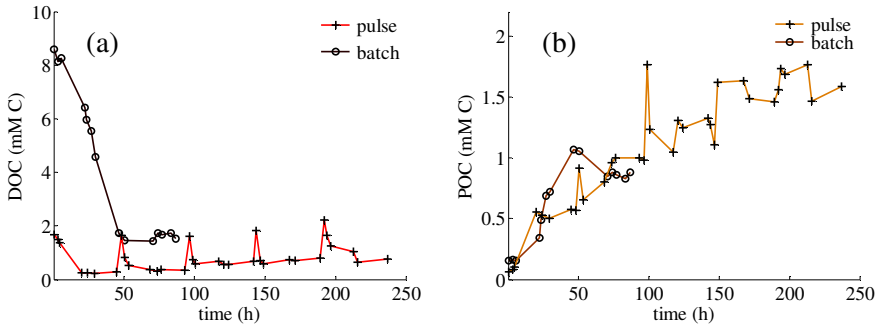

Figure III- 10: Dynamics of DOC (a) and POC (b) for B2 (o) and P (+) experiments.

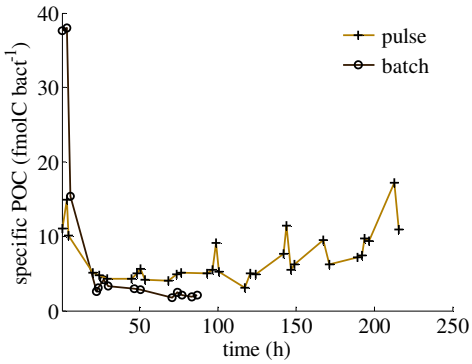

Figure III-11: Dynamics of specific POC during the time course of the experiments B2 (o) and P (+).

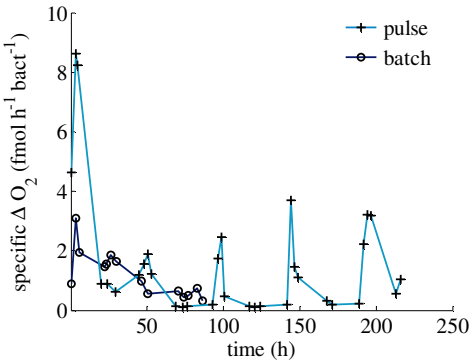

Figure III-12: Dynamics of specific O_2 consumption during the time course of the experiments B2 (o) and P (+).

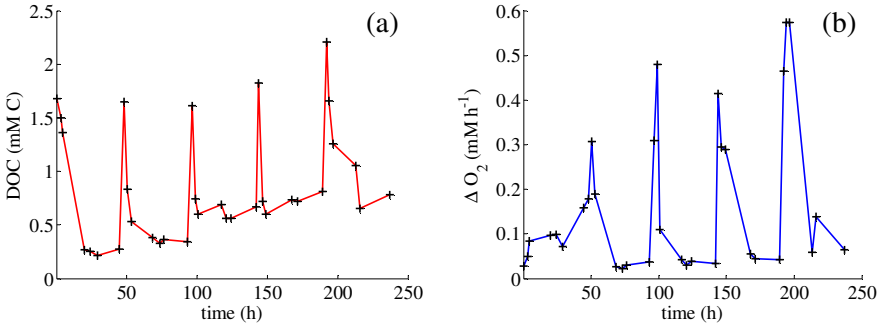

Figure III- 13: DOC (a) and respiration (b) dynamics during the time course of the P experiment.

3. Variation of the specific carbon content

The final R-DOC concentration was larger in the B2 (1.5 mM C) than in the P (0.8 mM C) experiments (Figure III-10-a), and may explain why smaller maximal bacterial biomass was observed for B2 (1.1 mM C) rather than P (1.8 mM C) experiments (Figure III-10-b). However, maximum bacterial density was higher in the batch than in the pulse experiments (a maximum of 4.7 10^8 bact cm^{-3} and 3.4 10^8 bact cm^{-3}, respectively) (Figure III-8 a and III-9 a), suggesting that bacteria were smaller in the B2 experiment. This is further supported by the POC content per cell during the growth and stationary phases of the batch experiment compared to the pulse experiment, except during the first hours (Figure III-11).

4. Maintenance process

Our results showed high specific O_2 consumption during the lag phase for B2 and P experiments (Figure III-12), suggesting a high bacterial consumption rate to adapt to the new medium and to start growth. The maintenance respiration, during the stationary phases, is highly visible in the pulse experiment. Indeed, the specific O_2 consumption increased rapidly and almost instantaneously after the addition of a substrate pulse, and decreased also very quickly when bacteria have used all the apparent L-DOC and were still in stationary phase.

5. Instantaneous response to a perturbation

The various measurements highlighted the instantaneous response of bacteria to an environmental perturbation. Indeed, we noticed that the apparent pulsed substrate, defined here as L-DOC, was always consumed within few hours by bacteria (Figure III-13-a). The apparent L-DOC concentration was consumed faster at each new pulse as the loaded concentration was the same for each pulse but the bacterial density increased during the time course of the experiment. This instantaneous response is more visible in the respiration data. Indeed, respiration measurements were generally carried out approximately 30 minutes after other measurements. However, these 30 minutes were sufficient for bacteria to increase their respiration by a factor 10 (Figure III-13-b). This increasing respiration lasted a few hours, the peak of respiration corresponding to the time needed to consume all the apparent substrate and to increase the biomass.

V. Bacterial degradation of organic matter in a variable and a constant environment: which system is the most efficient?

1. Experimental BGE estimation

BGE can be estimated experimentally from data sets by calculating the POC increase and the DOC removal with the following formula: $BGE = \frac{\Delta POC}{\Delta DOC}$. For both experiments, ΔPOC was estimated as the difference between the maximum and the initial POC values, and ΔDOC as the difference between the initial and the last DOC values for the batch experiment, and as the difference between the total DOC added in the culture and the last DOC value for the pulse experiment. BGE then amounts to 0.14 and 0.27 for the B2 and the P experiments, respectively, suggesting that bacteria are two fold more efficient with regular pulsed DOC input than with a unique DOC addition.

2. BGE estimation from models

i. Fitting

Parameter estimation is based on the minimization of the sum of squared deviations of model predictions to data points, using the Nelder Mead's simplex method (Lagaria et al. 1998). The calibration was carried out using the original data set for the pulse experiment and the corrected data set for the batch experiment, as DOC and POC values were corrected for bacteria that passed through the filters. The DEB and Marr-Pirt models fit the data for both experiments very well (Figure III-14 a-e). However, the parameter values are different for each experiment (Tables III-2 and III-3). After data modification, the Monod model fits the DOC dynamics of both experiments accurately, which is explained by the fact that the DOC absorption is governed by the same formulation for the three models. However, the Monod model fits POC data less accurately (Figure 14 c-f). The least square value for this model is indeed higher for the B2 batch experiment (Table III-2). We effectively avoided the problem of the production of R-DOC as this production cannot be incorporated in the Monod model, but the absence of the maintenance process does not allow reproducing experimental dynamics. This is clearly visible in the dynamics of the B2 experiment as the data showed a biomass decrease at the end of the experiment, but the Monod model is unable to reproduce this biomass loss.

ii. Comparison of BGE estimations from the three models

Each model allowed the estimation of a BGE for both experiments. In the Monod model, BGE is one of the parameters, in the Marr-Pirt model the BGE corresponds to the parameter Y_{VL} whereas it corresponds to the compound parameter $Y = \frac{y_{EL}}{y_{EV}}$ in the DEB model (Tables III-2 and III-3). For both experiments, BGE estimated from the Monod model is lower by at least 40 % than BGE estimated from other models. This is due to the fact that the Monod model does not comprise any maintenance term. The BGE estimations from the Monod model are also very close to the experimental BGE estimations. This is not surprising, especially for the experiment B2, as we have calculated the experimental BGE by subtracting the initial from the maximum POC value. Thus, this estimation does not take into account the maintenance which especially appears at the end of the experiment (Figure III-14). As Marr-Pirt and DEB models account for maintenance, the BGE has to be higher than for a model without maintenance to reach the same maximum growth. BGE estimated from the Marr-Pirt model exhibits a difference of only 4 % with the BGE estimated from the DEB model for the batch experiment, and of 12 % for the pulse experiment. BGE estimated from both models may thus be considered as equivalent.

Even if BGE estimated from the three models are different, we found that BGE was always higher for the pulse than for the batch experiment. This validates the result obtained with the experimental estimation. Nevertheless, the difference percentage between BGE for the pulse and the batch experiment is not the same for the different models. For the experimental estimation, the BGE is more than twice higher for the pulse than for the batch experiment, whereas this difference reaches only 65 % for the Monod model estimation. For the Marr-Pirt model, BGE is 88 % higher for the pulse compared to the batch experiment, and is 59 % higher when BGE was estimated from the DEB model.

Table III- 2: Parameter and least square values for each of the three models for the batch experiment B2. POC and DOC data were corrected for the bacteria passing through the filters. Parameters were estimated by the minimization of the sum of square deviations of model predictions to data points. As the Monod model cannot produce refractory material, DOC concentrations were held to 0, when bacteria were in stationary phase, by subtracting the R-DOC concentration at the end of the experiment to each DOC data point.

Parameters	**Monod**	**Marr-Pirt**	**Switch DEB**
α	0.167	0.104	0.212
k_E	-	-	0.201
y_{EL}	BGE = 0.142	$Y_{VL} = 0.203$	0.211
y_{EV}			1.000
$Y = \frac{y_{EL}}{y_{EV}} = 0.211$			
j_{EM}	-	-	0.021
j_{VM}	-	0.012	0.006
y_{RV}	-	1.000	1.000
Least square	**0.516**	**0.338**	**0.259**

Table III- 3: Parameter and least square values for each of the three models for the pulse experiment P. Parameters were estimated by the minimization of the sum of squared deviations of model predictions to data points. As the Monod model cannot produce refractory material, DOC concentrations were held to 0, when bacteria were in stationary phase between two pulses, by subtracting a linear regression on DOC data. This linear regression was estimated only on R-DOC data as they exhibit an increasing during the time course experiment, but it was applied on the whole data set.

Parameters	**Monod**	**Marr-Pirt**	**Switch DEB**
α	0.364	0.347	0.484
k_E	-	-	0.603
y_{EL}	BGE = 0.234	$Y_{VL} = 0.382$	0.500
y_{EV}			1.492
$Y = \frac{y_{EL}}{y_{EV}} = 0.335$			
j_{EM}	-	-	0.000
j_{VM}	-	0.004	0.008
y_{RV}	-	0.855	1.000
Least square	**1.722**	**1.595**	**1.728**

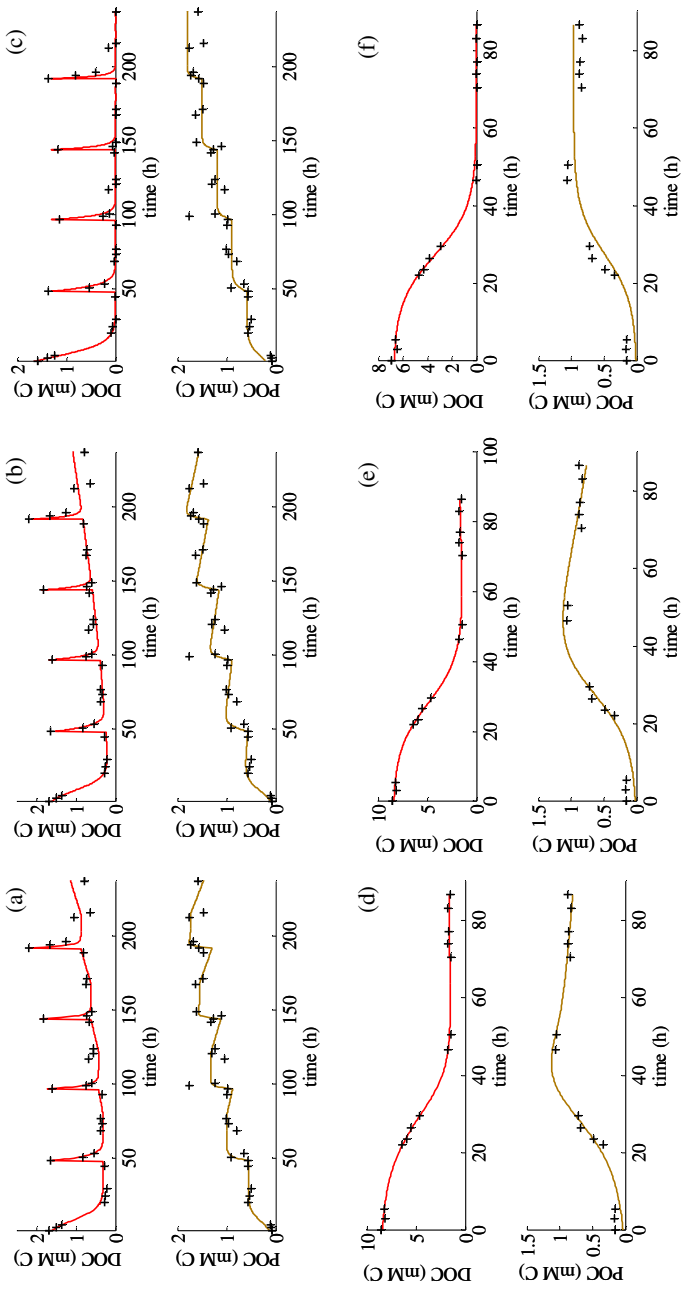

Figure III- 14: Dynamics of DOC and POC for the pulse experiment P and the DEB (a), Marr-Pirt (b) and Monod (c) models, and for the batch experiment B2 for the DEB (d), Marr-Pirt (e) and Monod (f) models. The crosses represent the original data for the pulse experiment and the corrected data (according to the percentage of bacteria passing through the filters) for the batch experiment. For the Monod model, DOC data were held to zero between two pulses or during stationary phase with a linear regression as no R-DOC cannot be produced.

VI. Discussion

This study has allowed pointing out several processes. Firstly, we have demonstrated that bacteria are able to produce refractory material. However, the nature of this material is unknown: it could consist of cell wall, suggesting that bacteria are a source of DOM and that bacteria-derived organic matter can be preserved for long periods (Nagata 2000), or it could consist of exopolysacharrides (EPS) as this bacterial strain produce it during the stationary phase (Raguénès et al. 1997). Chemical analyses are needed to identify the nature of this refractory material. To be sure that the studied system is fully limited by OC and not by a nutrient, it could be interesting to measure the pyruvate as well as the total DOC concentration. Such information could help us to understand whether the remaining DOC is only refractory or if it is made up of a part of not assimilated substrate. We could also measure the nutrient concentrations to follow their dynamics and eventually include them in models. However, this would complicate the experimental design by increasing the culture volume that needed considerably. An alternative would be the use of chemostats with a constant culture volume. The experimental design should be adjusted to allow the introduction of the pulses, for example by changing the dilution rate.

The respiration measurements allowed the study of maintenance during the stationary phase. The Monod model is not suitable for this purpose. Indeed, it considers that a proportion BGE is used for the growth, and that the remaining proportion (1-BGE) is used for the respiration. However, when considering the equations, substrate concentration (L) equal to zero would imply that the respiration (which amounts to (1-BGE) L M_V, where M_V stands for the bacterial biomass) is also null. This result is inconsistent with our experimental results. The choice of a model is highly influenced by the available data. Indeed, if our experiments stopped after the growth phase and if we did not measure the respiration, we would notice that the Monod model is sufficient for this experiment. In this study, Marr-Pirt and DEB models are almost equivalent in terms of dynamics and of BGE estimations. However, by including nutrient measurements for example, we could appreciate the relevance of mechanistic approach, as the DEB theory, considering processes as the assimilation, maintenance and growth of each element. It has been demonstrated that when considering a food chain with a bacteria, fed on glucose, and a predator, the Monod and Marr-Pirt models are not able to reproduce experimental dynamics, whereas the DEB model is (Kooi & Kooijman 1994). Consequently, experimental efforts and developments are necessary to assess bacterial processes that should be included in models.

The P experiment and especially the respiration measurements, showed the versatility of bacterial metabolism, which is difficult to observe in constant conditions. We may introduce the notion of population synchronisation as bacteria are constrained by the presence or absence of food. This synchronisation may be due to several factors, such as the stress generated by absence of substrate and the large energy requirement for maintenance. Consequently, all bacteria become active at the same moment to assimilate the substrate and to grow, and cells continue maintenance when the substrate has totally disappeared. This metabolic flexibility is necessary to cope with the vicissitudes of a largely oligotrophic and ever-changing environment, and may result from the uncoupling of anabolic and catabolic processes (del Giorgio & Cole 1998). We may believe that the situation is the same in natural seawater, as food is not continuously available (Hanegraaf & Kooi 2002) and bacteria may be faced with long periods of absence of one or more nutrients (Konopka 1999) and with short periods of high substrate availability. Thus, by carrying out batch biodegradation experiments using *in situ* samples, bacteria may be in one or another situation. The resulting BGE are of course affected by the temporal variation of substrate availability. We consequently have to be very cautious when comparing BGE from different study sites and periods, without considering the "story" of the water mass.

We also observed a highly significant autocorrelation between the various bacterial variables (POC, bacterial density and OD), especially for the batch experiments B1 and B2. It may be possible that calibration of two variables on the third would reduce the experimental cost and work considerably. For example, OD measurements do not require a large culture volume (2 cm^3 against 10 to 100 cm^3 for POC measurements) and are really fast and not expensive compared to POC and bacterial density measurements. However, it seems that this correlation is less accurate during the stationary phase compared to other growth phases, justifying that this kind of formulation should be applied cautiously. Moreover, three models have been used in this study to describe DOC and bacterial dynamics, and we have demonstrated that the Monod model is inaccurate for these data sets. Marr-Pirt and DEB models can thus be used in further work to determine critical variables and parameters to be measured.

On the other hand, the numerous variables measured also permitted to estimate the carbon content per bacteria, often called carbon conversion factor (CCF). This CCF is often considered constant and used to convert bacterial density into bacterial biomass-carbon. The mean CCF for marine bacteria is often considered to be 20 fgC $bacterium^{-1}$ (Lee & Fuhrman 1987). However, our study clearly showed that this CCF is not constant but varies

during the time course of the experiment. Indeed, in the experiment B2, CCF decreased rapidly from 450 to 30 fgC bacterium^{-1} (38 to 3 fmolC bacterium^{-1}) during the first lag phase, and then is quite stable during the rest of the experiment (Figure III-11). In the P experiment, the CCF also decreased from 180 to 60 fgC bacterium^{-1} (15 to 5 fmolC bacterium^{-1}) during the lag and exponential growth phases, and increased after each pulse (Figure III-11). The variation of the carbon content per cell has already been reported (Ducklow & Carlson 1992), being larger during growth phases than during stationary phase (Vrede et al. 2002). Due to the huge variation of the CCF during the several growth phases, the use of a constant CCF to deduce bacterial biomass-C from bacterial density should be avoided. By using a CCF of 20 fgC bacterium^{-1} for the first steps of the experiment B2, the error could be higher than 200 %.

The calibration of the Monod, Marr-Pirt and DEB models on these data sets demonstrated the weakness of the Monod model to reproduce this kind of dynamics. The presence of the maintenance process is necessary to assess these bacterial dynamics. However, it seems that the formulation of the maintenance process has little impact on the model outputs. Nevertheless, the DEB model, due to its mechanistic formulation, is more flexible than the Marr-Pirt model and is able to apply to more situations. The maintenance from the reserve has more importance in the B2 experiment than in the P experiment. Indeed, the parameter j_{EM} is negligibly small in the pulse experiment whereas it equals 0.021 h^{-1} in the batch B2 experiment (Tables III-2 and III-3). Contrary to the pulse experiment, the maintenance from reserve is higher than maintenance from the structure in the batch experiment (j_{EM} is more than three times higher than j_{VM}) (Table III-2). If the pulse experiment was realised with the initial conditions of the batch experiment B2 and with a longer pulse period, the Marr-Pirt model might have been unable to reproduce experimental dynamics as it does not comprise maintenance from reserve which is no more negligible (Figure III-15). Consequently, a mechanistic model like the DEB model may be useful in other conditions than that used in our pulse experiment, and may thus show dynamical differences with the Marr-Pirt model.

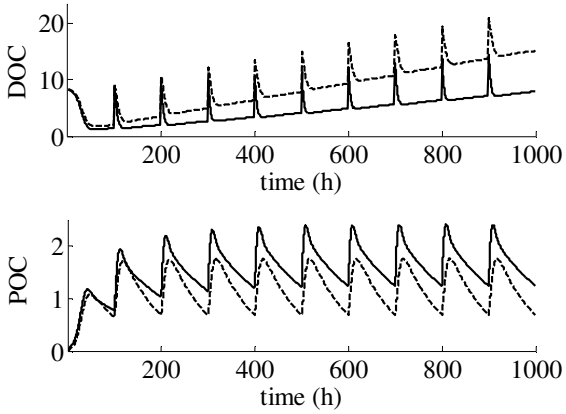

Figure III- 15: DOC and bacterial biomass dynamics for the DEB (solid line) and the Marr-Pirt (dashed line) models. For this simulation, we used parameters and initial conditions of the B2 experiment, and we applied a pulse period of 100 hours and a pulse concentration equal to the initial substrate concentration. In this case, both models show dynamical differences.

Finally, the coupling of the experimental and the modelling work has allowed the estimation of the BGE according to several methods: the experimental way (by calculating ΔDOC and ΔPOC) and the modelling way (by calibrating three models on the data sets). However, another way to estimate the experimental BGE is by considering that BCD = BP + BR contrary to BCD = ΔDOC and still considering that BP = ΔPOC. To estimate BR, experimentalists generally apply a linear regression on all O_2 concentration data and consider only one BR value for the whole experiment (Eichinger et al. 2006). However, these experiments clearly show that we can not consider one BR value per experiment as it varies greatly, being high during assimilation and low during starvation periods. The non systematic linearity of BR, and its impact on BGE estimation, was already demonstrated by performing continuous oxygen measurement with oxygen microprobes (Briand et al. 2004). We could also estimate a dynamic BGE with the models, by estimating the ratio between the variation of the biomass and the variation of the substrate. This is consistent with the definition of the BGE. For the Monod model, this calculation would result in $\frac{dM_V}{-dL} = BGE$ resulting in a constant BGE. However, for the Marr-Pirt model this calculation would result in a dynamic BGE, which is a function of the state variable L and

amounts to $\frac{dM_V}{-dL} = Y_{VL} - \frac{j_{VM}}{\alpha L}$. For the DEB model, the BGE is also variable and amounts to $\frac{dM_E + y_{EV}\, dM_V}{-dL} = y_{EL} - \frac{j_{EM}}{\alpha L}$ when $k_E M_E > j_{EM} M_V$ and to a more complex function in the other case. This dynamic estimation is also possible for the experimental BGE by calculating BGE from two consecutive data points. But for instance the variability between data does not allow a sufficient sensitivity to investigate such estimation. Nevertheless, it would be very interesting to compare these BGE for the different experiments and models, but we should previously choose a criterion for comparison as we can no longer compare single values but dynamics. Moreover, we would also have to solve some numerical problems as when L values approach 0, the dynamic BGE tends to infinity.

The values of the four constant BGE (one experimental BGE and three BGE resulting from models) differed, but it always results that the BGE is higher in the pulse than in the batch experiment. We can thus state that bacteria are more efficient in a transient than in a constant environment (Poggiale et al. 2005). It seems that they are unable to grow efficiently when a large amount of substrate is present, whereas there growth is stimulated when the same amount of substrate is brought periodically.

As the parameter α, the ratio between the maximum absorption rate j_{LA_m} and the half-saturation constant K, is also always higher for the pulse experiment (Tables III-2 and III-3), we can assume that bacteria also increase their maximum assimilation rate and/or increase their affinity to the substrate (decrease of K) in the pulse experiment. This is consistent with the fact that bacteria are faced with apparent "long" periods of absence of substrate, and that they subsequently have to increase their affinity to the substrate in order to increase their growth efficiency. The presence of two *K* systems has still been mentioned (Baxter & Sieburth 1984), where the low *K* system is constitutive and saturable, whereas the high *K* system may result from facilitated diffusion coupled with extracellular polymeric carbohydrate production. This hypothesis is consistent with our experiments as high affinities are observed in the P experiment showing the maximum products formation, which could correspond to EPS. Another hypothesis which might explain higher BGE values for the pulse experiment is by considering the competition. We can consider a ratio δ between the amount of available substrate and the bacterial density. Both experiments started with the same bacterial density but the substrate concentration was 5 times higher in the

batch experiment B2. Consequently, δ was higher in the B2 experiment which indicates a high substrate amount per bacterium. Thus, the competition for the substrate is negligible and bacteria do not need to increase their BGE or substrate affinity. By contrast, since the beginning of the pulse experiment, δ is small. Moreover, bacterial density increased in the time course of the experiment, and we periodically added the same substrate concentration in the culture. Consequently, δ decreased during the experiment, leading to a strong competition between bacteria which need to increase their BGE and affinity to the substrate. As bacteria are in strong limitation between two pulses, they also assimilate very rapidly each substrate pulse, which supports the increase of j_{LA_m}.

VII. Conclusion

Numerous studies have investigated how environmental factors influenced the BGE (del Giorgio & Cole 1998). It was still demonstrated that BGE is influenced by DOC quality in term of molecular weight (Amon & Benner 1996), DOC chemical nature (Carlson & Ducklow 1996, Cherrier et al. 1996, Cherrier & Bauer 2004), substrate C:N ratio (Goldman et al. 1987), distance from the seashore (del Giorgio & Cole 1998, La Ferla et al. 2005), season (Reinthaler & Herndl 2005, Eichinger et al. 2006) and depth (Eichinger et al. 2006). However, there have been only few investigations dealing with daily and detailed seasonal variation of natural BGE (del Giorgio & Cole 1998). We have demonstrated that the temporal variation in substrate availability influence the BGE greatly, which may be two times higher in a pulse than in constant experimental conditions. This outcome may have great impact on knowledge resulting from the long effort on BGE determination. Indeed, to determine BGE we need to uncouple DOC production from its consumption, however the time and space variability of DOC distribution in field makes BGE highly variable. More experiments are required to confirm our results, for example by improving the protocol by measuring also nutrient concentration and by progressively improving the protocol to incorporate the DOC source more naturally. However, we should still consider pulse load of substrate or other kinds of variable inputs. The outcome of this study is even more important knowing that model formulation and parameter estimation from experimental dynamics are often used in global models to investigate the oceanic carbon cycle.

APPENDIX III-A
Culture media

- **Composition of the several media used**

Zobell Medium (composition for 1 dm^3)

Large marine salt: 20 g
Peptones: 7 g
Yeast extract: 1 g
Agar: 15 g
$Fecl_3$ (5.04 g/L): 0.5 cm^3
Milli-Q water: qsp 1 L

Artificial seawater (Lyman & Fleming 1940), concentrated 10 times (composition for 2 dm^3)

NaF: 0,03 g = 30 mg
$SrCl_2$: 0,24 g = 240 mg
H_3BO_3: 0,26 g = 260 mg
KBr: 0,96 g = 960 mg
$NaHCO_3$: 1,92 g = 1920 mg
KCl: 6,6 g = 6600 mg
NH_4Cl: 7,2 g = 7200 mg
$CaCl_2$, 2 H_2O: 14.567 g = 14567 mg
$MgCl_2$, 6 H_2O: 105.8 g = 105800 mg
Na_2SO4: 39 g = 39000 mg
H_2O: qsp 2L

Vitamins (composition for 1 dm^3)

Cobalamine: 0.5 mg
Biotine: 5 mg
Thiamine: 50 mg
Riboflavine: 50 mg
Piridoxine: 50 mg
Folic acide: 50 mg
Nicotinic acide: 50 mg
Para amino benzoic acide: 50 mg
Panthoténic acide: 500 mg
Meso-inisitol: 500 mg

Milli-Q water: qsp 1 dm^3

Iron solution ($FeCl_2$) at 5.4 g dm^{-3}

$FeCl_2$, 4 H_2O: 616 mg
Milli-Q water: 100 cm^3

Phosphate solution (KH_2PO_4) at 20 g dm^{-3}

KH_2PO_4: 2g
Milli-Q water: 100 cm^3

Culture medium (for 1 dm^3)

Artificial seawater, concentrated 10 times: 100 cm^3
NaCl: 11,75 g
$FeCl_2$ (5,4 g dm^{-3}): 0,5 cm^3
Carbon source (sodium pyruvate $CH_3COCOONa$): 0,061 g for a DOC concentration of 1,6 mM C
KH_2PO_4 (20 g dm^{-3}): 1,122 cm^3
Vitamines: 1 cm^3
Milli-Q water: qsp 1 dm^3

- **Preparation of the media**

Zobell medium

All constituents are dissolved in a clean Erlenmeyer. pH is adjusted to 7.5, the solution is autoclaved 20 min at 110°C, poured in Petri boxes under laminar flow air bench. After solidification, the medium was stored in cold (4°C) room.

Artificial seawater

For artificial seawater, the products are successively added one by one in pre-combusted glass bottle. The product has to be dissolved before adding the following. The artificial seawater is divided into 20 flashes of 100 cm^3, so that 1 flash will serve for 1 dm^3 of culture medium as the seawater is concentrated 10 times.

Culture medium

The different products, without vitamins, are mixed. pH is adjusted to 7.5, the solution is autoclaved 20 min at 110°C and vitamins are added when the medium temperature is near 25°C. Vitamins are filtered on 0.2 µm before their introduction in order to sterilise them.

- **Start of a preculture**

The bacterial strain *Alteromonas infernus* was conserved on Petri box on Zobell medium and regularly mended. The colonies were mended a few days before starting a new preculture in order to have active and "in good health" bacteria. To start a new preculture, one colony was selected in the Petri box under the laminary flow air bench and added in 10 cm^3 of culture medium in a sterile tube. The tube was vortexed until having a homogeneous bacterial culture. The precultures were started with a concentration of 5.10^6 bact cm^{-3}, we thus had to calculate the volume to take among the 10 cm^3 to obtain this bacterial density. In this way, we took 900 mm^3 of the latter solution and we added 100 mm^3 of formol at 20 % to fix the bacteria. The fixation step lasted 15 min. Then, a few mm^3 were collected from this formol-mixture and added to a few cm^3 of MilliQ water in a sterile tube. Five-six drops of DAPI (2.5 µg cm^{-3}) were added to stain bacteria, in the dark at constant temperature and during 10 min. Then, bacteria were filtered on 0,2 µm filter and on a dark membrane. After the filtration, the dark filter, with the stained bacteria, were carefully recovered and placed between a slide and a cover slip. A drop of immersion oil was added on the slide and on the plate for the observation under the microscope. Then, bacteria were counted under the UV lamp and a x100 objective. 30 slides were counted in order to obtain a representative result of the bacterial density with the formula (III-C-1) (Appendix III-C-1).

The preculture has to be inoculated at a concentration of $5.\ 10^6$ bact cm^{-3}, we estimated thus the volume to take out from the sample according to the following formula:

$$V_1 = \frac{C_2\, V_2}{C_1}$$

with
V1 = volume to take out
C1 = N = density of bacteria counted
V2 = volume of the sample to inoculate
C2 = final concentration = 5.10^6 bact cm^{-3}

We then introduced the volume V_1, with the bacteria, in the new medium V_2 that had the same composition. This preculture is incubated in the dark at 25°C during 3 days, in order to start the culture with starved bacteria.

- **Start of a culture**

The cultures were started from the previous preculture. The inoculation scheme is almost the same than for the preculture. Indeed, a few cm^3 of this preculture was collected, and the DAPI stained bacteria were counted by epifluorescent microscopy. After bacterial addition, the culture was homogenised and this time corresponded to the time 0 of the experiment.

APPENDIX III-B
O_2 consumption estimation

1. The oxygraph

The Oroboros-2k oxygraph is composed of two independent measurement chambers housed in a Peltier copper block designed to regulate the temperature. In each chamber, a rotating electromagnetic field drives the stirrer bar to ensure the homogenisation of the sample (Figure III-B-1). Artefacts due to oxygen diffusion through the measurement chambers are minimised by using appropriate materials inert with O_2, such as glass for chambers and titanium for stoppers and injection cannulas. Each chamber is equipped with a polarographic oxygen sensor (POS). Oxygen diffuses from the sample to the cathode surface through (1) an unstirred layer of the sample at the outer membrane surface, (2) the membrane and (3) the electrolyte layer (KCL, 1M). To minimize the unstirred layer of the sample, a high and constant stirring of the sample medium is required. At the cathode the oxygen pressure is effectively held at zero. Under steady-state conditions, the oxygen flux to the cathode depends on the external oxygen pressure, and the electrochemical reduction of oxygen yields an oxygen-dependent consumption of oxygen by the POS which is converted into an electrical signal. This signal is directly transferred on-line by the software DatLab (OROBOROS, Austria), and converted in real time in oxygen concentration and flux independently for the two chambers (Figure III-B-2). Subsequently, sections of the experiment are selected for averaging and tabulating oxygen flux (from http://www.oroboros.at).

(a) (b)

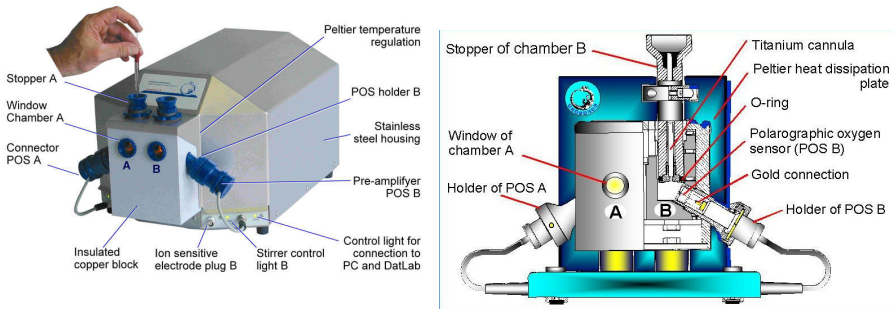

Figure III-B-1: Picture of the OROBOROS-2K oxygraph with its elements (a) and longitudinal scheme (b) (from http://www.oroboros.at).

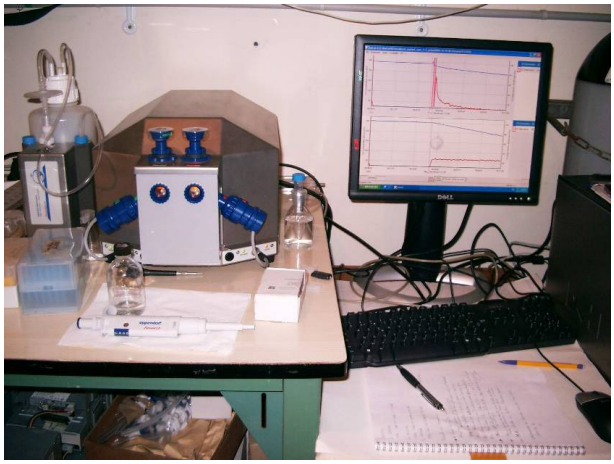

Figure III-B-2: Picture of the OROBOROS-2K oxygraph with an example of outputs of the on-line software DatLab.

2. Estimation of the consumption

As each sample was in contact with atmospheric O_2 before each measurement, we cannot deduce the instantaneous O_2 concentration in the batch cultures. However, the decreasing O_2 concentration allowed estimating the continuous O_2 consumption at each time point. O_2 consumption was calculated by considering a linear regression on the O_2 concentration curve, where the slope corresponds to the consumption. In order to get rid of the thermodynamic effects induced by the movement of the stopper when opening and closing the chambers (Figure III-B-3), the O_2 consumption estimation started a few times after the stopper closing. Several tries were realised to determine this interval time and to determine on how many points the linear regression has to be applied to calculate the consumption. To choose these times, we have tried several times after the closing and applied the linear regression on several data numbers, and we have chosen the times were the values of the slope did not change if we still increased the times (Figure III-B-4). So, the linear regression was applied 600 seconds (300 data points) after the stopper closing and on 200 seconds measurement (100 data points) (Figure III-B-5). This routine was programmed in a Matlab code in order to keep the same criteria for each time point. With this method, we obtained one consumption value for each time point of the experiment.

Each day, a control sample was made with a sterile medium sample to determine the consumption of the POS. This value was then subtracted from each O_2 consumption value measured the same day. We used the same

method to calculate the O_2 consumption of the control sample than for the culture sample, except that we did not have the thermodynamic effect due to the stopper closing. Thus, the O_2 consumption was estimated by calculating the mean of the slopes, with a time interval of 100 seconds, from the closing to the end of the recording.

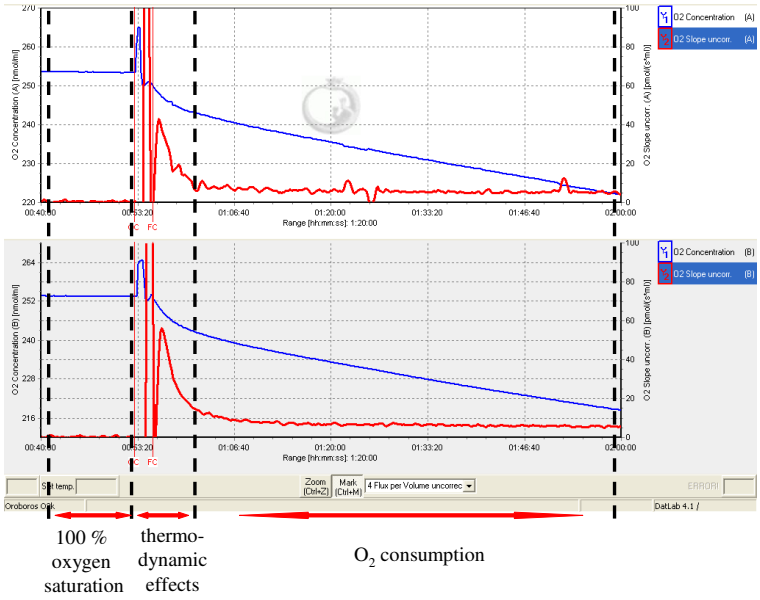

Figure III-B-3: Example of outputs of the on-line software DatLab. The upper panel represents curves of the chamber A and the other panel the curves of the chamber B. The upper curve corresponds to the O_2 concentration (in nmol cm^{-3}) and the lower curve to the dynamic of the O_2 consumption (in pmol cm^{-3} s^{-1}), calculated with the software but not used in this study. "OC" corresponds the time when the chambers were open and "FC" to the closing of the chambers. The first part of this dynamic corresponds to the 100 % oxygen saturation (stable part), the second linear part to the O_2 consumption by bacteria. The non-stable parts between these two parts correspond to moments where we have opened or closed the stoppers. The figure shows that during almost 10 minutes, the O_2 consumption is not stable due to the thermodynamic effects.

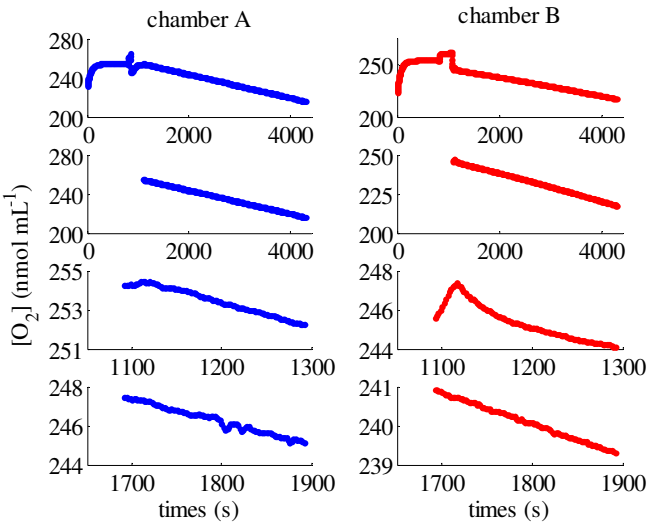

Figure III-B-4: Dynamics of O_2 concentration (nmol cm^{-3}) in chamber A (left panel) and B (right panel), used as duplicate for the t_0 of the pulse experiment. The upper panel represents the complete dynamic of O_2 concentration during the recording. This dynamic is identical to the dynamic from DatLab (previous figure). The second panel corresponds to the same dynamic but focused after the stopper closing (we have removed the 100 % oxygen saturation part). The third panel is a zoom of the second one on a period of 200 seconds just after the stopper closing. On the right graph, we see the effect of the stopper closing as the concentration is not stable. The last panel is also a zoom of the second one also on a period of 200 seconds, but 600 seconds after the stopper closing. The dynamic is indeed more stable than in the third panel.

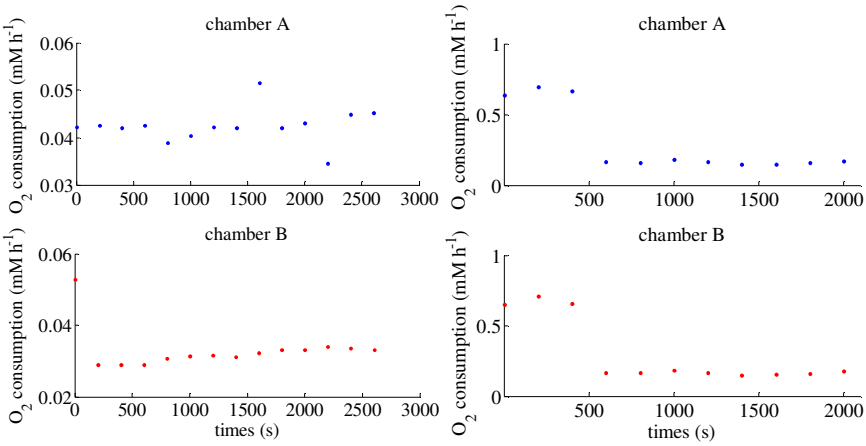

Figure III-B-5: Two examples of independent dynamics of the O_2 consumption. Both panels represent the O_2 consumption values calculated, for one sample, with a linear regression on 100 points (200 seconds) and every 200 seconds. Here, time 0 corresponds to the time of the stopper closing. The left panel corresponds to the same sample than the previous figure (t_0) (Figure III-B-4) and we see that the O_2 consumption stabilizes after 200 seconds. However, for the second panel (which corresponds to another time point), we see that the O_2 consumption needs at least 600 seconds to stabilize. Finally, the O_2 consumption value retained for each sample was the value 600 seconds after the stopper closing (the fourth point).

APPENDIX III-C
Cell counts

1. Microscopy

For each slide, 30 fields were counted, and the bacterial abundance N (in cell cm^{-3}) was estimated according to the following formula:

$$N = \frac{n_{mean}}{S_{grid}} \frac{D^2 \pi}{V_{filtered}} \frac{V_{prepared}}{V_{sample}} \qquad \text{(III-C-1)}$$

with
n_{mean} = average bacterial number per field
S_{grid} = surface of the count grid = 6400 μm^2 (10000 μm^2) if the microscope used was the Olympus BH 2 (Olympus BX 61)
D = diameter of the filtration surface = 15500 µm (18300 µm) if the filterer used was a turret (multiposition rosette)
$V_{filtred}$ = volume of the filtered sample
$V_{prepared}$ = prepared volume (with formol) = 1000 mm^3
V_{sample} = total volume of the sample (without formol) = 900 mm^3

2. Flow cytometry

The flow cytometer MoFlo cell sorter is equipped with a water cooled Argon laser providing a 352 nm (UV) and a 488 nm (blue) laser beam set up on a regulated 50 mW outpout power on UV. Three optical properties were measured for each single particle analyzed. Two light scatter intensities based on the 488 nm laser beam were measured, namely forward angle light scatter (related to the particle size) and right angle light scatter (related to cell structure and shape). The bacteria fluorescence induced by the DAPI after nucleic acid staining and UV excitation was also specifically recorded using a 405 ± 30 nm band pass-filter placed just in front of the photodetector. All the parameters were acquired in logarithmic scale, and the trigger acquisition was based on the right angle light scatter intensity in order to detect all the particles in the sample (bacteria, debris). The data were acquired in real time and list-mode using the SUMMIT 4.3 software (Dako, Dk). Flow cytometry data files (in Flow Cytometry Standard 3.0 format) were also analyzed using the same software.

In order to avoid doublets and hard coincidences, samples were diluted in sterile medium in order to keep a flow rate lower than 8,000 events analysed

per second, a mandatory condition to ensure accurate counting. The sheath tank of the flow cytometer was filled with 0.2 µm filtered distilled water. Sheath pressure was kept constant at 60.0 PSI, and sample pressure at 60.1 PSI. Analyses were performed during 1 minute. The exact volume analyzed was derived from a preliminary calibration phase during which a sample was weighed before and after a 3 minutes analysis in order to determine the average flow rate (in $mm^3\ s^{-1}$). The procedure is repeated 3 times and the average flow rate is calculated. Bacteria were optically resolved from the cytogram Right angle light scatter (au) *versus* DAPI fluorescence intensity (au). A manual region was drawn around them and the SUMMIT software automatically displayed the bacteria count. Dividing the bacteria count by the volume analyzed provides the cell abundance.

CHAPTER IV

Application of the DEB theory on data obtained in a perturbed environment

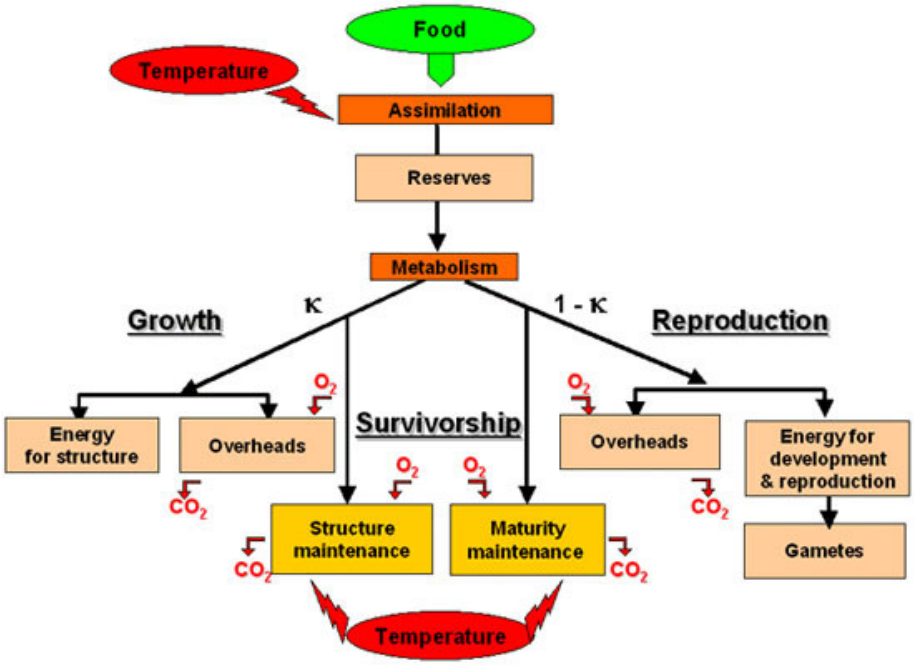

Abstract

We developed a model for the biodegradation of organic compounds based on a set of data from an experiment with pulse donation of substrate. Experiments were realised with a monospecific bacterial strain and a unique carbon substrate. The mechanistic model has a reserve compartment as well as two maintenance terms and represents an application of the Dynamic Energy Budget (DEB) theory. The measured variables were the dissolved organic carbon (DOC) corresponding to the substrate concentration in addition to other DOC forms, and the particulate organic carbon (POC) corresponding to the carbon bacterial biomass. The model, comprising 4 state variables and 7 parameters, matches the data very well, but the complexity of this model makes it difficult to implement it in ecosystem models. We showed that the DEB model can be simplified to a model with two state variables and a logistic-like growth, with a variable carrying capacity. The other two state variables of the DEB model reduce to functions of the state variables of the simplified model. Using parameter values that correspond to the experimental results, simulations of the DOC and POC kinetics for the DEB model and its simplification are similar. The reduction of the DEB model to a model with two state variables offers the advantage that the reduced model can be numerically integrated with simplicity. Computational costs are greatly decreased, which is of great interest for further coupling of this bacterial growth model with biogeochemical and hydrodynamical transport models. Moreover, this simplification gives a mechanistic basis to the logistic equation.

I. The DEB theory for micro-organisms

1. General concepts

The Dynamic Energy Budget (DEB; (Kooijman 2000)) theory provides rules for uptake and use of energy by organisms. It exploits conservation laws and stoichiometric constraints. Energy and mass fluxes through the organisms and their surroundings are central in the DEB framework. One advantage of this theory is that, due to its mechanistic basis, small changes are sufficient to adapt the model from one to another organism.

The DEB theory assumes that an organism is partitioned into a reserve and a structural compartment. The structural biomass is continuously degraded and reconstituted, whereas the reserve material is used and replenished. The DEB theory focuses on three major processes: assimilation, maintenance and growth. Food (substrate) uptake is proportional to the surface area of the organism. The food (or substrate) is always assimilated in the reserve compartment, and reserves are subsequently used to pay the several costs. For each species of organism, a fixed part κ of this catabolic flux is used to pay somatic maintenance and growth, the remaining $(1- \kappa)$ is used for development and/or reproduction. This law is called the "κ rule" in the DEB context. Typically three life stages are delineated, embryos don't feed or reproduce, juveniles feed but don't reproduce and adults feed and reproduce. For micro-organisms, which classify as juvenile, somatic and maturity maintenance can be combined and growth and maturation can be combined, which makes that we can set $\kappa = 1$ without loss of generality. Maintenance has always priority above growth, thus growth stops if all the mobilised reserve for maintenance + growth is used for maintenance. The latter is paid to maintain the integrity of the cells and to maintain gradients across the cell membrane. Maintenance costs are assumed to be proportional to the structural volume. The specific growth costs are assumed to be constant during the life of an organism. This hypothesis implies that the structural biomass has a constant chemical composition: this is known as the strong homeostasis assumption in the DEB framework. It is also assumed that reserves respect the strong homeostasis assumption. However, since the proportion of structure and reserve can change during the life of an organism, the macro-chemical composition of the whole organism can vary.

DEB theory provides also rules for the coupling between energy and mass fluxes. Experimental observations are mostly made on mass. Thus, we need robust rules to compare observations to model outputs. Models resulting

from the DEB theory are also constructed from mass balance equations. Thus, flux of one element may be deduced from fluxes of other elements. In the last part of this chapter, we demonstrate how dioxygen flux can be linked to assimilation, maintenance and growth processes, thus to carbon fluxes. This result is supported by experimental data.

2. The DEB theory for bacteria

i. General considerations

To deal with bacteria, we need to state some assumptions. First of all, bacteria are treated as V1-morph, that is as organism growing only in one dimension. For V1-morph individuals, the surface area is always proportional to the volume at the power 1. The main advantage of modelling bacteria as V1-morphs is that a population behaves in the same way as an individual. Consequently, the theory of structured population dynamics is not required to describe a population of bacteria, as we can work with the sum of the structural and reserve masses of the individuals.

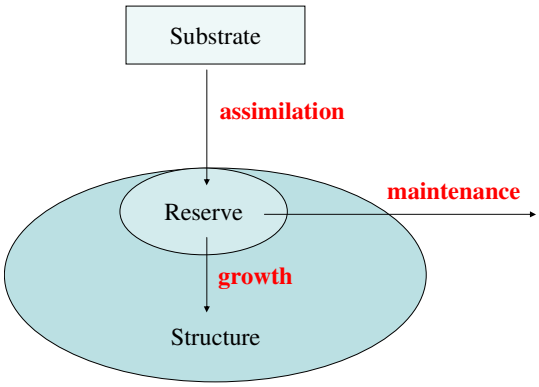

Figure IV-1: General scheme of fluxes in the DEB theory for micro-organisms. Words in black represent state variables of the model and words in red represent the main processes involved in the model. An individual is divided in a reserve and a structure compartment, and the reserve play central role as it fuels energy through the organism.

The basic DEB theory assumes three main processes: assimilation (of one substrate), maintenance (from a unique reserve) and growth (of one kind of structural volume) (Figure IV-1). In the case of bacteria, reproduction and development processes are not required since they are combined with growth and maintenance, respectively. This simplifies the model. The theory gives

also rules for adapting the general scheme for the assimilation of several substrates. In this case, the model requires several kinds of reserves, typically one for each kind of substrate. Phototrophy is an example where two substrates (carbon dioxide and light) are required for one reserve (carbohydrate). There is a flux of maintenance from each kind of reserve, but stoichiometric restrictions apply for how the various reserves fuel the growth of a single structural component. This generates a need to define the fate of fluxes that arrive at the synthesizing unit for growth, but are rejected. Chemical compounds, such as lipids, carbohydrates and proteins belong to one or more reserves and/or to structure. In this study, the model only considers the carbon and then is constructed by considering only one substrate, one reserve and one structure. Nevertheless, some improvements in the model conception are made according to the experimental results (see II).

Table IV-1 summarizes the various symbols used in this study for the basic DEB theory. Other variables will be added during the study.

ii. Uptake

The uptake rate is proportional to the surface area of the organism. For bacteria, substrate absorption is realised across the cell membrane. The uptake rate is proportional to the maximum specific uptake rate, a hyperbolic functional response and the structural mass of an individual (because we treat bacteria as V1-morphs). The first advantage of using a hyperbolic functional response is that a hyperbolic function of a hyperbolic function results in a hyperbolic function. We thus do not need to know the exact number of steps for the absorption process. Secondly, the hyperbolic functional response comprises only one parameter: the half-saturation constant K. The consumption of the substrate can thus be expressed as the following equation:

$$\frac{dX}{dt} = J_{X_m} \; f \; M_V \qquad \text{(IV.1)}$$

$f = \dfrac{X}{K + X}$ is the functional response

Table IV-1: Description of variables, parameters and symbols used in the DEB theory. The unity "J" (joule) is used for symbols dealing with energy.

Symbol	Equiv.	Unit	Description
State Variables			
M_E		mM C	Reserve mass
m_E	$\frac{M_E}{M_V}$	-	Reserve mass relative to the structural body mass
M_V		mM C	Structural body mass
Parameters			
J_{X_m}		mM C h^{-1}	Maximum uptake rate
K		mM C	Half-saturation constant
k_E		h^{-1}	Reserve turnover rate
General symbols			
J_{*1*2} or J_{*1}^{*2}		mM C h^{-1}	Flux of compound $*_1$ associated with process $*_2$
j_{*1*2}	$\frac{J_{*1*2}}{M_V}$	h^{-1}	Specific flux of compound $*_1$ associated with process $*_2$
y_{*2*1} or Y_{*2*1}		-	Yield coefficient of compound $*_1$ on compound $*_2$
n_{*1*2}		-	Number of atoms of element $*_1$ present in compound $*_2$
$\dot{p}_{*1}$		J h^{-1}	Energy flux (power) of process $*_1$
κ		-	Fraction of catabolic power energy spent on maintenance plus growth

Table IV-1 continued

Processes ($\dot{p}_*$)	
A	Assimilation
C	Catabolism
M	Maintenance
G	Growth
General compounds	
Organic	
X	Substrate
V	Structure
E	Reserve
P	Product
Mineral	
C	CO_2
H	H_2O
O	O_2
N	nitrogenous waste (ammonia)

iii. Reserve and structural body masses dynamics

The substrate is converted into reserve during the assimilation process with a fixed conversion efficiency y_{EX}. Reserve is used for maintenance and growth. Thus, the change in the amount of reserve is a function of the input (assimilation) and the energy requirements of the different cellular processes (maintenance + growth). Dynamic of the reserve mass can be described as follows:

$$\frac{dM_E}{dt} = J_{EA} - J_{EC} \qquad \text{(IV.2)}$$

where J_{EA} and J_{EC} represent the flux of reserve related to assimilation and catabolism, respectively. J_{EA} is directly related to the assimilation of substrate (equation IV.1) by using the conversion efficiency y_{EX} whereas the reserve used for catabolism (J_{EC}) is the combination of the maintenance (J_{EM}) and growth (J_{EG}) uses of the reserve.

$$J_{EA} = y_{EX} \frac{dX}{dt} = y_{EX}\ J_{X_m}\ f\ M_V$$
$$J_{EC} = J_{EM} + J_{EG}$$

The costs for maintenance are proportional to structural biomass and the costs for growth to the change in the structural biomass:

$$J_{EC} = j_{EM}\ M_V + y_{EV} \frac{dM_V}{dt} \qquad \text{(IV.3)}$$

where y_{EV} and j_{EM} represent the yield coefficient from the structure to the reserve and the maintenance flux from reserve, respectively.

The reserve density dynamics m_E may be defined as the specific assimilation flux minus m_E loss, due to growth and maintenance. As k_E is the turnover rate of reserve, we can write:

$$\frac{dm_E}{dt} = j_{EA} - k_E m_E \qquad \text{(IV.4)}$$

From equation (IV.2) we deduce:

$$J_{EC} = J_{EA} - \frac{dM_E}{dt} = J_{EA} - M_V \frac{dm_E}{dt} - m_E \frac{dM_V}{dt} \qquad \text{(IV.5)}$$

From equations (IV.3) and (IV.5):

$$y_{EV}\frac{dM_V}{dt}+j_{EM}\ M_V = J_{EA}-M_V\frac{dm_E}{dt}-m_E\frac{dM_V}{dt} \qquad \text{(IV.6)}$$

From equations (IV.6) and (IV.4):

$$\left(y_{EV}+m_E\right)\frac{dM_V}{dt} = J_{EA}-M_V\left(j_{EA}-k_E\ m_E\right)-j_{EM}\ M_V$$

$$\frac{dM_V}{dt} = \frac{k_E\ m_E\ M_V - j_{EM}\ M_V}{y_{EV}+m_E}$$

$$\frac{dM_V}{dt} = \frac{k_E M_E - j_{EM}\ M_V}{y_{EV}\ M_V + M_E}M_V \qquad \text{(IV.7)}$$

From equations (IV.2), (IV.3) and (IV.7), we can now deduce the reserve mass equation:

$$\frac{dM_E}{dt} = J_{EA}-J_{EC} = y_{EX}\ J_{X_m}\ f\ M_V - y_{EV}\frac{dM_V}{dt} - j_{EM}\ M_V$$

$$\frac{dM_E}{dt} = y_{EX}\ J_{X_m}\ f\ M_V - j_{EM}\ M_V - y_{EV}\frac{k_E M_E - j_{EM}\ M_V}{y_{EV}\ M_V + M_E}M_V \qquad \text{(IV.8)}$$

iv. Complete growth model

Finally, from equations (IV.1), (IV.7) and (IV.8) we can write the complete growth model:

$$\begin{cases} \dfrac{dX}{dt} = J_{X_m}\ \dfrac{X}{K+X}\ M_V \\ \dfrac{dM_E}{dt} = y_{EX}\ J_{X_m}\ \dfrac{X}{K+X}M_V - j_{EM}\ M_V - y_{EV}\dfrac{k_E M_E - j_{EM}\ M_V}{y_{EV}\ M_V + M_E}M_V \\ \dfrac{dM_V}{dt} = \dfrac{k_E M_E - j_{EM}\ M_V}{y_{EV}\ M_V + M_E}M_V \end{cases} \qquad \text{(IV.9)}$$

This model is the basic model for V1-morph individuals. Changes due to addition of processes must be made from this model.

II. Mechanistic model simplification for implementation in biogeochemical models: case of bacterial DOC degradation in a variable system

Eichinger M, Kooijman SALM, Sempéré R and Poggiale JC
Submitted to Ecological Modelling

1. Introduction

The dissolved organic carbon (DOC) is recognized as the largest pool of reduced carbon on the planet (Hedges 1992, Carlson & Ducklow 1995). This DOC is almost exclusively consumed by bacteria in the water column, and is thus either transformed in CO_2 or transferred to higher trophic level. Recent studies have indicated that a better understanding of organic matter (OM) dynamics, thus of DOC dynamics, in models requires an appropriate knowledge of bacterial dynamics (Talin et al. 2003). However, despite their ecological role, bacteria are rarely or poorly represented (Arhonditsis & Brett 2004). Most biogeochemical models use the Monod model (Monod 1942), that is Michaelis-Menten kinetics (Michaelis & Menten 1913), to describe bacterial growth (Baretta-Bekker et al. 1995, Blackburn et al. 1996, Anderson & Williams 1998, 1999, Lancelot et al. 2002, Raick et al. 2005). Later extensions included maintenance process (known as the Marr-Pirt model) (Marr et al. 1963, Pirt 1965) as a kind of death rate (but forming different products).

However, some studies have demonstrated that the Monod or Marr-Pirt models are too simplistic and that the addition of a reserve compartment as well as a maintenance term is necessary (1) to fit bacterial dynamics in a food chain (Kooi & Kooijman 1994) and (2) to obtain the area of bacterial depletion, as function of the C:P and C:N ratio in chemostat and batch experiments (Martinussen & Thingstad 1987). Indeed, this reserve compartment and the maintenance term may play crucial roles in bacterial dynamics as the first one acts as a buffer and allows bacteria to survive during depletion period and the second one represents the energetic cost for a cell to survive. The dynamic energy budget (DEB) theory (Kooijman 2000) accounts for these two processes. This theory has been widely tested against experimental data and used to construct numerous models for bacterial dynamics, e.g. trophic chains in a chemostat (Kooi & Kooijman 1994), biodegradation of multiple substrates (Brandt et al. 2003), adaptation to changing substrate availability (Brandt et al. 2004) and application of mass energy conservation laws (Kooijman et al. 1999).

Nowadays, two major currents concerning modelling studies are in expansion: the development of mechanistic models that account for more and more realistic processes, as stated previously, and the improvement of ecosystem models which is possible due to the progress in modern computing power and the advances in ecosystem and ecological theory (Fulton et al. 2004, Raick et al. 2006). Developing mechanistic models is a major challenge in oceanography as it allows improving our understanding of how the marine organisms respond to direct or indirect environmental or anthropic perturbations. However, the inclusion of complex formulations in biogeochemical models often leads to model that are inexorably too large, difficult to parameterise and to deal with (Raick et al. 2006). A long pattern of studies try to estimate the effect of physiological details on model performance (Murray & Parslow 1999, Fulton et al. 2004, Raick et al. 2006, Lawrie & Hearne 2007). The methods used to investigate the impact of complexity on model performance are various: some authors compare several levels of sophistication in the model formulation and compare their performance to observations (Fulton et al. 2004, Baklouti et al. 2006b, Raick et al. 2006) or compare the qualitative dynamics of two levels of models (Murray & Parslow 1999, Baird et al. 2003, Guven & Howard 2007). These studies generally lead to the conclusion that simpler models do capture the crucial dynamics of the complex models. However, to construct a mechanistic model and testing its performance towards reduced models, we need biological information (Flynn 2005). The relevant physiological processes are poorly known (Baird et al. 2003) and the results of experiments carried out on bacterial populations are typically too scattery to allow the application of complex models.

Models describing bacterial dynamics are often based on biodegradation experiments with batch cultures, i.e. with a certain quantity of substrate and of bacteria in the beginning of the experiment and where the system evolves without any modification during the time course of the experiment (Zweifel et al. 1993, Carlson & Ducklow 1996, Sempéré et al. 2000, Carlson et al. 2002, Sempéré et al. 2003, Cherrier & Bauer 2004, Eichinger et al. 2006). The Monod model is typically used to fit data from batch experiments and also to describe bacteria-substrate interactions in biogeochemical models. The chemical composition in ecosystems can differ substantially for that used in the batch cultures, which can affect the biodegradation process. Another weakness of this scale transfer from laboratory to the ecosystem environment is that the local environment in the ecosystem is typically much more dynamic. Organisms are continuously subjected to perturbations and the bacterial carbon demand is fuelled by episodic input of dissolved OM. Indeed, food is not continuously available in natural environment (Hanegraaf

& Kooi 2002), contrary to the batch experiments generally carried out to determine parameters as the bacterial growth efficiency (del Giorgio & Cole 1998). Long periods of absence of one or more nutrients (Konopka 1999) alternate with short periods of high substrate availability. The transient behaviour of DOC is very dynamic: the DOC concentration (1) shifts during a phytoplankton bloom (Miki & Yamamura 2005b), (2) varies greatly due to the DOC release by phytoplankton (Grossart & Simon 2007), fluctuates (3) seasonally, as well as non-periodically, as temporal input due to the rain (Miki & Yamamura 2005a), or (4) cyclically as a result of the hydrological effects in floodplains, like in Amazonian ecosystems (Farjalla et al. 2006) or in the Okavango Delta of Botswana (Mladenov et al. 2005, Mladenov et al. 2007), (5) changes by upwelling events (Mcmanus & Peterson 1988). This episodic character of the DOC as substrate for heterotrophic bacteria has thus to be considered in the experiments as well as in the models.

Here we describe in the first section an experiment that has specifically been set up to mimic the availability of substrate under field conditions. Then, we specify a mechanistic model, constructed from the DEB theory (Kooijman 2000) and taking into account the reserve and the maintenance processes, as these latter processes seem necessary when dealing with variable environment. In the next section we simplify it for implementation in biogeochemical models. The mechanistic model and its simplification are dynamically compared in the fourth section. The results are discussed in a wider modelling context in the last section.

2. Description of the experiments

The carbon substrate pyruvate was periodically added during 10 days to a batch culture of the bacterial strain *Alteromonas infernus*. Since other nutrients are in excess, the fed-bacth culture was carbon-limited with pyruvate as the only carbon source. The culture was incubated in a temperate room in the dark at 25 ± 1°C and gently swirled. The initial carbon substrate concentration [C(0)] was about 1.6 C mM C, whereas substrate pulses of [C(0)] concentration were added every 48 hours. This pulse period was chosen so that bacteria were starved between two pulses, allowing the study of the cell maintenance and the relevance of a reserve compartment. The experiment lasted approximately 230 hours, so there were 5 pulses, including the initial pulse at time zero. The measured variables are DOC, which includes the substrate and all other DOC forms that may be produced during the time course of the experiment, and particulate organic carbon (POC), which corresponds to the bacterial biomass-carbon. The reproducibility of the results of this experiment was demonstrated (Eichinger et al., unpublished

data), justifying the use of deterministic methods to describe the DOC assimilation and bacterial growth.

3. Specification of the DEB model

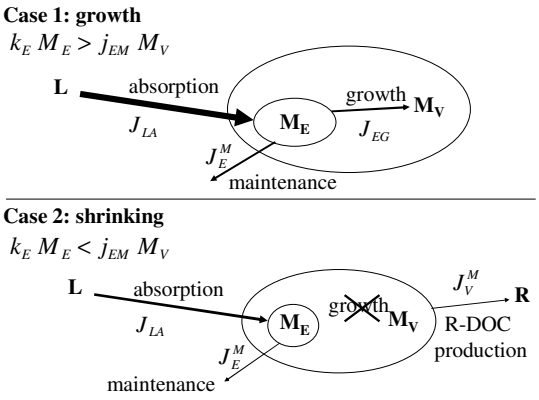

Figure IV-2: Schematic representation of the switch DEB model. The several compounds involved are: L (substrate), M_E (reserve mass), M_V (structural body mass) and R (refractory DOC or R-DOC). The various processes involved are: absorption (A), maintenance (M) and growth (G). J_{*1}^{*2} or J_{*1*2} represent the absolute flux of compound $_{*1}$ associated with process $_{*2}$. The notation J_{*1}^{*2} is here specifically used when dealing with maintenance.

The model was constructed on the basis of the DEB theory (Kooijman 2000) using a single reserve and a single structure compartment for a bacterial cell (Figure IV-2). We also assumed that the surface of the cell (which is linked to the uptake rate) is proportional to the structural volume (which is linked to the maintenance costs). This is the defining property for what is called V1-morphs. A population consists of a set of growing and dividing individuals, which all divide at a particular structural volume. It has been shown that in this case, there is no need to distinguish between the level of the individual and that of the population (Kooijman 2000, p. 315) and we can work with the sum of the structural and reserve masses of the individuals. Carbon substrate (and nutrients) is transformed into reserve (M_E), and reserve is mobilised at a rate that depends on the reserve density (m_E), i.e.

the ratio of the amounts of reserve and structure (M_V). As the experiment exhibits starvation period between two pulses, the model was constructed by assuming two maintenance fluxes: one from the reserve (J_E^M) and one from the structural body mass (J_V^M). Maintenance is paid from mobilized reserve if the flux is large enough, but otherwise structure is used to pay the remaining part of the maintenance costs, which causes shrinking of the cell. Growth is fuelled from the mobilized reserve flux minus the maintenance costs, so maintenance has priority over growth. We use a switch formulation as discussed in Tolla et al. (2007) to describe the use of one and/or another type of maintenance. Since the reserve dynamics is such that the reserve density can never be equal to zero (exactly), maintenance is never fully paid from structure. Part of it is always paid from reserve.

The data showed a DOC accumulation during the experiment (Figure IV-3). We modelled this by fractioning the DOC pool into two components: labile DOC (L-DOC) corresponding to the substrate, and non-labile or refractory DOC (R-DOC) that we assume to originate from structure when it is used to pay maintenance costs. The detailed nature of this fraction is unknown, but it might consist of cell wall material (Nagata 2000) or of exopolysaccharide (EPS) when bacteria are in stationary phase (Raguénès et al. 1997). Consequently, the model comprises four state variables:

L, the L-DOC concentration, which represents the pyruvate concentration (mM C)

R, the R-DOC concentration, which represents the refractory DOC pool (mM C) that accumulates during the experiment

M_E, the reserve mass (mM C)

M_V, the structural body mass (mM C)

The changes in these state variables are specified as follows:

$$\frac{dL}{dt} = -\,\text{absorption}$$

$$\frac{dM_E}{dt} = \text{efficiency}\left(\text{L} \rightarrow \text{M}_\text{E}\right) \text{x absorption} - \textbf{reserve maintenance} - \left\{ \begin{array}{ll} \dfrac{1}{\text{efficiency}\left(\text{M}_\text{E} \rightarrow \text{M}_\text{V}\right)} \text{x } \textbf{growth} & \textit{if } \text{growth} > 0 \\ \textbf{structural maintenance} & \textit{if } \text{growth} < 0 \end{array} \right\}$$

$$\frac{dM_V}{dt} = \left\{ \begin{array}{ll} +\,\textbf{growth} & \textit{if } \text{growth} > 0 \\ -\,\textbf{structural maintenance} & \textit{if } \text{growth} < 0 \end{array} \right\}$$

$$\frac{dR}{dt} = \left\{ \begin{array}{ll} 0 & \textit{if } \text{growth} > 0 \\ \text{efficiency}\left(\text{M}_\text{V} \rightarrow \text{R}\right) \text{x } \textbf{structural maintenance} & \textit{if } \text{growth} < 0 \end{array} \right\}$$

where only the maintenance and the growth formulations (bold characters) change according to the switch. In formulae we have:

$$\frac{dL}{dt} = -j_{LAm}\,\frac{L}{K+L}\,M_V$$

if $k_E\,M_E > j_{EM}\,M_V$

$$\begin{cases} \dfrac{dM_E}{dt} = j_{LAm}\,y_{EL}\,\dfrac{L}{K+L}\,M_V - j_{EM}\,M_V \\ \qquad\qquad - y_{EV}\,\dfrac{k_E\,M_E - j_{EM}\,M_V}{M_E + y_{EV}\,M_V}\,M_V \\ \dfrac{dM_V}{dt} = \dfrac{k_E\,M_E - j_{EM}\,M_V}{M_E + y_{EV}\,M_V}\,M_V \\ \dfrac{dR}{dt} = 0 \end{cases}$$

if $k_E\,M_E < j_{EM}\,M_V$

$$\begin{cases} \dfrac{dM_E}{dt} = j_{LAm}\,y_{EL}\,\dfrac{L}{K+L}\,M_V - k_E\,M_E \\ \qquad\qquad - \dfrac{j_{EM}\,M_V - k_E\,M_E}{M_E + \frac{j_{EM}}{j_{VM}}\,M_V}\,M_E \\ \dfrac{dM_V}{dt} = -\dfrac{j_{EM}\,M_V - k_E\,M_E}{M_E + \frac{j_{EM}}{j_{VM}}\,M_V}\,M_V \\ \dfrac{dR}{dt} = y_{RV}\,\dfrac{j_{EM}\,M_V - k_E\,M_E}{M_E + \frac{j_{EM}}{j_{VM}}\,M_V}\,M_V \end{cases}$$

For a detailed explanation of the model construction, see Appendix IV-A. When there is high substrate concentration (after a pulse), (1) the maintenance is fully paid from reserve ($\text{maintenance} = j_{EM}\,M_V$) and generates inorganic carbon products as CO_2 not considered in this study, (2) growth is positive ($\text{growth} = \dfrac{k_E\,M_E - j_{EM}\,M_V}{M_E + y_{EV}\,M_V}\,M_V$) allowing an increase of the structure and (3) there is no R-DOC production. On the contrary, when there is not enough (mobilized) reserve, which happens at a particular value of the reserve mass M_E relative to the structural body mass M_V, (1) the maintenance is realised from reserve plus structure (maintenance = $k_E\,M_E + \dfrac{j_{EM}M_V - k_E\,M_E}{M_E + \frac{j_{EM}}{j_{VM}}\,M_V}\,M_E$) the former still producing inorganic carbon, (2) structural growth is thus negative (growth= − structural maintenance = $-\dfrac{j_{EM}M_V - k_E\,M_E}{M_E + \frac{j_{EM}}{j_{VM}}\,M_V}\,M_V$) and (3) there is R-DOC production proportional to the decrease in structure.

Parameter estimation is based on the minimization of the sum of squared deviations of model predictions to data points, using the Nelder Mead's simplex method (Lagaria et al. 1998). To compare the state variables to the data values, we assumed that:

$$DOC = L + R$$
$$POC = M_V + M_E$$

Description and values of model parameters are given in Tables IV 2 and IV-3.

We conclude that our model fits qualitatively and quantitatively DOC and POC data very well (Figure IV-3).

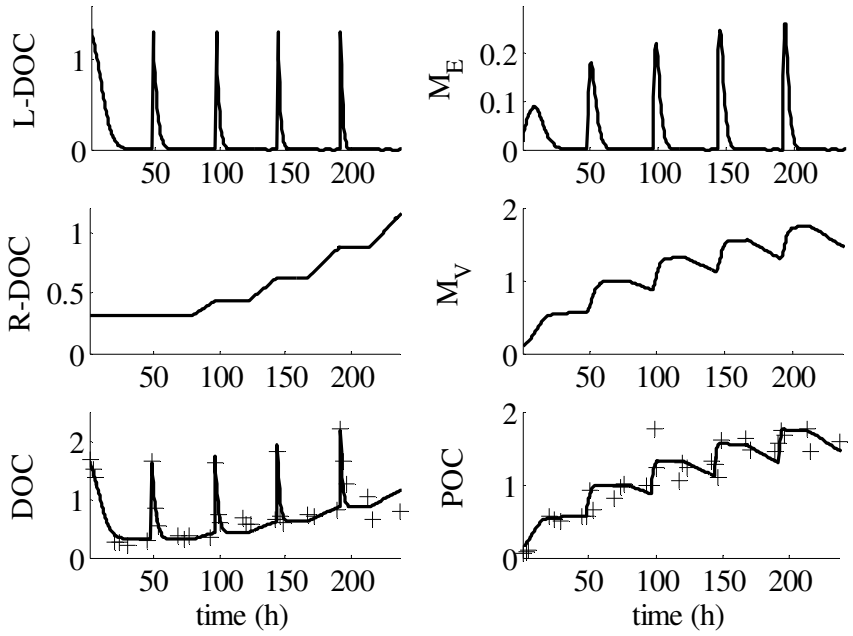

Figure IV-3: Dynamics of DOC (mM C) (left part) and bacterial state variables (mM C) (right part) for the switch DEB model. The crosses represent the data and the curves the outputs of the model with the fitted parameter set for the switch DEB model (Table IV-2). We remember that: $DOC = L + R$ and $POC = M_V + M_E$.

Table IV-2: Description and units of all variables and parameters used in this study.

Symbol	Equiv.	Unit	Description
State Variables			
L		mM C	L-DOC concentration
M_E		mM C	Reserve mass
m_E	$\frac{M_E}{M_V}$	-	Reserve mass relative to the structural body mass
M_V		mM C	Structural body mass
R		mM C	R-DOC concentration
Parameters in the switch DEB model			
j_{LAm}		h^{-1}	Maximum specific absorption rate
K		mM C	Half-saturation constant
y_{EL}		-	Yield coefficient from L-DOC to reserve masses
y_{EV}		-	Yield coefficient from structural to reserve masses
k_E		h^{-1}	Reserve turnover rate
j_{EM}		h^{-1}	Maintenance flux from reserve mass
j_{VM}		h^{-1}	Maintenance flux from structural mass
y_{RV}		-	Yield coefficient from structure to R-DOC
Parameters in the simplified model			
α	$\frac{j_{LAm}}{K}$	mM C^{-1} h^{-1}	Ratio between the maximum specific absorption rate and the half-saturation constant
r	k_E	h^{-1}	Growth rate
κ		mM C	Carrying capacity

Table IV-3: Parameter and initial condition values estimated for the switch DEB model.

Parameters	Values
α	0.484
k_E	0.603
y_{EL}	0.500
y_{EV}	1.492
j_{EM}	0.000
j_{VM}	0.008
y_{RV}	1.000
Initial conditions	
$C(0)$	1.369
$M_E(0)$	0.000
$M_V(0)$	0.098
$R(0)$	0.314

4. Simplification of the DEB model

i. Variable aggregation

Because the *L* values were negligible compared to the estimated *K* value, we can eliminate the maximum uptake rate and the half-saturation constant, and use a linear equation for the absorption with a new parameter: $\alpha = \frac{j_{LA_m}}{K}$ and $\frac{dL}{dt} = -\alpha L M_V$. However, despite the current improvement of computing power, such a model, with 4 state variables and now 7 parameters for only heterotrophic bacteria living on a single substrate shall be difficult to implement in a general biogeochemical and circulation models (Murray & Parslow 1999, Raick et al. 2006).

We need further simplification for such applications when scaling up from the physiological to the ecosystem level. Indeed, if the description of a

given process at the physiological level generally requires a fine scale of observation that subsequently generates intricate formulations, the resulting model can ultimately be simplified and adapted to a larger scale of observation (Baklouti et al. 2006a). Several methods exist to reduce a model, as statistical approaches or aggregation of state variables, where some processes are reformulated, short-circuited or not represented (Iwasa et al. 1989, Raick et al. 2006). Lots of studies use the aggregation of variables, but they often do that in a theoretical way without any data support, for example by using a static instead of a dynamical model when working on large time scale (Baklouti et al. 2006b) or by aggregating the physiological processes into less equations (Fulton et al. 2004).

In this study, the model was simplified by considering the mass balance on model equations and by applying the perturbation theory (Appenix IV-B). According to the reserve mass value to the structural mass value (switch value), we have considered several mass balances. In the first case (when growth is positive), C_{T_1} is the total C-mass in the system and is expressed as a weighted sum of the three state variables L, M_E and M_V (as derivative of R is null in this case). Using the perturbation theory, it results that C_{T_1} is not constant but varies as a function of time. M_E can now be expressed as a weighted sum of C_{T_1} and the two other state variables L and M_V. We also demonstrated that M_V can be described by a logistic-like function, where the growth rate (r) equals the reserve turnover rate of the DEB model (k_E) and the carrying capacity κ_1 is a function of L and C_{T_1}. In the second case (when growth is negative), mass balance is fractionated into two parts: C_{T_2} is a weighted sum of L and M_E, C_{T_3} of M_V and R. C_{T_3} is always constant, thus R can be expressed as a function of C_{T_3} and M_V. Using again the perturbation theory, we demonstrated that C_{T_2} is also constant. Thus M_E dynamic can be easily expressed as a function of C_{T_2} and L. The equation of M_V could also be reduced to a logistic-like growth where the growth rate still equals the reserve turnover rate of the DEB model (k_E) but where the carrying capacity κ_2 is a function of L and M_V, which complicates the expression. Consequently, the complete DEB model with four state variables reduces to a system of two differential equations (derivatives of L and M_V),

dynamics of M_E and R being estimated as functions of L, M_V and the three weighted sums of C-mass C_{T_*}.

$$\frac{dL}{dt} = -\alpha\, L\, M_V$$

if $M_E\, k_E > j_{EM}\, M_V$

$$\frac{dM_V}{dt} = r\, M_V \left(1 - \frac{M_V}{\kappa_1\left(L, C_{T_1}\right)}\right)$$

if $M_E\, k_E < j_{EM}\, M_V$

$$\frac{dM_V}{dt} = \frac{k_E\, C_{T_2}(0) - k_E\, y_{EL}\, L - j_{EM} M_V}{C_{T_2}(0) - y_{EL}\, L + \frac{j_{EM}}{j_{VM}} M_V} M_V$$

$$\kappa_1\left(L, C_{T_1}\right) = \frac{C_{T_1}(t) - y_{EL}\, L(t)}{y_{EV}}$$

$$C_{T_2}(0) = y_{EL}\, L(0) + M_E(0)$$

$$C_{T_1}(t) = C_{T_1}(0)\, e^{-\frac{j_{EM}}{y_{EV}} t}$$

$$M_E(t) = C_{T_2}(0) - y_{EL}\, L(t)$$

$$C_{T_1}(0) = y_{EL}\, L(0) + M_E(0) + y_{EV}\, M_V(0)$$

$$R(t) = y_{RV}\left(C_{T_3}(0) - M_V(t)\right)$$

$$M_E(t) = C_{T_1}(t) - y_{EL}\, L(t) - y_{EV}\, M_V(t)$$

$$C_{T_3}(0) = M_V(0) - \frac{R(0)}{y_{RV}}$$

ii. Comparison between the complete and the simplified models

The DEB model and its simplification were dynamically compared (Figure IV-4), by using the same parameter values (Table IV-3). It results that both models exhibit perfectly the same dynamics, even if the simulation time is longer than the time of the experiment. However, the simplified model comprises only two state variables, L and M_V, dynamics of M_E and R being estimated later as functions of both state variables, and the three weighted sums of C-mass C_{T_*}. C_{T_2} and C_{T_3} are constant, but C_{T_1} is a function of time and has thus to be numerically integrated. As it only depends on time, C_{T_1} can be integrated independently, and its values can be recorded to estimate afterward L and M_V dynamics. Finally, once L and M_V have been integrated, dynamics of M_E and R can be estimated. Contrary to this, all state variables of the DEB model need to be numerically integrated at the same time. The reduction of the DEB model in a model with two differential

equations offers the advantage that the simpler model can be numerically integrated with simplicity.

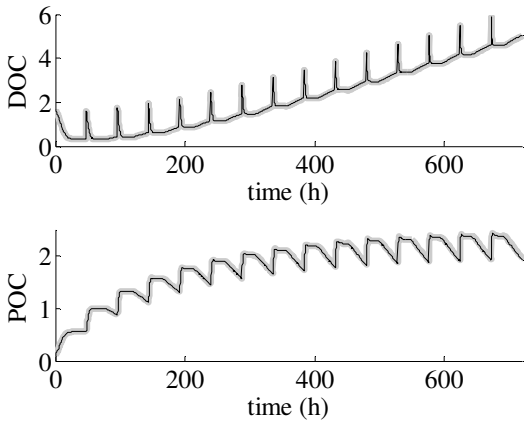

Figure IV-4: Dynamics of DOC (mM C) and POC (mM C) for the switch DEB (dark line) and the simplified DEB (grey line) models for a time equivalent to 15 pulses. Parameter values are the same for both models (Table IV-3) and $DOC = L + R$ and $POC = M_V + M_E$ for both models.

5. Bacterial growth in biogeochemical models

Biogeochemical models often use the Monod model to describe bacterial growth (Baretta-Bekker et al. 1995, Anderson & Williams 1998, 1999, Lancelot et al. 2002, Raick et al. 2006). However, we have proven that growth formulation (when growth is positive) can be expressed by a logistic-like equation, with a variable carrying capacity depending on the total C-mass and L. The logistic growth equation is even easier than the Monod model, but gives exactly the same dynamics than the mechanistic DEB model. When growth is negative, the model also reduces to two state variables. For both parts of the models, not any processes were eliminated, but their expressions were simplified. Reserve mass dynamic is now described as a function of the total carbon mass, L and the structural mass when growth is positive, and as a function of L when growth is negative. On the same way, R only depends on the structural body mass dynamic. Thus, we do not loose any model performance, but we gain in model simplicity. This result is very different from most results obtained from previous studies

on model reduction, as these latter studies generally search the best compromise between model performance and complexity, but they always loose performance to gain simplicity (Murray & Parslow 1999, Fulton et al. 2004, Baklouti et al. 2006b, Raick et al. 2006). For example, by using a Monod or a Marr-Pirt model, which are both special cases of the DEB model and thus simplifications of our model, we should eliminate the reserve mass variable. DEB model simulations show that the reserve mass dynamics are indeed faster than structural mass dynamics, and that reserve mass values are also smaller than structural mass values (Figure IV-3). Consequently, reserve mass dynamics could be neglected compare to other state variable dynamics. This would effectively lead in further model simplifications. Nevertheless, it has still been proven that bacteria are able to store carbon in carbon limited systems (Baxter & Sieburth 1984) and in non carbon limited systems (Kooijman 2000). If growth is limited by nutrients such as nitrate or phosphate, the carbon reserve can become important (Kooijman and Troost, 2007). Confrontation between data and models have also demonstrated that the addition of the reserve and the maintenance are necessary in the Monod model to reproduce dynamics of a tri-trophic food chain including bacteria (Kooi & Kooijman 1994, Nisbet et al. 2000). To conclude, our model reduction doesn't reduce model insight as it still comprises necessary processes to describe bacterial growth. Computational costs are greatly decreased, which is of great interest for further coupling of this bacterial growth model with biogeochemical and hydrodynamical transport models (Baklouti et al. 2006b). Moreover, this simplification gives a mechanistic basis to the logistic equation considered as an empirical formulation.

6. Conclusion

The comparison of mechanistic models to their simplifications, and moreover based on data set as in this study, allows the examination of the effects of alternative process formulations on model behaviour (Murray & Parslow 1999). The outcome of this kind of study takes all its importance when we can demonstrated that a simplified model behaves and fits equally than the complex formulation, as the simpler model uses less number of parameters, less of development time and less time to validate, verify and calibrate (Fulton et al. 2004). This simplification step is crucial when we aim to implement mechanistic-growth model in global models. The coupling between experimentation and modelling approaches is very important as it allows model simplification on an experimental data basis, and not only on theoretical dynamics.

However, other experiments with other kinds of perturbations and inclusion of trophic relation should be done to test the relevance of a reserve compartment for marine bacteria. Our expectations for when reserve might be important should be tested with experiments. The application of mechanistic models is only feasible if the critical variables have been measured (Flynn 2005). However, these complex models are difficult to calibrate accurately without accurate data sets. Nevertheless, even if physiological details are not necessarily needed for global models, such models can still be used to identify critical variables: if a detailed model does not match an experimental data set well, it is likely that it does miss an essential process (Flynn 2005).

III. Implementation of the respiration in DEB models

1. Development of the O_2 flux formulation

The DEB theory allows the evaluation of respiration, i.e. the use of dioxygen. During the experiments, O_2 consumption was also measured at each point in time. We have thus decided to use this data set in a modelling purpose. This will give a best insight of bacterial metabolism. Since energy for the conversion of substrate into reserve is extracted from substrate, assimilation has an anabolic as well as a catabolic aspect. Moreover, energy for the reserve conversion into structure is extracted from reserve, thus growth has also an anabolic and a catabolic aspect. The O_2 flux was determined from Table IV-4.

From this table we can first deduce each yield coefficient by multiplying the line of the considered yield coefficient by the line of the considered element C, H, O or N, the sum of this multiplication being 0 to respect the mass balance law. For example, to determine Y_{OL}^{a}, we have to multiply the line of the anabolic assimilation with the line of oxygen indices:

$$Y_{HL}^{a} + 2\,Y_{OL}^{a} - 1 - n_{OE} = 0$$

$$Y_{OL}^{a} = \frac{\left(1 + n_{OE} - Y_{HL}^{a}\right)}{2}$$

Table IV-4: Table resuming yield coefficients, chemical indexes and specific rates associated to each process and state variable. Y^{*p}_{*2*1} is the yield coefficient of compound $_{*1}$ on element $_{*2}$ associated with the process $_{*p}$, which may be catabolic (cat or c) or anabolic (ana or a).

symbol	processes	C : CO_2	H : H_2O	O : O_2	N : NH_3	L : L-DOC	R : R-DOC	M_E : reserve	M_V : structure	specific rates
A_c	assim (cat)	Y^c_{CL}	Y^c_{HL}	Y^c_{OL}	Y^c_{NL}	-1	0	0	0	$j_{EA_c} = (y_{XE} - 1) j_{EA}$
A_a	assim (ana)	0	Y^a_{HL}	Y^a_{OL}	Y^a_{NL}	-1	0	1	0	$j_{EA_a} = j_{EA}$
M_E	E-maint	Y^c_{CE}	Y^c_{HE}	Y^c_{OE}	Y^c_{NE}	0	0	-1	0	j^M_E
M_V	V-maint	Y^c_{CV}	Y^c_{HV}	Y^c_{OV}	Y^c_{NV}	0	y_{RV}	0	-1	j^M_V
G_c	growth (cat)	Y^c_{CE}	Y^c_{HE}	Y^c_{OE}	Y^c_{NE}	0	0	-1	0	$j_{EG_c} = (1 - y_{VE}) j_{EG}$
G_a	growth (ana)	0	Y^a_{HE}	Y^a_{OE}	Y^a_{NE}	0	0	-1	1	$j_{EG_a} = y_{VE}\ j_{EG}$
C	carbon	1	0	0	0	n_{CL}	1	1	1	
H	hydrogen	0	2	0	3	n_{HL}	n_{HR}	n_{HE}	n_{HV}	
O	oxygen	2	1	2	0	n_{OL}	n_{OR}	n_{OE}	n_{OV}	
N	nitrogen	0	0	0	1	n_{NL}	n_{NR}	n_{NE}	n_{NV}	

In the same way, we can obtain each yield coefficient:

$$Y^c_{CL} = n_{CL} \qquad Y^c_{OE} = \left(n_{OE} - 2 - Y^c_{HE}\right)/2$$
$$Y^c_{HL} = \left(n_{HL} - 3\, n_{NL}\right)/2 \qquad Y^c_{NE} = n_{NE}$$
$$Y^c_{OL} = \left(n_{OL} - Y^c_{HL} - 2\right)/2 \qquad Y^c_{CV} = 1 - y_{RV}$$
$$Y^c_{NL} = n_{NL} \qquad Y^c_{HV} = \left(n_{HV} - n_{HR}\ y_{RV} - 3\, Y^c_{NV}\right)/2$$
$$Y^a_{CL} = 0 \qquad Y^c_{OV} = \left(n_{OV} - n_{OR}\ y_{RV} - Y^c_{HV} - 2\, Y^c_{CV}\right)/2$$
$$Y^a_{HL} = \left(n_{HL} - n_{HE} - 3\, Y^a_{NL}\right)/2 \qquad Y^c_{NV} = n_{NV} - n_{NR}\ y_{RV}$$
$$Y^a_{OL} = \left(n_{OL} - n_{OE} - Y^a_{HL}\right)/2 \qquad Y^a_{CE} = 0$$
$$Y^a_{NL} = n_{NL} - n_{NE} \qquad Y^a_{HE} = \left(n_{HE} - n_{HV} - 3\, Y^a_{NE}\right)/2$$
$$Y^c_{CE} = n_{CE} \qquad Y^a_{OE} = \left(n_{OE} - n_{OV} - Y^a_{HE}\right)/2$$
$$Y^c_{HE} = \left(n_{HE} - 3\, n_{NE}\right)/2 \qquad Y^a_{NE} = n_{NE} - n_{NV}$$

From this table, we can also deduce the mass balance matrix $j = Y\,.\,k$, where Y is the yield coefficient matrix and k the vector of specific rates. We can thus describe mathematically the O_2 flux j_O by the following formula:

$$j_O = Y^c_{OL}\ j_{EA_c} + Y^a_{OL}\ j_{EA_a} + Y^c_{OE}\ j^M_E + Y^c_{OV}\ j^M_V + Y^c_{OE}\ j_{EG_c} + Y^a_{OE}\ j_{EG_a}$$

As we have previously determined each yield coefficient, we can express the O_2 flux j_O in function of the various chemical indexes n_{*1*2}:

$$j_O = \frac{1}{2}\left[\begin{array}{l}
\left(n_{OL} - 2 - \dfrac{\left(n_{HL} - 3\, n_{NL}\right)}{2}\right)\left(y_{LE} - 1\right) j_{EA} + \left(n_{OL} - n_{OE} - \dfrac{\left(n_{HL} - n_{HE} - 3\, Y^a_{NL}\right)}{2}\right) j_{EA} + \\
\left(n_{OE} - 2 - \dfrac{\left(n_{HE} - 3\, n_{NE}\right)}{2}\right) j^M_E + \left(n_{OV} - n_{OR}\ y_{RV} - \dfrac{\left(n_{HV} - n_{HR}\ y_{RV} - 3\, Y^c_{NV}\right)}{2} - 2\left(1 - y_{RV}\right)\right) j^M_V + \\
\left(n_{OE} - 2 - \dfrac{\left(n_{HE} - 3\, n_{NE}\right)}{2}\right)\left(1 - y_{VE}\right) j_{EG} + \left(n_{OE} - n_{OV} - \dfrac{\left(n_{HE} - n_{HV} - 3\, Y^a_{NE}\right)}{2}\right) y_{VE}\ j_{EG}
\end{array}\right]$$

After having replaced each yield coefficient by the corresponding chemical indexes and grouped these indexes with respect to the various processes, we obtain the following formula:

$$j_O = \frac{1}{4}\left[\begin{array}{l}\left(4-3\,n_{NE}-2\,n_{OE}+n_{HE}\right)j_{EA}+\left(-4+3\,n_{NL}+2\,n_{OL}-n_{HL}\right)y_{LE}\;j_{EA}+\left(-4+3\,n_{NE}+2\,n_{OE}-n_{HE}\right)j_E^M+\\ \left(-4+3\,n_{NV}+2\,n_{OV}-n_{HV}+y_{RV}\left(4-3\,n_{NR}-2\,n_{OR}+n_{HR}\right)\right)j_V^M+\\ \left(-4+3\,n_{NE}+2\,n_{OE}-n_{HE}\right)j_{EG}+\left(4-3\,n_{NV}-2\,n_{OV}+n_{HV}\right)y_{VE}\;j_{EG}\end{array}\right]$$

The substrate L is pyruvic acid, with a known composition: $CH_3COCOOH$. If we report all elements to the number of carbon ($n_{CL}=1$), we thus obtain:

$$n_{CL}=1 \qquad n_{OL}=1$$
$$n_{HL}=4/3 \qquad n_{NL}=0$$

For sake of simplicity, especially to reduce the number of parameters to estimate, we have merged all chemical indexes according to their origin (reserve, structure or refractory material):

$$n_E = -n_{HE}+3\,n_{NE}+2\,n_{OE}$$
$$n_V = -n_{HV}+3\,n_{NV}+2\,n_{OV}$$
$$n_R = -n_{HR}+3\,n_{NR}+2\,n_{OR}$$

Now, we can write the O_2 flux as:

$$j_O = \left(1-\frac{n_E}{4}\right)j_{EA}-\frac{5}{6}\,y_{LE}\;j_{EA}-\left(1-\frac{n_E}{4}\right)j_E^M-\left(1-\frac{n_V}{4}-y_{RV}\left(1-\frac{n_R}{4}\right)\right)j_V^M$$
$$-\left(1-\frac{n_E}{4}\right)j_{EG}+\left(1-\frac{n_V}{4}\right)y_{VE}\;j_{EG}$$

2. Implementation in the model

Changes in O_2 concentration, or O_2 consumption, can be written as follows:

$$\frac{dO_2}{dt} = \dot{J}_O = j_O \, M_V$$

As j_O depends on the fluxes implemented in the switch model, we must describe O_2 consumption for each case of the model. In all cases, we have:

$$j_{EA} = j_{LA_m} \, y_{EL} \, \frac{L}{K+L}$$

if $M_E \, k_E > j_{EM} \, M_V$	*if* $M_E \, k_E < j_{EM} \, M_V$
$j_E^M = j_{EM}$	$j_E^M = \dfrac{k_E \, j_{EM} / j_{VM} + j_{EM}}{m_E + j_{EM} / j_{VM}} m_E$
$j_V^M = 0$	$j_V^M = \dfrac{j_{EM} - k_E \, m_E}{m_E + j_{EM} / j_{VM}}$
$j_{EG} = y_{EV} \dfrac{k_E \, m_E - j_{EM}}{m_E + j_{EM}}$	$j_{EG} = 0$
$\dfrac{dO_2}{dt} = \dfrac{5}{6}\dfrac{dL}{dt} + \left(1 - \dfrac{n_E}{4}\right)\dfrac{dM_E}{dt} + \left(1 - \dfrac{n_V}{4}\right)\dfrac{dM_V}{dt}$	$\dfrac{dO_2}{dt} = \dfrac{5}{6}\dfrac{dL}{dt} + \left(1 - \dfrac{n_E}{4}\right)\dfrac{dM_E}{dt} + \left(1 - \dfrac{n_V}{4}\right)\dfrac{dM_V}{dt} + \left(1 - \dfrac{n_R}{4}\right)\dfrac{dR}{dt}$

We finally found that O_2 consumption depends on the variation of each of the other state variables. The introduction of the respiration process in the model implied the addition of three new parameters n_E, n_V and n_R which must also be calibrated.

3. Calibration and simulation

The three new parameters were calibrated at the same time than other parameters which are included in the growth model. We thus utilised simultaneously all available data, which are DOC concentrations, POC concentrations and O_2 consumptions, to calibrate the model by minimising

the sum of square deviations between data and model outputs. Values of the three parameters accounting for the respiration were:

$$n_E = 1.179$$
$$n_V = 16.247$$
$$n_R = 42.884$$

Values of other model parameters are the same as in Table IV-3. The model was simulated by accounting for respiration in this case (Figure IV-5), dynamics of other state variables being the same as in Figure IV-3.

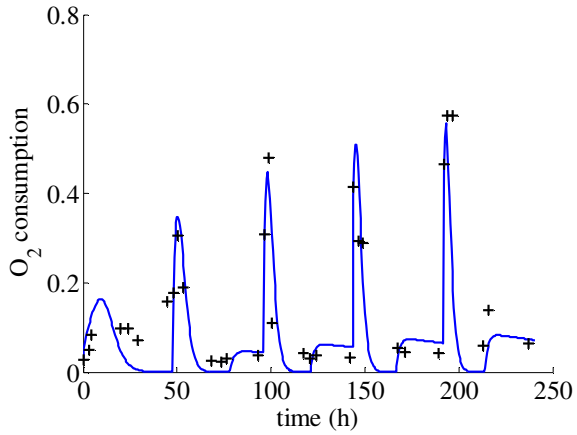

Figure IV-5: Dynamic of O_2 consumption (mM h^{-1}) for the switch DEB model. The crosses represent the data and the curves the outputs of the model with the fitted parameter set for the switch DEB model (Table IV-3 and respiration parameters n_E, n_V and n_R given previously).

4. Conclusion

The application of mass balance with the DEB theory allows estimating elemental fluxes, as O_2 in this study. However, this implies the introduction of several new parameters (9 in our case) for the addition of only 1 state variable. We have thus merged these various parameters from 9 to 3 for simplifying the calibration, especially as the O_2 consumption data were not sufficient to calibrate 9 parameters. We first notice that model outputs match well O_2 consumption data. However, after each peak (which corresponds to the introduction of a substrate pulse), O_2 consumption drops to 0, which is

quite surprising. Indeed, we might assume that bacteria never stop respiration due to maintenance, and thus consumption should not fall near zero values. This dynamic may be due to the calibration, as it doesn't include any biological insight but just try to minimise the difference between model outputs and observations. As we do not have any data which could confirm that O_2 consumption should not drop to 0, we cannot prove our assumptions.

On the other hand, our parameter values for the chemical indexes which have allowed respiration calibration are also difficult to interpret. For example, for the bacterial species *Klebsiella aerogenes* growing on glycerol, the following parameter values were found (Hanegraaf 1997, Kooijman 2000, p 314):

$$n_{HE} = 1.66 \quad n_{OE} = 0.422 \quad n_{NE} = 0.312$$
$$n_{HV} = 1.64 \quad n_{OV} = 0.379 \quad n_{NV} = 0198$$

We can assume that chemical indexes are in the same order of magnitude for organisms that can be considered equivalent on a physiological point of view (both are heterotrophic and aerobic bacteria). This would result in our study to parameter values that amount to:

$$n_E = 0.120$$
$$n_V = -0.288$$

These values are really far from values we have estimated. However, if O_2 consumption was simulated from this parameter set, with n_R value being a weighted sum of n_E and n_V, model outputs didn't match data well. The best strategy would consist in measuring these chemical indexes. But these measurements would be highly difficult because (1) the experimental protocol would be difficult for this kind of measurements, (2) if we succeeded to measure these indexes for this bacterial species in culture, we could not discriminate the composition between reserve and structure, (3) for instance we can not separate the R-DOC from L-DOC.

APPENDIX IV-A
Construction of the switch DEB model

Refer to Table IV-2 for explanations of the notation and description of the several state variables and parameters used. The model was developed according to the following table and the conservation law matrix:

symbol	processes	L : L-DOC	R : R-DOC	M_E : reserve	M_V : structure	specific rates
A_c	assim (cat)	-1	0	0	0	$j_{EA_c} = (y_{LE} - 1)\, j_{EA}$
A_a	assim (ana)	-1	0	1	0	$j_{EA_a} = j_{EA}$
M_E	E-maint	0	0	-1	0	j_E^M
M_V	V-maint	0	y_{RV}	0	-1	j_V^M
G_c	growth (cat)	0	0	-1	0	$j_{EG_c} = (1 - y_{VE})\, j_{EG}$
G_a	growth (ana)	0	0	-1	1	$j_{EG_a} = y_{VE}\ j_{EG}$

This table gives rise to the differential equations of the 4 state variables by multiplying the column of the considered state variable (L, R, M_E and M_V) by the column of the specific rate and by the structural biomass M_V:

$$\frac{dL}{dt} = j_L\, M_V$$
$$\frac{dM_E}{dt} = j_{M_E}\, M_V$$
$$\frac{dM_V}{dt} = j_{M_V}\, M_V$$
$$\frac{dR}{dt} = j_R\, M_V$$

where j_*, the specific fluxes, are defined by the previous table:

$$j_L = -j_{EA_C} - j_{EA_a} = -y_{LE}\ j_{EA}$$
$$j_{M_E} = j_{EA_a} - j_E^M - j_{EG_c} - j_{EG_a} = j_{EA} - j_E^M - j_{EG}$$
$$j_{M_V} = -j_V^M + j_{EG_a} = y_{VE}\ j_{EG} - j_V^M$$
$$j_R = y_{RV}\ j_V^M$$

The specific fluxes j_{*1*2} or j_{*1}^{*2} of compound $*1$ associated with the process $*2$ are defined by the DEB theory (Kooijman 2000). As the maintenance can be done either from the reserve or from the reserve plus structure, two kinds of maintenance have to be defined, the maintenance from reserve having always the absolute priority on maintenance from structure (Tolla et al. 2007). The total maintenance flux j_{EM} has to be constant, thus $j_{EM} = j_E^M + j_V^M$ is constant. If the amount of reserve is sufficient to ensure all the maintenance, thus $j_E^M = j_{EM}$. This is the case when $j_{EC} > j_{EM}$, where j_{EC} is the catabolic flux from reserve, i.e. the reserve loss flux, and can be calculated from:

$$\frac{dm_E}{dt} = j_{EA} - k_E\ m_E \qquad \text{(Kooijman, 2000)}$$
$$\frac{dM_E}{dt} = M_V \frac{dm_E}{dt} + m_E \frac{dM_V}{dt} = M_V \left(j_{EA} - k_E\ m_E \right) + \dot{r}\ M_E$$
$$j_E = \frac{dM_E / dt}{M_V} = j_{EA} - m_E \left(k_E - \dot{r} \right) = j_{EA} - j_{EC}$$

Thus $j_{EC} = m_E \left(k_E - \dot{r} \right)$, and when $m_E \left(k_E - \dot{r} \right) > j_{EM}$, $j_E^M = j_{EM}$ and consequently $j_V^M = 0$. For the other case, when $m_E \left(k_E - \dot{r} \right) < j_{EM}$, we have $j_E^M = j_{EC} = m_E \left(k_E - \dot{r} \right)$ and thus $j_V^M = \left(j_{EM} - j_E^M \right) \frac{j_{VM}}{j_{EM}}$, where $\frac{j_{VM}}{j_{EM}}$ represents the quantity of energy spent to transform compounds from reserve to structure and then from structure to maintenance, which is obviously more costly than the direct transformation from reserve to maintenance.

On the same way, if maintenance is fully done from reserve, the remaining of the energy can be spent for the growth which amounts to $j_{EG} = y_{EV}\ \dot{r}$ (Kooijman 2000), and if maintenance is also done from structure, growth of the structure is no more possible and $j_{EG} = 0$. We can thus write:

$$j_E^M = \min\left(j_{EM}, m_E\left(k_E - \dot{r}\right)\right)$$
$$j_V^M = \max\left(0, j_{EM} - j_E^M\right)\frac{j_{VM}}{j_{EM}}$$
$$j_{EG} = \max(0, \dot{r}\ y_{EV})$$

We now have to determinate the specific growth rate $\dot{r}$:

if $m_E\left(k_E - \dot{r}\right) > j_{EM}$	if $m_E\left(k_E - \dot{r}\right) < j_{EM}$
$\dot{r} = \frac{k_E\ m_E - j_{EM}}{m_E + y_{EV}}$	$\dot{r} = \frac{k_E\ m_E - j_{EM}}{m_E + j_{EM}/j_{VM}}$

It should be also noted that $m_E\left(k_E - \dot{r}\right) > j_{EM} \Leftrightarrow m_E\ k_E > j_{EM}$.

For a unique substrate, the assimilation flux is always $j_{EA} = j_{LAm}\ y_{EL}\frac{L}{K+L}$ (Kooijman 2000). We finally can write the complete model:

$$\begin{cases} \dfrac{dL}{dt} = j_L\ M_V = -y_{LE}\ j_{EA}\ M_V = -j_{LAm}\dfrac{L}{K+L}M_V \\ \dfrac{dM_E}{dt} = j_{M_E}\ M_V = \left(j_{LAm}\ y_{EL}\dfrac{L}{K+L} - \min\left(j_{EM}, m_E\left(k_E - \dot{r}\right)\right) - \max(0, \dot{r}\ y_{EV})\right)M_V \\ \dfrac{dM_V}{dt} = j_{M_V}\ M_V = \left(y_{VE}\ \max(0, \dot{r}\ y_{EV}) - \max\left(0, j_{EM} - j_E^M\right)\dfrac{j_{VM}}{j_{EM}}\right)M_V \\ \dfrac{dR}{dt} = j_R\ M_V = y_{RV}\ \max\left(0, j_{EM} - j_E^M\right)\dfrac{j_{VM}}{j_{EM}}M_V \end{cases}$$

This model can also be written as follows:

if $k_E M_E > j_{EM} M_V$

$$\begin{cases} \dfrac{dM_E}{dt} = j_{LAm}\, y_{EL} \dfrac{L}{K+L} M_V - j_{EM} M_V \\ \qquad\qquad - y_{EV} \dfrac{k_E M_E - j_{EM} M_V}{M_E + y_{EV} M_V} M_V \\ \dfrac{dM_V}{dt} = \dfrac{k_E M_E - j_{EM} M_V}{M_E + y_{EV} M_V} M_V \\ \dfrac{dR}{dt} = 0 \end{cases}$$

if $k_E M_E < j_{EM} M_V$

$$\begin{cases} \dfrac{dM_E}{dt} = j_{LAm}\, y_{EL} \dfrac{L}{K+L} M_V - k_E M_E \\ \qquad\qquad - \dfrac{j_{EM} M_V - k_E M_E}{M_E + j_{EM} / j_{VM} M_V} M_E \\ \dfrac{dM_V}{dt} = - \dfrac{j_{EM} M_V - k_E M_E}{M_E + j_{EM} / j_{VM} M_V} M_V \\ \dfrac{dR}{dt} = y_{RV} \dfrac{j_{EM} M_V - k_E M_E}{M_E + j_{EM} / j_{VM} M_V} M_V \end{cases}$$

APPENDIX IV-B
Switch DEB model simplification

In this appendix, we show how the simplified model is obtained from the complete one.

1. Case 1: $M_E\, k_E > j_{EM}\, M_V$

Since the parameter j_{EM} is very small, we set $j_{EM} = \varepsilon\, j'_{EM}$ where ε is a small unitless parameter. Moreover, as the sum of squared deviations gives the minimum for a very high K value, we have assumed $K >> L$ and we set $\alpha = \frac{j_{LA_m}}{K}$. It follows:

if $k_E\, M_E > \varepsilon\, j'_{EM}\, M_V$

$$\begin{cases} \dfrac{dL}{dt} = -\alpha\, L\, M_V \\ \dfrac{dM_E}{dt} = \alpha\, y_{EL} L\, M_V - \varepsilon\, j'_{EM}\, M_V - y_{EV} \dfrac{k_E\, M_E - \varepsilon\, j'_{EM}\, M_V}{M_E + y_{EV}\, M_V} M_V \\ \dfrac{dM_V}{dt} = \dfrac{k_E\, M_E - \varepsilon\, j'_{EM}\, M_V}{M_E + y_{EV}\, M_V} M_V \\ \dfrac{dR}{dt} = 0 \end{cases}$$

Let $C_{T_1} = y_{EL}\, L + M_E + y_{EV}\, M_V$ represents the total amount of carbon (in reserve unit) in the system:

$\frac{dC_{T_1}}{dt} = y_{EL}\frac{dL}{dt} + \frac{dM_E}{dt} + y_{EV}\frac{dM_V}{dt} = -\varepsilon\, j'_{EM}\, M_V$ is the equation governing the mass balance in the system. We notice that there is a small carbon loss which is due to the maintenance process. This lost is very slow thus we can use perturbation theory in order to analyse and simplify the system. In a first step, since ε is small, we consider that ε is null. Then, in a second step, we study the case $\varepsilon \simeq 0$ which is considered as a perturbation of the previous one.

If $\varepsilon = 0$, $\frac{dC_{T_1}}{dt} = 0$ and C_{T_1} is a constant. As a consequence, we can replace M_E by the following expression:

$$M_E = C_{T_1} - y_{EL}\, L - y_{EV}\, M_V$$

This permits to rewrite the equation for the structural biomass as a usual logistic-like equation:

$$\frac{dM_V}{dt} = r\, M_V \left(1 - \frac{M_V}{\kappa_1(L)}\right)$$

where the carrying capacity depends on the variable L:

$$\kappa_1 = \frac{C_{T_1} - y_{EL}\, L}{y_{EV}}$$

and the growth rate is $r = k_E$.

Finally, when $M_E\, k_E > j_{EM}\, M_V$ and $\varepsilon = 0$, the complete model can be simplified and reads :

$$\begin{cases} \frac{dL}{dt} = -\alpha\, L\, M_V \\ \frac{dM_V}{dt} = r\left(1 - \frac{M_V}{\kappa_1(L)}\right) M_V \end{cases}$$

When the time t goes to infinity, we have: $L \to 0$, $M_V \to \kappa_1 = \frac{C_{T_1}}{y_{EV}}$ and $M_E \to 0$.

We now consider the case $\varepsilon \simeq 0$. It follows:

$$\frac{dC_{T_1}}{dt} = -\varepsilon\, j'_{EM}\, M_V$$

In other words, C_{T_1} slowly changes and since M_V changes faster, it reaches its equilibrium value rapidly, leading to the equation:

$$\frac{dC_{T_1}}{d\tau} = -j'_{EM}\, \frac{C_{T_1}}{y_{EV}}$$

where $\tau = \varepsilon t$. Since this equation is linear, its solution is $C_{T_1}(\tau) = C_{T_1}(0)\, e^{-\frac{j'EM}{y_{EV}}\tau}$

We can thus conclude:

$$\begin{cases} \dfrac{dL}{dt} = -\alpha\, L\, M_V \\ \dfrac{dM_V}{dt} = r\, M_V \left(1 - \dfrac{M_V}{\kappa_1\left(L, C_{T_1}\right)}\right) \end{cases}$$

with:

$\kappa_1\left(L, C_{T_1}\right) = \dfrac{C_{T_1}(\tau) - y_{EL}\, L(\tau)}{y_{EV}}$, $C_{T_1}(\tau) = C_{T_1}(0)\, e^{-\frac{j'_{EM}}{y_{EV}}\tau}$ and

$M_E = C_{T_1}(\tau) - y_{EL}\, L(\tau) - y_{EV}\, M_V(\tau)$.

2. Case 2: $M_E\, k_E < j_{EM}\, M_V$

The model reads:

$$\begin{cases} \dfrac{dL}{dt} = -\alpha\, L\, M_V \\ \dfrac{dM_E}{dt} = \alpha\, y_{EL}\, L\, M_V - k_E\, M_E - \dfrac{j_{EM}\, M_V - k_E\, M_E}{M_E + j_{EM}/j_{VM}\, M_V} M_E \\ \dfrac{dM_V}{dt} = -\dfrac{j_{EM}\, M_V - k_E\, M_E}{M_E + j_{EM}/j_{VM}\, M_V} M_V \\ \dfrac{dR}{dt} = y_{RV}\, \dfrac{j_{EM}\, M_V - k_E\, M_E}{M_E + j_{EM}/j_{VM}\, M_V} M_V \end{cases}$$

Let us define $C_{T_2} = y_{EL}\, L + M_E$ and $C_{T_3} = M_V + \dfrac{R}{y_{RV}}$. Moreover, since we have $M_E\, k_E < j_{EM}\, M_V = \varepsilon\, j'_{EM}\, M_V$, it follows that M_E is very

small in this case. In other words, $y_{EL}\ L$ is very close to C_{T_2} thus we set $L = \frac{1}{y_{EL}} C_{T_2} - \varepsilon L'$ and consequently $M_E = \varepsilon\ y_{EL}\ L'$. We thus finally get:

$$\frac{dC_{T_2}}{dt} = -\varepsilon \left(\frac{k_E / j_{VM} + 1}{y_{EL}\ L' + j'_{EM} / j_{VM}\ M_V} \right) j'_{EM}\ y_{EL}\ M_V\ L'$$

and

$$\frac{dC_{T_3}}{dt} = 0$$

We use again the perturbation theory in order to analyse and simplify the model formulation. We first consider the situation $\varepsilon = 0$. In this case, $\frac{dC_{T_2}}{dt} = 0$ and consequently C_{T_2} and C_{T_3} are constant. The structure dynamics is thus governed by the equation:

$$\frac{dM_V}{dt} = \frac{k_E\ y_{EL}\ L' - j'_{EM}\ M_V}{y_{EL}\ L' + \frac{j'_{EM}}{j_{VM}} M_V} M_V$$

The condition $M_E\ k_E < j_{EM}\ M_V$ also reads $k_E y_{EL} L' < j'_{EM}\ M_V$. In this case and when $\varepsilon = 0$, the system of differential equations can be simplified as follows:

$$\begin{cases} \frac{dL'}{dt} = -\alpha\ L' M_V \\ \frac{dM_V}{dt} = \frac{k_E y_{EL} L' - j'_{EM}\ M_V}{y_{EL} L' + \frac{j'_{EM}}{j_{VM}} M_V} M_V \end{cases}$$

when the time $t \to \infty$: $L' \to 0$, $M_V \to 0$, $M_E \to C_{T_2}$ and $R \to y_{RV}\ C_{T_3}$. In order to understand the dynamics in the situation $\varepsilon \simeq 0$, we replace the fast previous variables by their equilibrium values and we still define $\tau = \varepsilon t$, we get: $\frac{dC_{T_2}}{d\tau} = o(\varepsilon)$. In other words, the variable C_{T_2} changes so slowly

that it cannot be seen during the experiment. We can thus consider $\frac{dC_{T_2}}{d\tau} = 0$ and C_{T_2} is constant.

We can thus conclude:

$$\begin{cases} \frac{dL}{dt} = -\alpha\, L\, M_V \\ \frac{dM_V}{dt} = \frac{k_E\, C_{T_2}(0) - k_E\, y_{EL}\, L - j_{EM} M_V}{C_{T_2}(0) - y_{EL}\, L + \frac{j_{EM}}{j_{VM}} M_V} M_V \end{cases}$$

with :

$C_{T_2} = C_{T_2}(0) = y_{EL}\, L(0) + M_E(0)$

$M_E(t) = C_{T_2}(0) - y_{EL}\, L(t)$ and $R(t) = y_{RV}\left(C_{T_3}(0) - M_V(t)\right)$

CHAPTER V

General conclusions and Perspectives

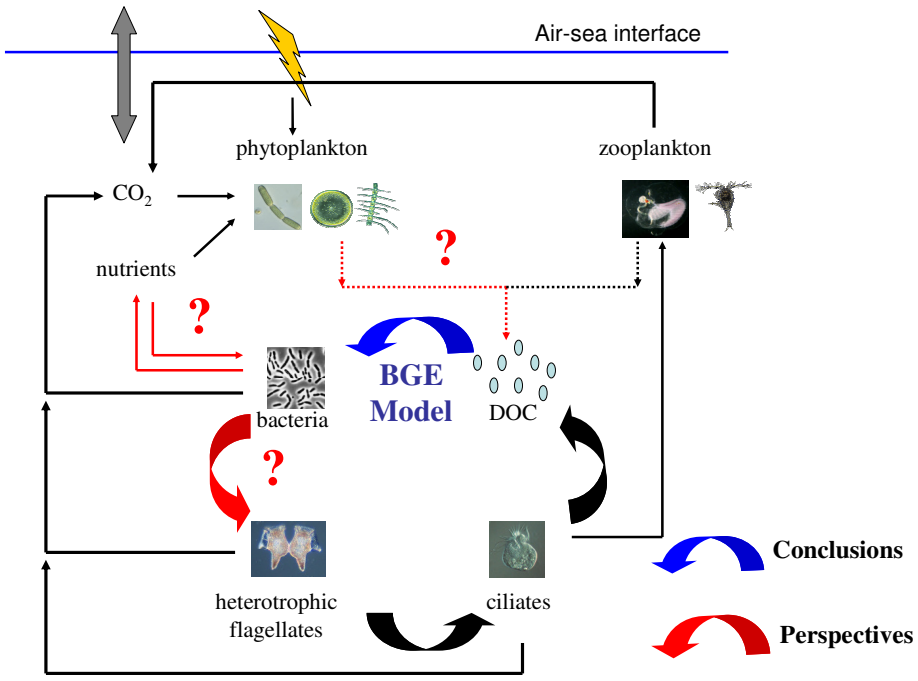

I. Bacterial growth efficiency

This thesis highlighted several patterns in the dynamics of BGE. Utilisation of the Monod model on *in situ* data has demonstrated that the BGE varies according to depth and season, with higher values in surface layer and during warm seasons (Eichinger et al., 2006 – chapter II). To our knowledge, BGE variation with depth was never shown previously. The fact that the BGE dynamic depends on the season, or on the temperatures, was already demonstrated, but not by using a modelling approach.

The third chapter also deals with the BGE variability, but in artificial culture conditions. The experiments were here carried out to determine the influence of the input regime on bacterial and BGE dynamics. We have demonstrated that the way of introducing the substrate in the batch has a profound impact on the BGE value. The substrate quantity and quality were the same in both experiments, they thus may not have an impact in this case. The pulse experiment simulated a transient environment in terms of DOC availability. We have shown that this kind of environment, closer to natural environment from a qualitative point of view, is more efficient for bacterial degradation than a constant environment, generally investigated to estimate BGE. Consequently, the method of BGE estimation should be reviewed by trying to incorporate more realistic substrate dynamics. However, our experimental design is still far from natural conditions in terms of the amount of substrate, and experimental efforts should be done to be closer to natural DOC and bacterial concentrations.

Chapters II and III both used models to estimate the BGE. This method seems suitable as we have proven in chapter II that BGE estimated from the Monod model and from experimental data are qualitatively and quantitatively equivalent. However, the BGE value estimated from models will of course depend on the model used. The Monod model does not incorporate maintenance process, and thus exhibits higher BGE values than models which do. BGE estimation from Monod model seems to be closer to the experimental estimation for both studies investigated in this thesis (chapters II and III). As the Marr-Pirt and DEB models include maintenance, they exhibit smaller BGE values than the Monod estimation. The BGE estimated from the Marr-Pirt and the DEB models are very similar and considered as equivalent. However, it is difficult from these results to determine which of these estimations matches better with the “true” or “natural” BGE. The diversity of methods used in BGE investigation makes BGE dynamics difficult to study. This variability can only be demonstrated when BGE are

estimated with the same method in the same study. We may talk about an "absolute" BGE. Indeed, even if BGE values are not identical with the different methods, they always show the same pattern: smaller in deep waters and during cold seasons, and smaller in a constant than in a transient environment.

Nevertheless, a dynamic BGE could be investigated. Indeed, models provide tools to represent experimental dynamics by implementing the required processes. This tool could allow the representation of the BGE dynamics during an experiment and thus highlighting events or processes responsible for BGE changes. However, in this case the comparison between several estimations is difficult as we should compare dynamics and not individual BGE values. Nevertheless, this method should be considered.

II. Bacterial growth models

In this thesis, several bacterial growth models have been used and for different purposes. The Monod model was used to describe bacterial growth (1) from *in situ* data, as the data did not allowed the application of more complex models, and also (2) from artificial culture data to test its pertinence in transient conditions. The model matched the data well in the first case but not in the second case, as experiments realised in artificial conditions were carried out for a sufficient long time to exhibit biomass decrease which could not be simulated by the Monod model due to the absence of maintenance. Consequently, the adequacy of a model to describe data is primarily determined by the type of data, and simple models can often be sufficient to represent some dynamics.

The Marr-Pirt and DEB models were utilised in chapter III for representing bacterial culture dynamics. The application of these models was required as experimental data showed the presence of maintenance. Both models equally fitted data, but we have also shown that the Marr-Pirt model could be less efficient if the pulse experiment was realised in the conditions of the batch experiment. This showed that the fit success may be determined by the data set, and that only small variations in the experimental setup could change the type of model that should be used. The advantage of the DEB formulation is that it is more flexible and thus suitable in all cases, as it can be reduced to Monod or Marr-Pirt models.

We also have demonstrated that the growth part of the Monod (chapter II) and DEB (chapter IV) models may be simplified in a logistic equation, with a constant and a variable carrying capacity, respectively. The utilisation of this logistic equation reduces the model complexity in terms of calibration and simulation costs, without affecting model performance. This simplification step is required if we use these models in a biogeochemical context. The key role of bacteria in the oceanic ecosystems has still been proven and we have demonstrated in this study that they need to be modelled accurately at the global level to obtain a good representation of the aquatic carbon cycle. Once a suitable formulation has been found, it should be simplified if this latter is complex in terms of number of parameters or state variables with respect to the number of organisms or elements. Model reduction facilitates calibration, simulation and understanding of the underlying processes. However, model reduction should only be envisaged when the complete model is constructed from experimental data, thus when the complete model might provide realistic representation of experimental or environmental dynamics.

III. Experimentation – modelling coupling

The conclusions of this thesis were possible because we coupled experimentation and modelling. This coupling is essential to obtain realism. For example, measurements made in chapter II (bacterial production and respiration) did not demonstrate the maintenance that occurred in these natural bacteria assemblages. Consequently, a model including maintenance was not required. On the contrary, experiments carried out in artificial conditions were specifically designed to place bacteria in starvation conditions and highlight the necessity of the maintenance process in bacterial modelling. Consequently, experiments should be planned in a modelling framework. We won't find an appropriate formulation for bacterial growth without thinking before about which kind of processes they could implement. Then, the experimental design can be prepared by planning which kind of experiments and measurements should be used to quantify the various processes. The utilisation of models also requires numerous data for the calibration and validation, especially when dealing with transient environments, as the pulse experiment of chapter III. Of course, this requires a profound investment in terms of effort and finances. Then, model outputs could serve to improve the sampling strategy, the type of measurements to be made, the design of the future experiments. Chapter III discussed what experiments could discriminate between the DEB and the Marr-Pirt models.

Consequently, the best strategy alternates repeatedly between experiment and modelling.

Another important fact highlighted in this thesis is the necessity to use artificial conditions to reveal key processes (chapter III). Indeed, the diversity of uncertainties, when dealing with natural samples (chapter II), complicates the analysis of results and makes the utilisation of complex model inappropriate as processes are difficult to isolate from uncertainties. The utilisation of artificial seawater and monospecific bacteria is of course far from *in situ* conditions, but we first need a better understanding of the key processes. Moreover, we can easily control external conditions and thus add several limitations or introducing other organisms as we go along.

IV. Perspectives

My conclusions lead me to think that hypotheses asserted in this thesis should be check experimentally. We have assumed that DOC accumulation in batches (chapters III and IV) is due to its refractory nature. This assumption could be check by measuring substrate (pyruvate) concentration as well as DOC concentration in the cultures. However, we should first improve our protocol of pyruvate detection. This kind of analysis is delicate and not much used currently. Nevertheless, it will be probably feasible soon with the method perfected by Tedetti et al. (2006) at LMGEM. We should also measure N and P concentrations (or NH_4^+ and PO_4^{3-} concentrations) to be sure that the systems were not limited by inorganic nutrients. The measurements of N and P, in the culture medium as well as in the bacterial biomass, could also be useful for improving the DEB model. As done by Martinussen and Thingstad (1987), we could so take into account three reserves and have a more accurate idea on bacterial dynamics. Then, we could test several limitations, for example by pulsing periodically two nutrients (C and N or C and P), and then by pulsing the three of them (C, N and P). We could so have more insights about bacterial physiology, for example on the regulation of bacterial C:N and C:P ratios in transient environments. The investigation of Thingstad (1987) showed that a Monod-type model may effectively be sufficient in many purposes, but that a model with a reserve for each kind of compound allows an easier incorporation of biologically plausible concepts. In addition, the depletion areas, in function of C:P and C:N ratios, of batch and chemostat cultures are accurately represented by this model with three reserves (Martinussen & Thingstad 1987). This kind of approach would also allow a better understanding about

the storage capacity, and test the prediction of DEB theory that nutrient reserves accumulate under energy limitation. Nevertheless, the addition of all of these measurements needs an improvement of the experimental protocol, since the time required for doing all carbon measurements carried out in this thesis was already substantial, and the addition of other measurements would imply either a reduction of the number of data points between two pulses, or another experimental design.

One of the solutions would be the utilisation of chemostats instead of batch systems. The culture volume that is required to perform all measurements is a point of concern. The sampling protocol could so be automated. To mimic transient environments we should vary either the dilution rate or the substrate concentration in the input.

The real complexity of the natural medium let me suggest that it is necessary to test prey-predator interactions in the context of the DEB theory. Kooi and Kooijman (1994) showed the necessity of adding a storage compartment as well as the maintenance process to the Monod model for representing data of a trophic chain implying one substrate, one bacterial species and one predator. We could imagine the same kind of protocol by pulsing the substrate. The model should include the DOC production by the predator (grazer), and it would thus comprise two DOC sources (the input substrate as well as DOC produced from grazing), with a differentiate preference in the uptake. In the DEB context, the grazer would have two nutritive sources: bacterial reserve and structure. In the same way, we could test an interaction between a phytoplankton and bacterial species. Bratbak and Thingstad (1985) tested this kind of interaction with chemostat experiments, where the nutritive resource was phosphate, and showed that bacterial density increased whereas phytoplankton density decreased at low dilution rates. They have also constructed a model where both organisms are in competition for the limiting resource but where the phytoplankton produces organic carbon assimilated by bacteria. This approach could be used by including more realist nutrient dynamics, as the pulse input of substrate in this thesis. The model should thus include two DOC sources and bacteria would compete for the inorganic nutrients with phytoplankton. Then, we could test the effect of these processes in a biogeochemical model, after having simplified their formulation.

To sum up, more coupling between experimental and modelling work should be investigated. In the bacterial context, studies that deal with both approaches at the same time are seldom. Some investigations succeed to

demonstrate experimentally some theoretical results obtained few decades earlier. For example, the study of Becks et al. (2005) demonstrated the existence of chaotic behaviour in a microbial food web with chemostat experiments. The existence of chaos in simple ecological systems was however demonstrated with models since a long time. In this thesis, model comparison with experimental data (chapter III) showed that a complex model is not currently necessary to represent bacterial dynamics in a pulse DOC environment. Nevertheless, models provide tools to test assumptions and/or the influence of the addition of processes in system dynamics. In this context, the influence of the incorporation of physiological details in ecosystem models on global dynamics could be tested. For example, we can test the DEB formulations on the 1-D model of Anderson & Williams (1999), which simulates the DOC distribution in the water column, by keeping the same global model structure. Then, we can observe if these detailed formulations imply dynamical differences and judge the necessity of using mechanistic models at the global scale.

References

Amon RMW, Benner R (1996) Bacterial utilization of different size classes of dissolved organic matter. Limnology and Oceanography 41:41-51

Anderson TR, Ducklow HW (2001) Microbial loop carbon cycling in ocean environments studied using a simple steady-state model. Aquatic Microbial Ecology 26:37-49

Anderson TR, Williams PJleB (1998) Modelling the seasonal cycle of dissolved organic carbon at station E-1 in the English Channel. Estuarine Coastal and Shelf Science 46:93-109

Anderson TR, Williams PJleB (1999) A one-dimensional model of dissolved organic carbon cycling in the water column incorporating combined biological-photochemical decomposition. Global Biogeochemical Cycles 13:337-349

Arhonditsis GB, Brett MT (2004) Evaluation of the current state of mechanistic aquatic biogeochemical modeling. Marine Ecology-Progress Series 271:13-26

Azam F, Fenchel T, Field JG, Gray JS, Meyer-Reil LA, Thingstad TF (1983) The ecological role of water-column microbes in the sea. Marine Ecology-Progress Series 10:257-263

Baird ME, Walker SJ, Wallace BB, Webster IT, Parslow JS (2003) The use of mechanistic descriptions of algal growth and zooplankton grazing in an estuarine eutrophication model. Estuarine Coastal and Shelf Science 56:685-695

Baklouti M, Diaz F, Pinazo C, Faure V, Queguiner B (2006a) Investigation of mechanistic formulations depicting phytoplankton dynamics for models of marine pelagic ecosystems and description of a new model. Progress in Oceanography 71:1-33

Baklouti M, Faure V, Pawlowski L, Sciandra A (2006b) Investigation and sensitivity analysis of a mechanistic phytoplankton model implemented in a new modular numerical tool (Eco3M) dedicated to biogeochemical modelling. Progress in Oceanography 71:34-58

Baretta-Bekker JG, Baretta JW, Hansen AS, Riemann B (1998) An improved model of carbon and nutrient dynamics in the microbial food web in marine enclosures. Aquatic Microbial Ecology 14:91-108

Baretta-Bekker JG, Baretta JW, Rasmussen EK (1995) The microbial food web in the European Regional Seas Ecosystem Model. Netherland Journal of Sea Research 33:363-379

Baretta-Bekker JG, Riemann B, Baretta JW, Koch Rasmussen E (1994) Testing the microbial loop concept by comparing mesocosm data with results from a dynamical simulation model Marine Ecology-Progress Series 106:187-198

Bauer JE, Williams PM, Druffel ERM (1992) C-14 Activity of Dissolved Organic-Carbon Fractions in the North-Central Pacific and Sargasso Sea. Nature 357:667-670

Baxter M, Sieburth JMN (1984) Metabolic and ultrastructural response to glucose of two eurytrophic bacteria isolated from seawater at different enriching concentrations. Applied and Environmental Microbiology 47:31-38

Becks L, Hilker FM, Malchow H, Jürgens K, Arndt H (2005) Experimental demonstration of chaos in microbial foo web. Nature 435:1226-1229

Bendtsen J, Lundsgaard C, Middelboe M, Archer D (2002) Influence of bacterial uptake on deep-ocean dissolved organic carbon. Global Biogeochemical Cycles 16:Art. No. 1127

Billen G, Becquevort S (1991) Phytoplankton Bacteria Relationship in the Antarctic Marine Ecosystem. Polar Research 10:245-253

Bissett WP, Walsh JJ, Dieterle DA, Carder KL (1999) Carbon cycling in the upper waters of the Sargasso Sea: I. Numerical simulation of differential carbon and nitrogen fluxes. Deep-Sea Research Part I - oceanographic research papers 46:205-269

Blackburn N, Zweifel UL, Hagstrom A (1996) Cycling of marine dissolved organic matter .II. A model analysis. Aquatic Microbial Ecology 11:79-90

Brandt BW, Kelpin FDL, van Leeuwen IMM, Kooijman SALM (2004) Modelling microbial adaptation to changing availability of substrates. Water Research 38:1003-1013

Brandt BW, van Leeuwen IMM, Kooijman SALM (2003) A general model for multiple substrate biodegradation. Application to co-metabolism

of structurally non-analogous compounds. Water Research 37:4843-4854

Briand E, Pringault O, Jacquet S, Torréton P (2004) The use of oxygen microprobes to measure bacterial respiration for determining bacterioplankton growth efficiency. Limnology and Oceanography: Methods 2:406-416

Cajal-Medrano R, Maske H (1999) Growth efficiency, growth rate and the remineralization of organic substrate by bacterioplankton - revisiting the Pirt model. Aquatic Microbial Ecology 19:119-128

Cajal-Medrano R, Maske H (2005) Growth efficiency and respiration at different growth rates in glucose-limited chemostats with natural marine bacteria populations. Aquatic Microbial Ecology 38:125-133

Carlson CA (2002) Production and removal processes. In: Hansell DA, Carlson CA (eds) Biogeogemistry of marine dissolved organic matter. Academic Press, San Diego, p 91-151

Carlson CA, Bates NR, Ducklow HW, Hansell DA (1999) Estimation of bacterial respiration and growth efficiency in the Ross Sea, Antarctica. Aquatic Microbial Ecology 19:229-244

Carlson CA, Ducklow HW (1995) Dissolved organic carbonin the upper ocean of the central equatorial Pacific Ocean, 1992: Daily and finescale vertical variations. Deep-Sea Research Part II-Topical Studies in Oceanography 42:639-656

Carlson CA, Ducklow HW (1996) Growth of bacterioplankton and consumption of dissolved organic carbon in the Sargasso Sea. Aquatic Microbial Ecology 10:69-85

Carlson CA, Ducklow HW, Hansell DA, Smith WO Jr (1998) Organic carbon partitioning during spring phytoplancton blooms in the Ross Sea polynya and the Sargasso Sea. Limnology and Oceanography 43:375-386

Carlson CA, Giovannoni SJ, Hansell DA, Goldberg SJ, Parsons R, Otero MP, Vergin K, Wheeler BR (2002) Effect of nutrient amendments on bacterioplankton production, community structure, and DOC utilization in the northwestern Sargasso Sea. Aquatic Microbial Ecology 30:19-36

Carlson CA, Giovannoni SJ, Hansell DA, Goldberg SJ, Parsons R, Vergin K (2004) Interactions among dissolved organic carbon, microbial processes, and community structure in the mesopelagic zone of the

northwestern Sargasso Sea. Limnology and Oceanography 49:1073-1083

Cherrier J, Bauer JE (2004) Bacterial utilization of transient plankton-derived dissolved organic carbon and nitrogen inputs in surface ocean waters. Aquatic Microbial Ecology 35:229-241

Cherrier J, Bauer JE, Druffel ERM (1996) Utilization and turnover of labile dissolved organic matter by bacterial heterotrophs in eastern north Pacific surface waters. Marine Ecology-Progress Series 139:267-279

Christian JR, Anderson TR (2002) Modeling DOM biogeochemistry. In: Hansell DA, Carlson CA (eds) Biogeochemistry of marine dissolved organic matter. Academic Press, London, p 774

Coffin RB, Connolly JP, Harris PS (1993) Availability of dissolved organic carbon to bacterioplankton examined by oxygen utilization. Marine Ecology-Progress Series 101:9-22

Connolly JP, Coffin RB (1995) Model of Carbon Cycling in Planktonic Food Webs. Journal of Environmental Engineering-Asce 121:682-690

Copinmontegut G, Avril B (1993) Vertical-Distribution and Temporal Variation of Dissolved Organic-Carbon in the North-Western Mediterranean-Sea. Deep-Sea Research Part I-Oceanographic Research Papers 40:1963-1972

Dafner E, Gonzalez-Davila M, Santana-Casiano JM, Sempéré R (2001) Total organic and inorganic carbon exchange through the Strait of Gibraltar in September 1997. Deep-Sea Research Part I-Oceanographic Research Papers 48:1217-1235

Davidson K (1996) Modelling microbial food webs. Marine Ecology-Progress Series 145:279-296

Dearman JR, Taylor AH, Davidson K (2003) Influence of autotroph model complexity on simulations of microbial communities in marine mesocosms. Marine Ecology-Progress Series 250:13-28

del Giorgio PA, Cole JJ (1998) Bacterial growth efficiency in natural aquatic systems. Annual Review of Ecology and Systematics 29:503-541

del Giorgio PA, Duarte CM (2002) Respiration in the open ocean. Nature 420:379-384

Droop MR (1968) Vitamin B12 and marine ecology. IV. The kinetics of uptake, growth and inhibition in *Monochrysis lutheri*. Journal of the Marine Biological Association of the United Kingdom 48:689-733

Druffel ERM, Williams PM, Bauer JE, Ertel JR (1992) Cycling of Dissolved and Particulate Organic-Matter in the Open Ocean. Journal of Geophysical Research-Oceans 97:15639-15659

Ducklow H, Carlson C, Smith W (1999) Bacterial growth in experimental plankton assemblages and seawater cultures from the Phaeocystis antarctica bloom in the Ross Sea, Antarctica. Aquatic Microbial Ecology 19:215-227

Ducklow HW, Carlson CA (1992) Oceanic Bacterial Production. Advances in Microbial Ecology 12:113-181

Eichinger M, Kooijman SALM, Sempéré R, Poggiale JC (submitted) Mechanistic model simplification for implementation in biogeochemical models: case of bacterial DOC degradation in a perturbed system. Ecological Modelling

Eichinger M, Poggiale JC, Van Wambeke F, Lefèvre D, Sempéré R (2006) Modelling DOC assimilation and bacterial growth efficiency in biodegradation experiments: a case study in the Northeast Atlantic Ocean. Aquatic Microbial Ecology 43:139-151

Fagerbakke KJ, Heldal M, Norland S (1996) Content of carbon, nitrogen, oxygen, sulfur and phosphorus in native aquatic and cultured bacteria. Aquatic Microbial Ecology 10:15-27

Farjalla VF, Azevedo DA, Esteves FA, Bozelli RL, Roland F, Enrich-Prast A (2006) Influence of hydrological pulse on bacterial growth and DOC uptake in a clear-water Amazonian lake. Microbial Ecology 52:334-344

Farrington J (1992) Overview and key recommendations. Marine organic geochemistry workshop, January 1990. Marine Chemistry 39:5-9

Flynn KJ (2005) Castles built on sand: dysfunctionality in plankton models and the inadequacy of dialogue between biologists and modellers. Journal of Plankton Research 27:1205-1210

Fujii M, Murashige S, Ohnishi Y, Yuzawa A, Miyasaka H, Suzuki Y, Komiyama H (2002) Decomposition of phytoplankton in seawater. Part 1: Kinetic analysis of the effect of organic matter concentration. Journal of Oceanography 58:433-438

Fulton EA, Parslow JS, Smith ADM, Johnson CR (2004) Biogeochemical marine ecosystem models II: the effect of physiological detail on model performance. Ecological Modelling 173:371-406

Goldman JC, Caron DA, Dennett MR (1987) Regulation of gross growth efficiency and ammonium regeneration in bacteria by susbtrate C:N ratio. Limnology and Oceanography 32:1239-1252

González N, Anadón R, Marañón E (2002) Large-scale variability of planktonic net community metabolism in the Atlantic Ocean: importance of temporal changes in oligotrophic subtropical waters. Marine Ecology-Progress Series 233

Grossart HP, Simon M (2007) Interactions of planktonic algae and bacteria: effects on algal growth and organic matter dynamics. Aquatic Microbial Ecology 47:163-176

Grover JP (1991) Resource Competition in a Variable Environment - Phytoplankton Growing According to the Variable-Internal-Stores Model. American Naturalist 138:811-835

Guidi L, Stemman L, Legendre L, Picheral M, Prieur L, Gorsky G (2007) Vertical distribution of aggregates (> 110 µm) and mesoscale activity in the northeastern Atlantic: Effects on the deep vertical export of surface carbon. Limnology and Oceanography 52:7-18

Guven B, Howard A (2007) Identifying the critical parameters of a cyanobacterial growth and movement model by using generalised sensitivity analysis. Ecological Modelling 207:11-21

Hanegraaf PPF (1997) Mass and energy fluxes in microorganisms according to the Dynamic Energy udget theory for filaments. Vrije Universiteit, Amsterdam

Hanegraaf PPF, Kooi BW (2002) The dynamics of a tri-trophic food chain with two-component populations from a biochemical perspective. Ecological Modelling 152:47-64

Hanegraaf PPF, Muller EB (2001) The dynamics of the macromolecular composition of biomass. Journal of theoretical biology 212:237-251

Hansell DA (2002) DOC in the global ocean carbon cycle. In: Hansell DA, Carlson CA (eds) Biogeochemistry of marine dissolved organic matter. Academic Press, London, p 774

Hansell DA, Bates NR, Gundersen K (1995) Mineralization of dissolved organic carbon in the Sargasso Sea. Marine Chemistry 51:201-212

Hansell DA, Carlson CA (1998a) Deep-ocean gradients in the concentration of dissolved organic carbon. Nature 395:263-266

Hansell DA, Peltzer ET (1998) Spatial and temporal variations of total organic carbon in the Arabian Sea. Deep-Sea Research Part Ii-Topical Studies in Oceanography 45:2171-2193

Harvey HR, Tuttle JH, Bell JT (1995) Kinetics of Phytoplankton Decay during Simulated Sedimentation - Changes in Biochemical-Composition and Microbial Activity under Oxic and Anoxic Conditions. Geochimica Et Cosmochimica Acta 59:3367-3377

Hedges JI (1992) Global biogeochemical cycles: Progress and problems. Marine Chemistry 39:67-93

Heldal M, Norland S, Fagerbakke KJ, Thingstad TF, Bratbak G (1996) The elemental composition of bacteria: a signature of growth conditions? Marine Pollution Bulletin 33:3-9

Herbert D (1958) Some principles of continuous culture. In: Tunevall G (ed) Recent progress in microbiology, Vol 7. Almquist and Wiksell, Stockholm, p 381–396

Iwasa Y, Levin SA, Andreasen V (1989) Aggregation in Model-Ecosystems .2. Approximate Aggregation. Ima Journal of Mathematics Applied in Medicine and Biology 6:1-23

Jahnke RA, Craven DB (1995) Quantifying the Role of Heterotrophic Bacteria in the Carbon-Cycle - a Need for Respiration Rate Measurements. Limnology and Oceanography 40:436-441

Jorgensen NOG, Kroer N, Coffin RB, Hoch MP (1999) Relations between bacterial nitrogen metabolism and growth efficiency in an estuarine and an open-water ecosystem. Aquatic Microbial Ecology 18:247-261

Karayanni H, Christaki U, Van Wambeke F, Denis M, Moutin T (2005) Influence of ciliated protozoa and heterotrophic nanoflagellates on the fate of primary production in the northeast Atlantic Ocean. Journal of Geophysical Research-Oceans 110: Art. No. C07S15

Kirchman DL (1993) Leucine incorporation as a measure of biomass production by heterotrophic bacteria. In: Kemp PF, Cole JJ, Sherr BF, Sherr EB (eds) Handbook of Methods in Aquatic Microbial Ecology. Lewis Press, New York, p 509-512

Konopka A (1999) Theoretical analysis of the starvation response under substrate pulses. Microbial Ecology 38:321-329

Kooi BW, Kooijman SALM (1994) The Transient-Behavior of Food-Chains in Chemostats. Journal of Theoretical Biology 170:87-94

Kooijman SALM (2000) Dynamic Energy and Mass Budgets in Biological Systems, Vol. Cambridge University Press, Cambridge

Kooijman SALM, Kooi BW, Hallam TG (1999) The application of mass and energy conservation laws in physiologically structured population models of heterotrophic organisms. Journal of Theoretical Biology 197:371-392

Kooijman SALM, Muller EB, Stouthamer AH (1991) Microbial growth dynamics on the basis of individual budgets. Antonie Van Leeuwenhoek 60:159-174

Kooijman SALM, Troost TA (2007) Quantitative steps in the evolution of metabolic organisation as specified by the dynamic energy budget theory. Biological Reviews 82:1-30

La Ferla R, Azzaro F, Azzaro M, Caruso G, Decembrini F, Leonardi M, Maimone G, Monticelli LS, Raffa F, Santinelli C, Zaccone R, Ribera d'Alcalá M (2005) Microbial contribution to carbon biogeochemistry in the Central Mediterranean Sea: Variability of activities and biomass. Journal of Marine Systems 57:146-166

Lagaria JC, Reeds JA, Wright MH, Wright PE (1998) Convergence properties of the Nelder-Mead simplex method in low dimensions. SIAM journal of optimization 9:112-147

Lancelot C, Staneva J, Van Eeckhout D, Beckers JM, Stanev E (2002) Modelling the Danube-influenced north-western continental shelf of the Black Sea. II: Ecosystem response to changes in nutrient delivery by the Danube River after its damming in 1972. Estuarine Coastal and Shelf Science 54:473-499

Lawrie J, Hearne J (2007) Reducing model complexity via output sensitivity. Ecological Modelling 207:137-144

Lee S, Fuhrman JA (1987) Relationships between Biovolume and Biomass of Naturally Derived Marine Bacterioplankton. Applied and Environmental Microbiology 53:1298-1303

Legendre L, Rassoulzadegan F (1995) Plankton and nutrient dynamics in marine waters. Ophelia 41:153-172

Lyman J., Fleming R. (1940) Composition of sea water. Journal of Marine Research 3:134-146

Maixandeau A, Lefèvre D, Fernandez IC, Sempéré R, Sohrin R, Ras J, Van Wambeke F, Caniaux G, Quéguiner B (2005) Mesoscale and seasonal variability of community production and respiration in the surface waters of the NE Atlantic Ocean. Deep-Sea Research Part I-Oceanographic Research Papers 52:1663-1676

Marr AG, Nilson EH, Clark DJ (1963) The maintenance requirement of Escherishia coli. Annals of the New York Academy of Sciences 102:536-548

Martinussen I, Thingstad TF (1987) Utilization of Organic-N, Organic-P and Organic-C by Heterotrophic Bacteria .II. Comparison of Experiments and a Mathematical-Model. Marine Ecology-Progress Series 37:285-293

Mcmanus GB, Peterson WT (1988) Bacterioplankton Production in the Nearshore Zone during Upwelling Off Central Chile. Marine Ecology-Progress Series 43:11-17

Memery L, Reverdin G, Paillet J, Oschlies A (2005) Introduction to the POMME special section: Thermocline ventilation and biogeochemical tracer distribution in the northeast Atlantic Ocean and impact of mesoscale dynamics. Journal of Geophysical Research-Oceans 110: Art. No. C07S01

Merien D (2003) Variabilité biooptique à différentes échelles spatiales et temporelles dans l'Atlantique nord-est: interprétations biogéochimiques. University of Pierre and Marie Curie (Paris VI)

Michaelis L, Menten ML (1913) Die Kinetik der Invertinwirkung. Biochem. Z. 49:333-369

Middelboe M, Jorgensen NOG, Kroer N (1996) Effects of viruses on nutrient turnover and growth efficiency of noninfected marine bacterioplankton. Applied and Environmental Microbiology 62:1991-1997

Miki T, Yamamura N (2005a) Effects of asynchronous fluctuations in DOC supply and bacterial growth on biodegradation efficiency. Ecological Modelling 183:281-299

Miki T, Yamamura N (2005b) Theoretical model of interactions between particle-associated and free-living bacteria to predict functional composition and succession in bacterial communities. Aquatic Microbial Ecology 39:35-46

Mladenov N, McKnight DM, Wolski P, Murray-Hudson M (2007) Simulation of DOM fluxes in a seasonal floodplain of the Okavango Delta, Botswana. Ecological Modelling 205:181-195

Mladenov N, McKnight DM, Wolski P, Ramberg L (2005) Effects of annual flooding on dissolved organic carbon dynamics within a pristine wetland, the Okavango Delta, Botswana. Wetlands 25:622-638

Monfort P, Baleux B (1992) Comparison of flow cytometry and epifluorescence microscopy for counting bacteria in aquatic ecosys terns. Cytometry 13:188-192

Monod J (1942) Recherches sur la croissance des cultures bactériennes. University of Paris

Murray AG, Parslow JS (1999) The analysis of alternative formulations in a simple model of a coastal ecosystem. Ecological Modelling 119:149-166

Nagata T (2000) Production mechanisms of dissolved organic matter. In: Kirchman DL (ed) Microbial ecology of the oceans. Wiley-Liss, p 121-152

Nagata T, Kirchman DL (1999) Bacterial mortality: A pathway for the formation of refractory DOM? In: Brylinsky M, Bell C, Johnson-Grenn P (eds) New frontiers in Microbial Ecology: Proceedings of the Eighth International Symposium on Microbial Ecology. Atlantic Canda Society for Microbial Ecology, Halifax

Nisbet RM, Muller EB, Lika K, Kooijman SALM (2000) From molecules to ecosystems through dynamic energy budget models. Journal of Animal Ecology 69:913-926

Pahlow M, Vézina AF (2003) Adaptative model of DOM dynamics in the surface ocean. Journal of Marine Research 61:127-146

Panagiotopoulos C, Sempéré R, Obernosterer I, Striby L, Goutx M, Van Wambeke F, Gautier S, Lafont R (2002) Bacterial degradation of large particles in the southern Indian Ocean using in vitro incubation experiments. Organic Geochemistry 33:985-1000

Pirt SJ (1965) The maintenance energy of bacteria in growing cultures. Proceedings of the Royal Society of London. Series B: Biological Sciences 163:224-231

Poggiale JC, Auger P, Nerini D, Mante C, Gilbert F (2005) Global production increased by spatial heterogeneity in a population dynamics model. Acta Biotheoretica 53:359-370

Pomeroy LR (1974) The ocean's food web, a changing paradigm. Bioscience 24:499-504

Pomeroy LR, Sheldon JE, Sheldon WM, Peters F (1995) Limits to Growth and Respiration of Bacterioplankton in the Gulf-of-Mexico. Marine Ecology-Progress Series 117:259-268

Raguénès GHC, Peres A, Ruimy R, Pignet P, Christen R, Loaec M, Rougeaux H, Barbier G, Guezennec JG (1997) Alteromonas infernus sp. nov., a new polysaccharide-producing bacterium isolated from a deep-sea hydrothermal vent. Journal of Applied Microbiology 82:422-430

Raick C, Delhez EJM, Soetaert K, Gregoire M (2005) Study of the seasonal cycle of the biogeochemical processes in the Ligurian Sea using a 1D interdisciplinary model. Journal of Marine Systems 55:177-203

Raick C, Soetaert K, Gregoire M (2006) Model complexity and performance: How far can we simplify? Progress in Oceanography 70:27-57

Reinthaler T, Herndl GJ (2005) Seasonal dynamics of bacterial growth efficiencies in relation to phytoplankton in the southern North Sea. Aquatic Microbial Ecology 39:7-16

Rivkin RB, Legendre L (2001) Biogenic carbon cycling in the upper ocean: Effects of microbial respiration. Science 291:2398-2400

Saunders G (1976) Decomposition in fresh water. In: Anderson J, Macfadyen A (eds) The role of terrestrial and aquatic organisms in decomposition processes. Blackwell, p 341-374

Sempéré R, Dafner E, Van Wambeke F, Lefèvre D, Magen C, Allegre S, Bruyant F, Bianchi M, Prieur L (2003) Distribution and cycling of total organic carbon across the Almeria-Oran Front in the Mediterranean Sea: Implications for carbon cycling in the western basin. Journal of Geophysical Research-Oceans 108:Art. No. 3361

Sempéré R, Van Wambeke F, Azourmanian H, Chambaut AL, Ferrière L, Bianchi M (1998) On the use of batch systems to determine DOC bacterial lability and bacterial growth efficiency in seawater samples. In: Bayens J, Dehairs F, Goyens, L (eds) Inetgrated marine system analysis. European Network for integrated Marine System Analysis, p 233-238

Sempéré R, Yoro SC, Van Wambeke F, Charrière B (2000) Microbial decomposition of large organic particles in the northwestern

Mediterranean Sea: an experimental approach. Marine Ecology-Progress Series 198:61-72

Sherr EB, Sherr BF (1996) Temporal offset in oceanic production and respiration processes implied by seasonal changes in atmospheric oxygen: The role of heterotrophic microbes. Aquatic Microbial Ecology 11:91-100

Siegenthaler U, Sarmiento JL (1993) Atmospheric Carbon-Dioxide and the Ocean. Nature 365:119-125

Sohrin R, Sempéré R (2005) Seasonal variation in total organic carbon in the northeast Atlantic in 2000-2001. Journal of Geophysical Research-Oceans 110:-

Spitz YH, Moisan JR, Abbott MR (2001) Configuring an ecosystem model using data from the Bermuda Atlantic Time Series (BATS). Deep-Sea Research Part II-Topical Studies in Oceanography 48:1733-1768

Talin F, Tolla C, Rabouille C, Poggiale JC (2003) Relations between bacterial biomass and carbon cycle in marine sediments: An early diagenetic model. Acta Biotheoretica 51:295-315

Taylor AH, Joint I (1990) A Steady-State Analysis of the Microbial Loop in Stratified Systems. Marine Ecology-Progress Series 59:1-17

Tedetti M, Kawamura K, Charrière B, Chevalier N, Sempéré R (2006) Determination of low molecular weight dicarboxylic and ketocarboxylic acids in seawater samples. Analytical Chemistry 78:6012-6018

Tedetti M, Kawamura K, Narukawa M, Joux F, Charrière B, Sempéré R (2007) Hydroxyl radical-induced photochemical formation of dicarboxylic acids from unsaturated fatty acid (oleic acid) in aqueous solution. Journal of Photochemistry and Photobiology a-Chemistry 188:135-139

Thingstad TF (1987) Utilization of N, P, and Organic C by Heterotrophic Bacteria .I. Outline of a Chemostat Theory with a Consistent Concept of Maintenance Metabolism. Marine Ecology-Progress Series 35:99-109

Thingstad TF, Pengerud B (1985) Fate and Effect of Allochthonous Organic Material in Aquatic Microbial Ecosystems - an Analysis Based on Chemostat Theory. Marine Ecology-Progress Series 21:47-62

Tian RC, Vézina AF, Legendre L, Ingram RG, Klein B, Packard T, Roy S, Savenkoff C, Silverberg N, Therriault J-C, Tremblay J-E (2000)

Effects of pelagic food-web interactions and nutrient remineralization on the biogeochemical cycling of carbon: a modelling approach. Deep-Sea Research Part II-Topical Studies in Oceanography 47:637-662

Tolla C, Kooijman SALM, Poggiale JC (2007) A kinetic inhibition mechanism for maintenance. Journal of Theoretical Biology 244:576-587

Touratier F, Legendre L, Vezina A (1999) Model of bacterial growth influenced by substrate C:N ratio and concentration. Aquatic Microbial Ecology 19:105-118

Vallino JJ (2000) Improving marine ecosystem models: Use of data assimilation and mesocosm experiments. Journal of Marine Research 58:117-164

Vallino JJ, Hopkinson CS, Hobbie JE (1996) Modeling bacterial utilization of dissolved organic matter: optimization replaces Monod growth kinetics. Limnology and Oceanography 41:1591-1609

Verdugo P, Alldredge AL, Azam F, Kirchman DL, Passow U, Santschi PH (2004) The oceanic gel phase: a bridge in the DOM–POM continuum. Marine Chemistry 92:67-85

Vichi M, Oddo P, Zavatarelli M, Coluccelli A, Coppini G, Celio M, Umani SF, Pinardi N (2003) Calibration and validation of a one-dimensional complex marine biogeochemical flux model in different areas of the northern Adriatic shelf. Annales Geophysicae 21:413-436

Vrede K, Heldal M, Norland S, Bratbak G (2002) Elemental composition (C, N, P) and cell volume of exponentially growing and nutrient-limited bacterioplankton. Applied and Environmental Microbiology 68:2965-2971

Wheeler PA, Gosselin M, Sherr E, Thibault D, Kirchman DL, Benner R, Whitledge TE (1996) Active cycling of organic carbon in the central Arctic Ocean. Nature 380:697-699

Wiebinga CJ, de Baar HJW (1998) Determination of the distribution of dissolved organic carbon in the Indian sector of the Southern Ocean. Marine Chemistry 61:185-201

Williams PJleB, Jenkinson NW (1982) A Transportable Microprocessor-Controlled Precise Winkler Titration Suitable for Field Station and Shipboard Use. Limnology and Oceanography 27:576-584

Williams PJleB (2000) Heterotrophic bacteria and the dynamics of dissolved organic material. In: Kirchman DL (ed) Microbial ecology of the oceans. Wiley-Liss, p 153-199

Williams PM, Druffel ERM (1987) Radiocarbon in Dissolved Organic-Matter in the Central North Pacific-Ocean. Nature 330:246-248

Yoro SC, Panagiotopoulos C, Sempéré R (1999) Dissolved organic carbon contamination induced by filters and storage bottles. Water Research 33:1956-1959

Zweifel UL, Norrman B, Hagstrom A (1993) Consumption of Dissolved Organic-Carbon by Marine-Bacteria and Demand for Inorganic Nutrients. Marine Ecology-Progress Series 101:23-32

Summary

Bacterial degradation of dissolved organic carbon in the water column

An experimental and modelling approach

This thesis deals with the growth of heterotrophic pelagic bacteria which use the dissolved organic carbon (DOC) as nutritive resource. It is widely recognised that heterotrophic bacteria play a predominant role in the carbon cycle. Indeed, they represent the most important living biomass in aquatic ecosystems and constitute the major DOC consumers. DOC is the second most important stock of bioreactive carbon in ocean and its dynamics are important for understanding the global carbon cycle and changes of atmospheric CO_2. DOC may play an important role in the biogeochemistry of the oceanic carbon cycle as it contributes to the biological pump by the export of sinking biogenic particles. The carbon flow through the bacterial compartment is investigated by the bacterial growth efficiency (BGE). BGE provides an estimation of the DOC fraction that is used by bacteria for their growth, the rest being remineralised. Numerous studies investigated the influence of environmental factors on BGE values. These factors generally comprise temperature, season, distance from the shore and substrate quality.

This thesis aims to investigate heterotrophic bacterial growth by using both experimental and modelling approaches. The experimental work used natural as well as artificial seawater. Various models for bacterial growth, comprising different levels of complexity, were investigated to represent mathematically the dynamics of the different experiments. Two main axes merge in this work: (1) the study of growth models, constructed from experimental results, with a view to implement them in ecosystem models, and (2) the investigation of the environmental factors influencing the BGE with these models. The main objective consists of the study of bacterial growth in different environmental contexts and to deduce a suitable mathematical formulation for describing the interaction between growth and DOC to include this in a biogeochemical model later on.

We first studied bacterial and DOC dynamics from *in situ* samples. Numerous biodegradation experiments, implying natural DOC and bacterial assemblages, were realised in stable conditions in the Northeast Atlantic Ocean according to several seasons and depths. We utilised the Monod model for representing the data acquired during these experiments. This model is empirical, constructed with Michaelis-Menten kinetics and is the most widely used for describing bacterial growth in ecosystem models. BGE was estimated experimentally, as generally done by most authors, and also by using the model. We demonstrated that BGE varies according to season and depth, the dynamics being the same with both methods of estimation. As BGE is one parameter of the Monod model, this result proved that it is inaccurate for representing the utilisation of DOC by bacteria in ecosystem models.

We then decided to carry out experiments in artificial conditions, with a monospecific bacterial strain and a single DOC substrate. This setup provides data sets that are easier to analyse and allows the application of more complex models. To test the performance of several models, comprising several levels of complexity, including the Monod model, 2 kinds of experiments were performed: 1 experiment was realised in constant conditions with a single substrate load at the start of the experiment, as the previous study, the other experiment was carried out by pulsing the substrate supply periodically. The total amount of substrate was the same in both experiments, the only difference consists of the input regime. The substrate pulses mimic the spatial and temporal variability of DOC distribution. We demonstrated that the Monod model is inaccurate to represent bacterial dynamics when they are in starved conditions, which may often occur in natural environments. We also utilised a model implementing the bacterial maintenance, the Marr-Pirt model, and another model, constructed from the dynamic energy budget (DEB) theory, including maintenance as well as a reserve compartment. Both models match the data very well. However, the DEB model, due to its mechanistic basis, is more flexible and is able to adapt to more situations. BGE was estimated experimentally and with the 3 models for both experiments. We demonstrated that BGE is higher in the pulse experiment than in the experiment carried out in stable conditions with all methods of BGE estimation. Consequently, the spatial and temporal variability of DOC distribution has a profound impact on the estimation of BGE value.

Data of the pulse experiment were also used to formulate a mechanistic model, based on the DEB theory as stated previously. In a third section, we investigate this model more profoundly and its potential inclusion in

ecosystem models. We adapted a bacterial growth model with the theory in order to account for the processes highlighted by the experiment. The model was first improved by considering 2 maintenance processes: when mobilised reserves are sufficient, maintenance is realised from the reserve pool, the remaining energy being used for growth; however, when the reserve flux is not enough to sustain maintenance, growth ceases and maintenance is realised from the reserve plus the structural volume and the cell shrinks. When maintenance is performed from the structure, the model permits the release of refractory material in the medium by bacteria. Maintenance was modelled in this way to account for the increasing non-used DOC in the culture. This model is quite complex to represent only a bacterial component and is thus difficult to implement in ecosystem models. The original model, comprising 4 state variables, was thus reduced to a system of 2 differential equations which may be easier implemented in global models. This result has a profound impact in the context of global modelling, as model simplification allows easier calibration, simulation and the understanding of model outputs.

The results highlighted by this thesis were obtained thanks to the coupled experimentation-modelling approach. The experiments revealed key processes and facilitated the construction of models on the basis of biological insights, and models highlighted gaps in the knowledge which is required for a better representation of the system. Consequently, models may suggest new experiments to be performed and the best strategy alternates repeatedly between experiment and modelling.

Samenvatting

Bacteriële afbraak van opgelost organische koolstof in de water kolom

Een gecombineerde experimentele en modellerings benadering

Dit proefschrift behandelt de groei van pelagische bacteriën die opgelost organisch koolstof (DOC) als energie bron gebruiken. Het is algemeen bekend dat dit type bacteriën een dominante rol spelen in de koolstof cyclus. Zij vertegenwoordigen de belangrijkste levende biomassa in aquatische oecosystemen en vormen de voornaamste consumenten van DOC. DOC is de op één na belangijkste poel van biologisch beschikbaar koolstof in de oceaan en zijn dynamika is belangrijk voor het begrip van de koolstof cyclus en van veranderingen in het atmosferisch CO_2. DOC zou een belangrijke rol kunnen spelen in de biogeochemie van de koolstof cyclus in de oceaan aangezien het bijdraagt aan de biologische pomp die biogene deeltjes exporteert uit het oppervlakte water naar de diepte. De koolstof-stroom door het bacteriële compartiment wordt onderzocht aan de hand van de bacteriële groei efficientie (BGE). Deze efficientie geeft de fractie DOC aan dat door de bacteriën wordt gebruikt voor de groei, de rest wordt gemineraliseerd. Vele studies gaan over de invloed van omgevingsfactoren op BGE waarden. Deze factoren omvatten temperatuur, seizoen, afstand tot de kust en de kwaliteit van het substraat.

Dit proefschrift combineert experimetele en modelmatige benaderingen om de groei van heterotrofe bacteriën te onderzoeken. Het experimentele werk maakte van natuurlijk, maar ook van kunstmatig zeewater gebruik Verschillende modellen voor bacteriële groei van uiteenlopende complexiteit werden onderzocht op hun representatie van de resultaten van de experimenten. Twee denklijnen komen in dit proefschrift samen: (1) de studie van groei modellen die gebaseerd zijn op experimentele resultaten met het oog deze toe te passen in ecosysteem modellen, en (2) de studie van de effecten van omgevingsfactoren op de BGE met behulp van deze modellen. De belangrijkste doelstelling is de bacteriële groei in de verschillende omgevingen te begrijpen en af te leiden welke wiskundige formulering het meest geschikt is om later in biogeochemische toe te passen.

We hebben eerst de dynamica van bacteriën en DOC bestudeerd in *in situ* monsters. Vele biodegradatie experimenten betreffende DOC en microorganismen werden gedaan onder constante condities zoals die in de noordwestelijke Atlantische Ocean op de verschillende diepten en in de verschillende seizoenen gevonden worden. Wij hebben het Model model gebruikt om de resultaten van deze experimenten te beschrijven. Dit is een empirisch model dat gebruik maakt van Michaelis-Menten kinetika en is het vaakst gebruikte model voor bacteriële groei dat wordt toegepast in ecosysteem modellen De BGE werd rechtstreeks experimenteel geschat, zoals de meeste auteurs doen, maar ook met behulp van het Monod model. Wij hebben aangetoond dat de.BGE variëert met het seizoen en de diepte, en beide schattingsmethoden leverden dezelfde resultaten op. Aangezien de BGE een parameter van het Monod model is die niet zou mogen variëren laten deze resultaten zien dat het Monod model ongeschikt is om het gebruik van DOC door bacteriën te beschrijven in ecosysteem modellen.

Vervolgens besloten we experimenten onder kunstmatige condities uit te voeren met een zuivere bacterie stam en een enkelvoudige DOC bron. Deze proefopzet levert data op die makkelijker te analiseren zijn en de toepassing van meer complexe modellen mogelijk maakt. Om modellen van verschillend niveau van complexiteit met elkaar te vergelijken, waaronder het Monod model, hebben we twee soorten experimenten uitgevoerd: één waarbij al het substraat aan het begin van de proef werd toegevoegd, en één waarbij dit pulserend werd gedaan met tussenpozen. De totale hoeveelheid toegevoegde substraat was in beide gevallen gelijk, het enige verschil is in de wijze van toediening. De gepulseerde dosering bootst de ruimtelijke en in de tijd variërende concentratie DOC na. We laten zien dat het Monod model de bactiële dynamica slecht beschrijft tijdens hongering, hetgeen in de natuur vaak voorkomt. .We pasten ook modellen toe die rekening houden met bacteriële onderhouds-processen, het Marr-Pirt model en een model dat gebaseerd is op de dynamische energie budget (DEB) theorie en ook nog een reserve compartiment heeft. Beide modellen beschrijven de experimentele resultaten voortreffelijk. Dankzij zijn mechanische basis is het DEB model echter meer flexiebel en kan het in meer situaties gebruikt worden. De BGE werd wederom geschat zowel direct uit de experimentele data als met behulp van de drie modellen. We laten zien dat de BGE bij de puls-experimenten hoger is dan bij de eenmalige dosering, ongeacht de gebruikte schattingsmethode. We kunnen dus concluderen dat variaties van de concentratie DOC in ruimte en tijd een grote invloed hebben op de waarde van de BGE .

Data van het puls-experiment werden ook gebruikt om het DEB model te verfijnen. In het derde gedeelte onderzoeken we de eigenschappen van dit model meer in detail om het model later in te bouwen in ecosystem modellen. We onderscheiden een tweetal onderhoudsprocessen, één waarbij de stroom van gemobiliseerde reserve groot genoeg is voor het onderhoud van de cel, en één waarbij dit niet het geval is en deze stroom moet worden aangevuld met gemobiliseerde structuur, met het gevolg dat de cel krimpt. Bij dit krimp-proces wordt slecht afbreekbaar organisch koolstof gevormd, dat tijdens het experiment ophoopt waardoor de concentratie DOC toeneemt..Dit model is knap ingewikkeld voor toepassing in ecosysteem modellen. Om deze reden is het vereenvoudigd en zijn de 4 differentiaal-vergelijkingen die oorspronkelijk nodig waren tot 2 teruggebracht. Dit resultaat is van grote waarde voor globale modellering van de koolstof cyclus. Dit vereenvoudigt het schatten van parameter waarden de computer simulaties en de interpretatie van de simulatie resultaten.

De resultaten van dit proefschrift onderstrepen de kracht van een gecombineerde experimentele en modelmatige aanpak. De experimentele resultaten maakten het opstellen van een realistisch model mogelijk en de modellen legden gaten in de kennis bloot die nodig is om ecosysteem modellen te kunnen opstellen. Dit suggereert op zijn beurd weer het opzetten van gerichte nieuwe experimenten. De beste aanpak in biologisch onderzoek is het herhaaldelijk afwisselen van het doen van experimenten en het modelmatig analyseren van experimentele resultaten.

Acknowledgments

First, I would like to thank Jean-Christophe POGGIALE and Bas KOOIJMAN, my french and dutsch supervisors, who guided me in this enterprise which is the thesis. I would like to thank Jean-Christophe for his help, understandings and trust during these 3 years. He was always present when needed. I would like to thank Bas for proposing me this double-doctorat degree, for his welcome in his lab, his availability and kindness. Both transmitted me the liking for modelling work and to go deeper in thinks.

Then, many thanks to Richard SEMPERE, my second french supervisor, who gave me the means to undertake this thesis. His advices were always helpful and he always trusted on my choices. It was very interesting to collaborate with him.

I also sincerely thank Peter van BODEGOM, Tiago DOMINGO, Frédéric JEAN, Bob KOOI and Olivier MAURY who honour me for judging my work and accepting the jury role for this PhD defence in Netherlands.

I'm infinitely grateful to Dominique LEFEVRE who gave me the means to realise the experiments presented in this thesis. He believed in my project, gave me the time I needed, was always present to listen and pay attention to me and accompanied me during these long months of experimental work. For all of these I thank him.

I would also like to thank Gérald GREGORI, Bruno CHARRIERE and Marc GAREL who help me for constructing the experiments, gave me a hand when necessary and above all a lot of time. This thesis would not be the same without their help.

I don't forget to thank all my colleagues and friends of the fourth floor: Philippe CUNY, Claude DEGIOVANNI, Franck GILBERT, Claude MANTE, David NERINI, Brigitte PANTAT, Dominique POIROT, Georges STORA and Anne-Françoise YAO. It was a pleasure to work among these persons, with their exuberance, their kindness, their jokes. The coffee breaks were always the moments of friendly discussions. Many thanks also to Laura PISCHEDDA who supported me during these long months, for the good and

the bad moments. She was always here to give me more courage to continue or to console me. I like her humour, optimism and way of life. It was a pleasure to spend so many times with her and I know I will miss her.

To finish, all my thanks go to my parents, Fabien, and all my family who were always here for putting me up, who helped me since all these years of studies, and who love me for what I am. I'll never succeed without all of them.

List of most used acronym:

BCD	bacterial carbon demand
BGE	bacterial growth efficiency
BP	bacterial production
BR	bacterial respiration
C	carbon
CCF	carbon conversion factor
CO_2	carbon dioxide
DCAA	dissolved combined amino acid
DEB	dynamic energy budget
DFAA	dissolved free amino acid
DOC	dissolved organic carbon
DOM	dissolved organic matter
EPS	exopolysaccharides
H	hydrogen
HMW	high molecular weight
IBP	integrated bacterial production
IC	inorganic carbon
L-DOC	labile dissolved organic carbon
LMW	low molecular weight
MCHO	monosaccharide
N	nitrogen
O	oxygen
O_2	dioxygen
OC	organic carbon
OD	optical density
OM	organic matter
P	phosphorus
PER	percent extracellular release
POC	particulate organic carbon
POM	particulate organic matter
POMME	programme océan multidisciplinaire méso-échelle
POS	polarographic oxygen sensor
R-DOC	refractory dissolved organic carbon
RQ	respiratory quotient
SL-DOC	semi-labile dissolved organic carbon
TOC	total organic carbon
VHMW	very high molecular weight

Variables, parameters and notations used for the models

Symbol	Equiv.	Unit	Description
Chapter II – Monod model			
DOC		µM C	DOC concentration
BB		µM C	Bacterial biomass - carbon
$V_{\max}$		h^{-1}	Maximum specific assimilation rate
k		µM C	Half-saturation constant
BGE_N		-	Bacterial growth efficiency
α	$\frac{V_{\max}}{k}$	µM C^{-1} h^{-1}	Ratio between the maximum specific absorption rate and the half-saturation constant
Chapters III-IV Monod – Marr-Pirt – DEB models			
State Variables			
M_E		mM C	Reserve mass
m_E	$\frac{M_E}{M_V}$	-	Reserve mass relative to the structural body mass
M_V		mM C	Structural body mass
L		mM C	L-DOC concentration
R		mM C	R-DOC concentration
Parameters			
J_{X_m}		mM C h^{-1}	Maximum uptake rate
K		mM C	Half-saturation constant
k_E		h^{-1}	Reserve turnover rate
j_{LAm}		h^{-1}	Maximum specific absorption rate
y_{EL}		-	Yield coefficient from L-DOC to reserve masses
y_{EV}		-	Yield coefficient from structural to reserve masses
j_{EM}		h^{-1}	Maintenance flux from reserve mass
j_{VM}		h^{-1}	Maintenance flux from structural mass
y_{RV}		-	Yield coefficient from structure to R-DOC
α	$\frac{j_{LAm}}{K}$	mM C^{-1} h^{-1}	Ratio between the maximum specific absorption rate and the half-saturation constant
r	k_E	h^{-1}	Growth rate
κ_1		mM C	Carrying capacity

Symbol	Equiv.	Unit	Description
General symbols			
J_{*1*2}		mM C h^{-1}	Flux of compound $*_1$ associated with process $*_2$
j_{*1*2}	$\frac{J_{*1*2}}{M_V}$	h^{-1}	Specific flux of compound $*_1$ associated with process $*_2$
y_{*2*1} or Y_{*2*1}		-	Yield coefficient of compound $*_1$ on compound $*_2$
n_{*1*2}		-	Number of atoms of element $*_1$ present in compound $*_2$
$\dot{p}_{*1}$		J h^{-1}	Energy flux (power) of process $*_1$
κ		-	Fraction of catabolic power energy spent on maintenance plus growth
Processes ($\dot{p}_*$)			
A			Assimilation
C			Catabolism
M			Maintenance
G			Growth
D			Dissipation
P			Production
General compounds			
Organic			
X			Substrate
V			Structure
E			Reserve
P			Product
Mineral			
C			CO_2
H			H_2O
O			O_2
N			nitrogenous waste (ammonia)